

**AD-A257 769**

PL-TR-92-2218(I)



**DATA TO TEST AND EVALUATE THE  
PERFORMANCE OF NEURAL NETWORK  
ARCHITECTURES FOR SEISMIC SIGNAL  
DISCRIMINATION: DATA SETS #2-3**

Thomas J. Sereno, Jr.  
Gagan B. Patnaik  
Mari J. Mortell

Science Applications International Corporation  
10260 Campus Point Drive  
San Diego, California 92121

31 August 1992

Final Report (Volume I)  
1 September 1990 - 31 August 1992

DTIC  
ELECTE  
OCT 23 1992  
S E D

APPROVED FOR PUBLIC RELEASE; DISTRIBUTION UNLIMITED

92 10 1 15

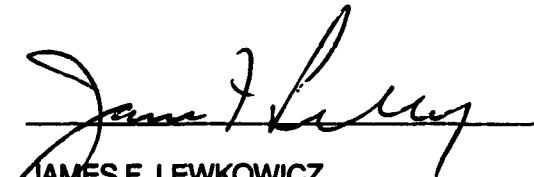
92-27739



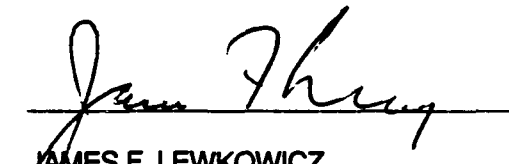
**PHILLIPS LABORATORY**  
**Directorate of Geophysics**  
**AIR FORCE MATERIEL COMMAND**  
**HANSCOM AIR FORCE BASE, MA 01731-5000**

The views and conclusions contained in this document are those of the authors and should not be interpreted as representing the official policies, either expressed or implied, of the Air Force or the U.S. Government.

This technical report has been reviewed and is approved for publication.



JAMES F. LEWKOWICZ  
Contract Manager  
Solid Earth Geophysics Branch  
Earth Sciences Division



JAMES F. LEWKOWICZ  
Branch Chief  
Solid Earth Geophysics Branch  
Earth Sciences Division



DONALD H. ECKHARDT, Director  
Earth Sciences Division

This document has been reviewed by the ESD Public Affairs Office (PA) and is releasable to the National Technical Information Service (NTIS).

Qualified requestors may obtain additional copies from the Defense Technical Information Center. All others should apply to the National Technical Information Service.

If your address has changed, or if you wish to be removed from the mailing list, or if the addressee is no longer employed by your organization, please notify PL/IMA, Hanscom AFB MA 01731-5000. This will assist us in maintaining a current mailing list.

Do not return copies of this report unless contractual obligations or notices on a specific document requires that it be returned.

REPORT DOCUMENTATION PAGE			Form Approved OMB No 0704-0188	
<small>Public reporting burden for this collection of information is estimated to average 1 hour per response, including the time for reviewing instructions, searching existing data sources, gathering and maintaining the data needed, and completing and reviewing the collection of information. Send comments regarding this burden estimate or any other aspect of this collection of information, including suggestions for reducing this burden, to Washington Headquarters Services, Directorate for Information Operations and Reports, 1215 Jefferson Davis Highway, Suite 1204, Arlington, VA 22202-4302, and to the Office of Management and Budget, Paperwork Reduction Project (0704-0188), Washington, DC 20503.</small>				
1. AGENCY USE ONLY (Leave blank)		2. REPORT DATE 31 August 1992		3. REPORT TYPE AND DATES COVERED Final Report (Volume I) 9/1/90-8/31/92
4. TITLE AND SUBTITLE Data to Test and Evaluate the Performance of Neural Network Architectures for Seismic Signal Discrimination: Data Sets #2-3			5. FUNDING NUMBERS PE 61101E PR 9T10 TA DA WU AA Contract F19628-90-C-0156	
6. AUTHOR(S) Thomas J. Sereno, Jr Gagan B. Patnaik Mari J. Mortell				
7. PERFORMING ORGANIZATION NAME(S) AND ADDRESS(ES) Science Applications International Corporation 10260 Campus Point Drive San Diego, CA 92121			8. PERFORMING ORGANIZATION REPORT NUMBER  SAIC- 92/1190	
9. SPONSORING/MONITORING AGENCY NAME(S) AND ADDRESS(ES) Phillips Laboratory Hanscom AFB, MA 01731-5000  Contract Manager: James Lewkowicz/GPEH			10. SPONSORING/MONITORING AGENCY REPORT NUMBER  PL-TR-92-2218 (I)	
11. SUPPLEMENTARY NOTES				
12a. DISTRIBUTION/AVAILABILITY STATEMENT  Approved for public release; distribution unlimited			12b. DISTRIBUTION CODE	
13. ABSTRACT (Maximum 200 words)  This report describes a data set that was developed to test and evaluate the performance of neural networks for automated processing and interpretation of regional seismic data. This data set may also be valuable for other applications related to seismic monitoring at regional distances, and it is available at the Center for Seismic Studies (CSS) in an Oracle database or in UNIX tar format on exabyte tapes. It consists of waveform and parametric data from >500 regional events recorded by the short-period elements of the NORESS and ARCESS arrays in Norway, and the GERESS array in Germany (the Oracle database at CSS also includes data from the FINESA array in Finland and a 3-component station in Poland called KSP). The epicentral distances are primarily 50-2000 km, and the magnitudes are primarily 1.0-5.0. Most of the events are mining explosions in the western part of the CIS, Sweden, Finland, Poland and Germany. Also included are 22 presumed underwater explosions, and 51 earthquakes in Fennoscandia that were identified in a regional bulletin produced by the University of Helsinki. Other presumed earthquakes (for which independent bulletin information was not available) include events in the Alps and Mediterranean region that were recorded by GERESS. The Oracle database is in CSS 3.0 format, and the exabyte tapes include waveforms in SAC binary format and parametric data in ASCII tables. Detailed documentation has been developed for each event, and is included in a 15-volume report at the CSS.				
14. SUBJECT TERMS Neural networks Seismic database NORESS/ARCESS/GERESS			15. NUMBER OF PAGES 80	
			16. PRICE CODE	
17. SECURITY CLASSIFICATION OF REPORT Unclassified	18. SECURITY CLASSIFICATION OF THIS PAGE Unclassified	19. SECURITY CLASSIFICATION OF ABSTRACT Unclassified	20. LIMITATION OF ABSTRACT SAR	

DTIC TAB

DTIC TAB ☒  
Unannounced ☐  
Justification

By  
Distribution/

Availability Codes

Dist Avail a, d/or Special

A-1

## Table of Contents

<b>1. SUMMARY</b>	1
<b>1.1 Objectives</b>	1
<b>1.2 Summary of the Data Sets</b>	1
1.2.1 Data Set #1	2
1.2.2 Data Set #2	2
1.2.3 Data Set #3	5
<b>1.3 Outline of the Report</b>	5
<b>2. DATA EXCHANGE FORMAT</b>	7
<b>2.1 Parametric Data</b>	7
<b>2.2 Waveform Data</b>	11
<b>2.3 Documentation</b>	12
<b>3. DATA SET #2</b>	21
<b>3.1 NORESS/ARCESS Arrays</b>	21
<b>3.2 Regional Events</b>	21
3.2.1 Selection Criteria	21
3.2.2 Event Description	27
3.2.3 Sample Waveforms	27
<b>4. DATA SET #3</b>	39
<b>4.1 GERESS Array</b>	39
<b>4.2 Regional Events</b>	39
4.2.1 Selection Criteria	39
4.2.2 Event Description	47
4.2.3 Sample Waveforms	47
<b>5. CONCLUSIONS</b>	67
<b>ACKNOWLEDGMENTS</b>	67
<b>REFERENCES</b>	69

## 1. SUMMARY

### 1.1 Objectives

The objectives of this two-year study are:

- (1) *Assemble three data sets to be used to test and evaluate the performance of neural networks for automated processing and interpretation of seismic data (Table 1).*

**Table 1.** Seismic Data Sets for DARPA's Artificial Neural Network Technology Program

Data Set	Description
<i>Data Set #1</i>	Data from approximately 300 events to develop and train neural networks to perform seismic data processing and interpretation tasks such as automated phase association, onset time estimation, typical and atypical event recognition, and event identification [ <i>Lacoss et al.</i> , 1990].
<i>Data Set #2</i>	Data from approximately 30 events to test the response of the neural networks to <i>novelty</i> signals. These data are recorded at the same stations as the events in Data Set #1, but are from different source types.
<i>Data Set #3</i>	Data from approximately 300 events to test the generality and adaptability of the neural networks. These events are recorded by stations in a different geologic environment than the stations used for Data Set #1.

These data sets are to be provided to a group at *MIT Lincoln Laboratory* who is developing and testing neural networks for the *Seismic Application* of DARPA's *Artificial Neural Network Technology* (ANNT) Program.

- (2) *Evaluate the results of the neural network program in the context of monitoring nuclear explosion testing.*

### 1.2 Summary of the Data Sets

Three data sets were developed to test and evaluate the performance of neural networks for automated processing and interpretation of regional seismic data. These data sets may also be valuable for other applications related to seismic monitoring at regional distances, and they are available at the Center for Seismic Studies (CSS) in an Oracle database or in UNIX tar format on exabyte tapes. The data sets consist of waveform and parametric data from >500 regional events recorded by the short-period elements of the NORESS and ARCESS arrays in Norway, and the GERESS array in Germany (the Oracle database at CSS also includes data from the FINESA array in

Finland and a 3-component station in Poland called KSP). The epicentral distances are primarily 50–2000 km, and the magnitudes are primarily 1.0–5.0. The Oracle database is in CSS 3.0 format, and the exabyte tapes include waveforms in the binary format used by SAC (*Seismic Analysis Code*) and parametric data in ASCII tables. SAC is a widely-used interactive analysis software package that was developed by Joseph Tull at Lawrence Livermore National Laboratory. Detailed documentation has been developed for each event in these data sets, and is included in a 13-volume report at the CSS.

### *1.2.1 Data Set #1*

This first data set consists of short-period single-channel waveforms (33 channels/array), beams, and parametric data from 241 regional events recorded by the NORESS and ARCESS arrays in Norway (Figure 1). The epicentral distances are primarily 200–1800 km, and the  $L_g$  magnitudes are primarily 1.5–3.2. Most of the events are mining explosions in the western part of the CIS, Sweden, and Finland. However, 18 of the events are earthquakes, and 22 are presumed to be underwater explosions. Most of the events were identified in a regional bulletin produced by the University of Helsinki. The others were identified by *Sereno* [1991] on the basis of location, origin time,  $S/P$  amplitude ratios, cepstral analysis, and past seismicity. Data Set #1 also includes parametric data from 249 other events (e.g., arrival times, amplitudes, polarization attributes, etc) recorded at NORESS and ARCESS during a continuous 10-day period.

These data were selected to support MIT Lincoln Laboratory's efforts to improve the automated performance of DARPA's *Intelligent Monitoring System* (IMS). The selection criteria were based on whether or not the automated IMS event solutions were accepted, modified or rejected by a seismic analyst [*Lacoss et al.*, 1990; *Lacoss et al.* 1991; *Sereno and Patnaik*, 1991]. These were further categorized by the quality of the IMS event solution (e.g., "high-quality" events were defined as those that were detected by both NORESS and ARCESS, and whose locations were constrained by at least 3 defining phases). The total data volume for Data Set #1 is about 1200 MBytes. This data set is described in detail by *Sereno and Patnaik* [1991], and in a 7-volume report that includes waveform and map displays for each event [*Patnaik and Sereno*, 1991a].

### *1.2.2 Data Set #2*

Data Set #2 consists of short-period single-channel waveforms (33 channels/array), beams, and parametric data from 33 presumed earthquakes recorded at regional distances by the NORESS and ARCESS arrays in Norway (Figure 2). The epicentral distances are primarily 200–2000 km, and the event magnitudes are primarily 1.0–2.9. Most of these events were reported to be earthquakes in the regional bulletin produced by the University of Helsinki.

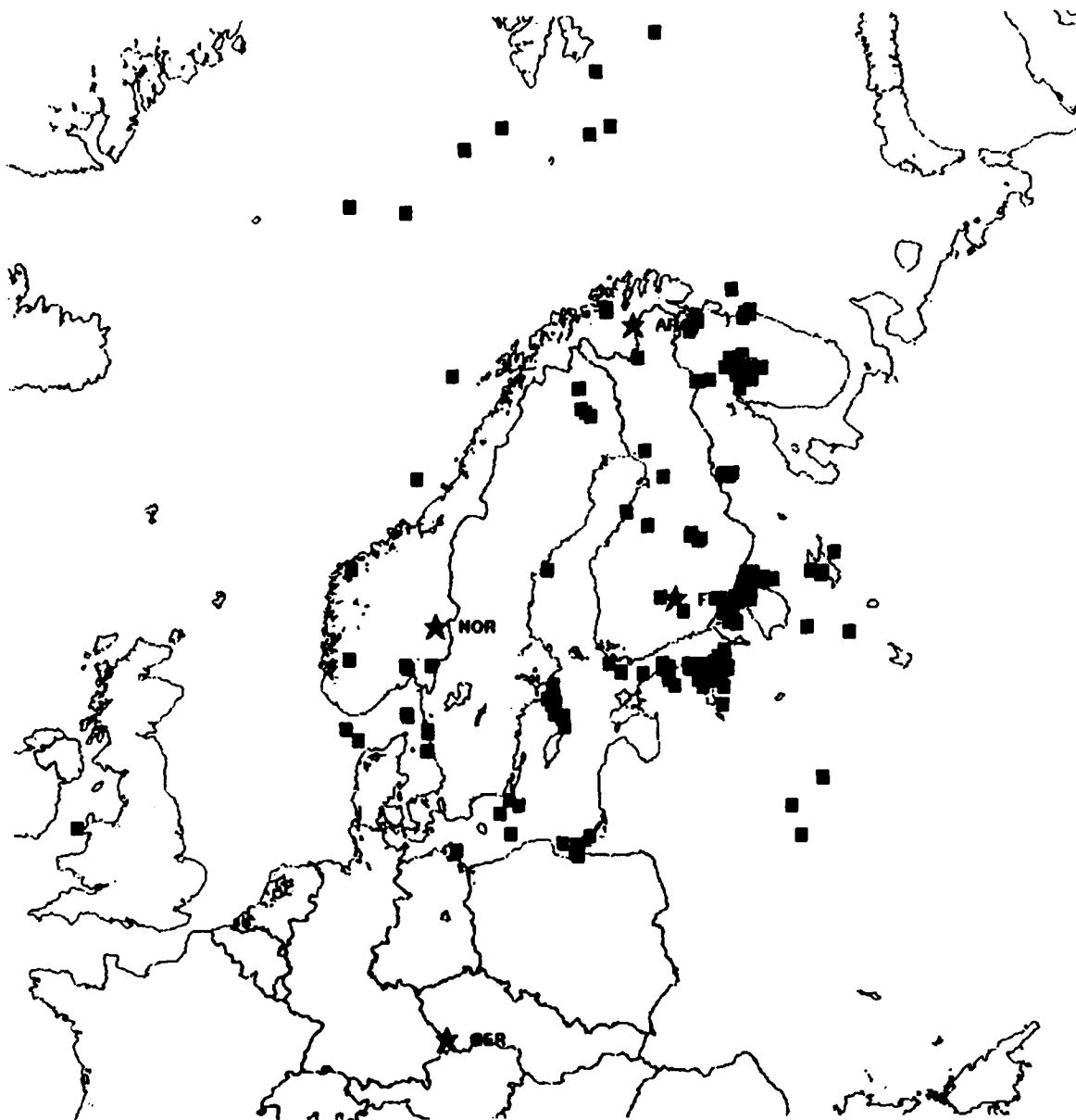


**Figure 1.** Epicenters are plotted for the 241 events with waveforms in Data Set #1.

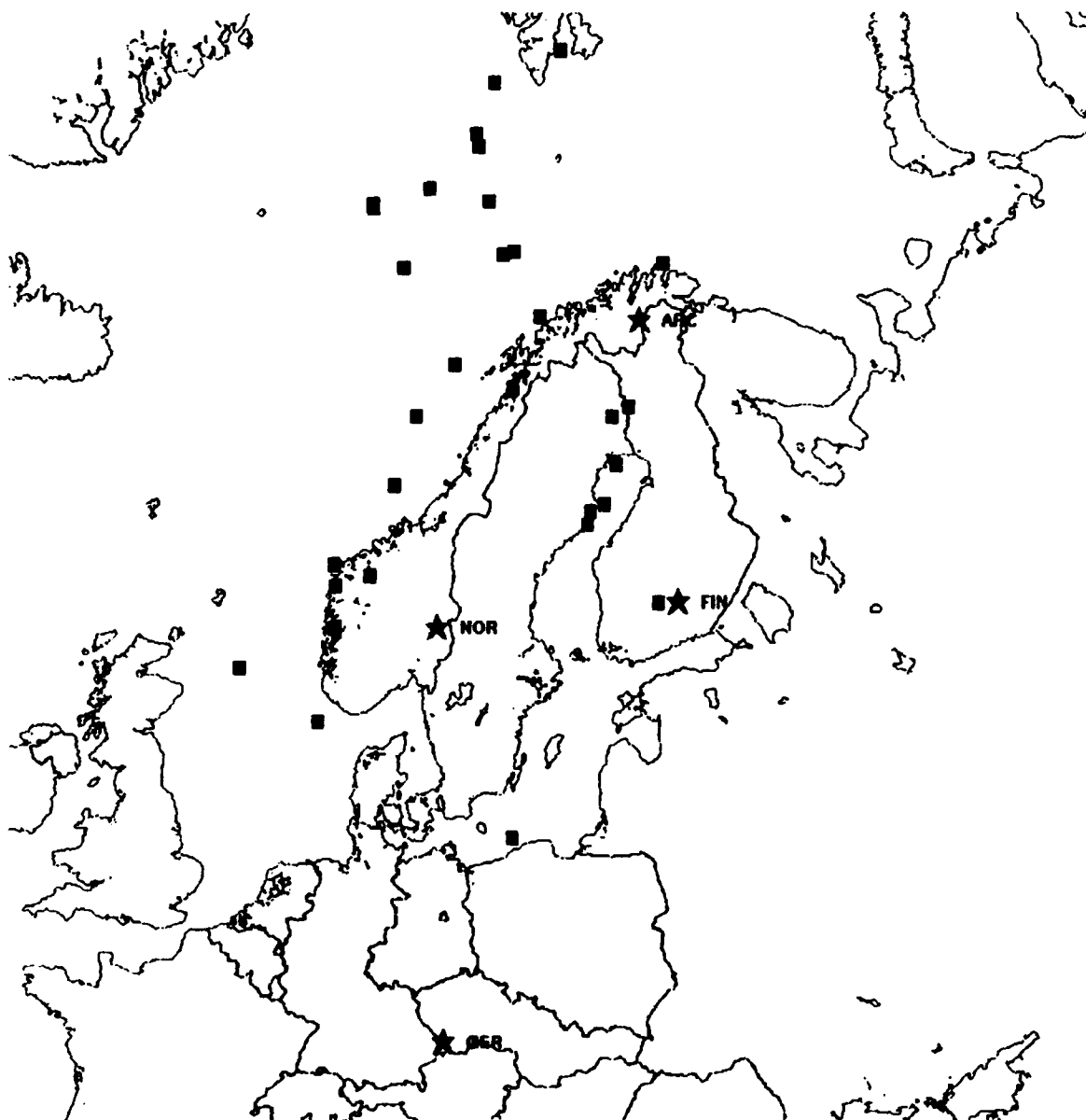


**Figure 2.** Epicenters are plotted for the 33 events in Data Set #2.



We selected earthquakes for Data Set #2 since over 90% of the events in Data Set #1 are explosions, and the objective of Data Set #2 was to test the response of the neural network to *novelty* signals (Table 1). The data volume for Data Set #2 is about 150 MBytes. This data set is described in detail in Section 3 of this report, and in a report that includes waveform and map displays for each of the 33 events [Mortell *et al.*, 1991].

### 1.2.3 Data Set #3

The third data set consists of short-period single-channel waveforms (33 channels), beams, and parametric data from 255 regional events recorded by the GERESS array in Germany (Figure 3). The epicentral distances are primarily 50–1700 km, and the magnitudes are primarily 2.0–5.0. We don't have independent bulletin information, but most of the events to the south of GERESS are probably earthquakes and most of the events to the north are probably mining explosions (e.g., there is an active mining region in Lubin, Poland).

GERESS is in a much different geologic and tectonic environment than the arrays in Norway, and this data set was developed to test the generality and adaptability of the neural networks that were trained with NORESS and ARCESS data. Events were selected with  $\geq 3$  defining phases, and at least one associated regional phase at GERESS. The data volume for Data Set #3 is about 450 MBytes. This data set is described in detail in Section 4 of this report, and in a 5-volume report that includes waveform and map displays for each event [Mortell *et al.*, 1992].

## 1.3 Outline of the Report

This final report is divided into two volumes. Volume I (this document) is a description of Data Sets #2–3 that were provided to *MIT Lincoln Laboratory* for their neural network study [Data Set #1 was described in our annual report; Sereno and Patnaik, 1991]. Volume II [Patnaik *et al.*, 1992] presents the results of evaluating *MIT Lincoln Laboratory's* neural network for regional phase identification (e.g.,  $P_n$ ,  $P_g$ ,  $S_n$ ,  $L_g$ ,  $R_g$ ), and our neural network for initial phase identification ( $P$  or  $S$ ) using polarization attributes derived from 3-component data [Patnaik and Sereno, 1991b].

The main technical sections of Volume I are Sections 2–4. The exchange format for waveform and parametric data is described in Section 2. Section 3 describes Data Set #2, and Section 4 describes Data Set #3. Section 3.1 describes the NORESS and ARCESS arrays and instrumentation. Section 3.2 gives a description of the regional events in Data Set #2 (e.g., location, magnitudes, distances, and identification). Similarly, Section 4.1 describes the GERESS array and instrumentation, and Section 4.2 describes the regional events in Data Set #3. Our conclusions regarding these regional seismic data sets are presented in Section 5.

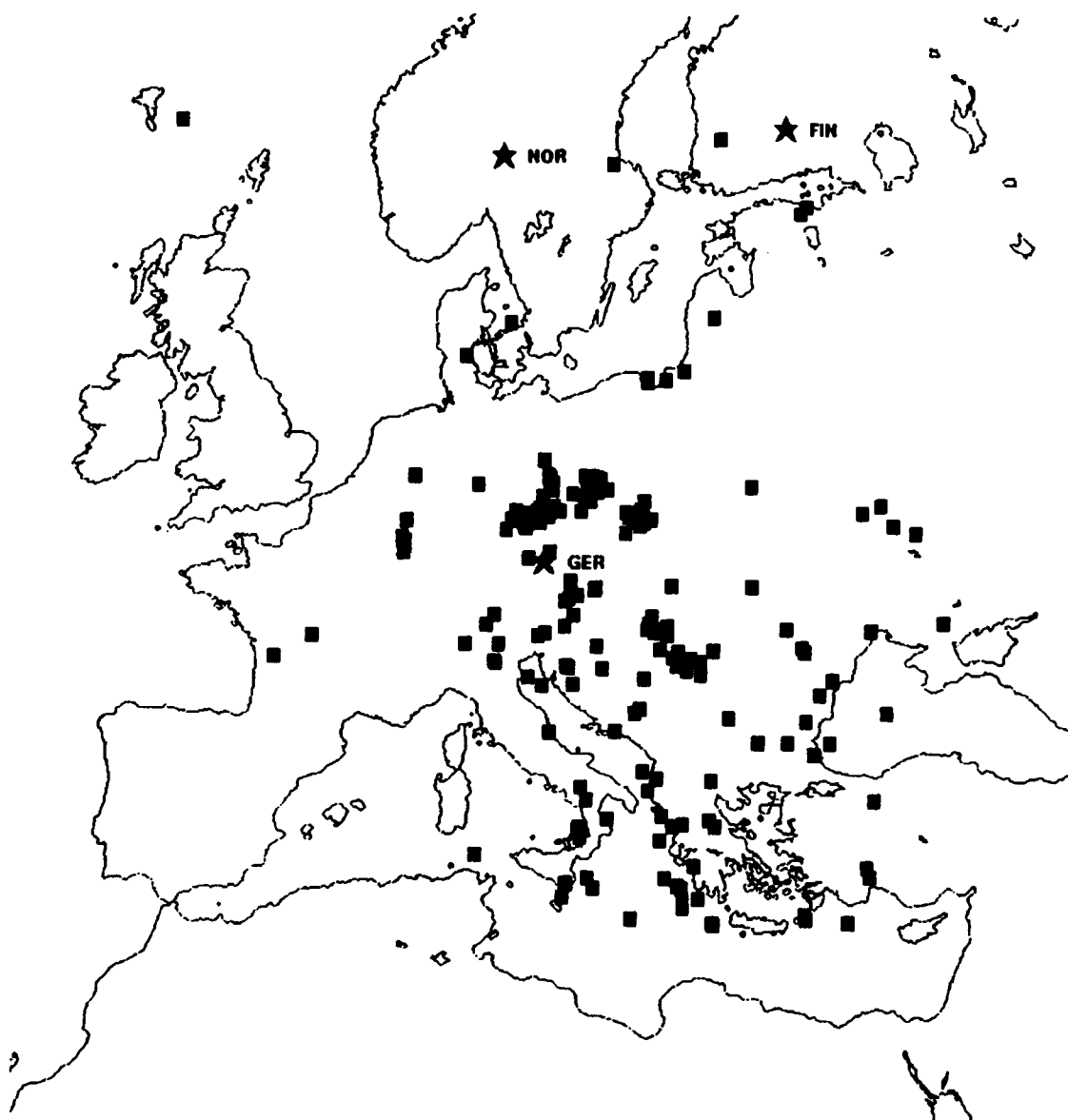


**Figure 3.** Epicenters are plotted for the 255 events in Data Set #3.

## 2. DATA EXCHANGE FORMAT

This section describes the exchange format for Data Sets #2-3. These data were provided to *MIT Lincoln Laboratory* on exabyte tape in UNIX tar format, and these tapes are available for general distribution at the Center for Seismic Studies (CSS). Reports that include displays and information for each event were also provided to *MIT Lincoln Laboratory* and the CSS. For each event, these reports include a map showing station and event location, a listing of event origin and detection data, waveform displays, and plots of each detecting and 3-component beam (described below). All three data sets are also available in an Oracle database at the CSS in Version 3.0 format [Anderson *et al.*, 1990; Swanger *et al.*, 1991].

### 2.1 Parametric Data

The data sets include parametric data generated by the automated IMS processing, and all changes made by seismic analysts. The parametric data are stored in ASCII files, and the format of these files are described in detail in Appendix A of *Sereno and Patnaik* [1991]. Figures 4 and 5 show the directory structure for Data Sets #2-3 (directories are printed in bold-face type, and files are printed in italics). The top-level directory includes a sub-directory called **DB1** that has the waveform and parametric data for each event, and sub-directories for documentation and static data (e.g., data that are the same for all events).

*Documentation Directory.* The documentation directory for Data Set #1 includes a description of the data exchange format. The format for Data Sets #2-3 differ only slightly from the format for Data Set #1, and these differences are described in their documentation directories. The only significant difference between the format of Data Set #2 and Data Set #1 is the definition of the channel names used to identify the detecting beam. Events recorded prior to November 1990 used an integer called *chanid* to identify the detecting beam [Sereno and Patnaik, 1991]. After that, the detecting beam was identified by a character channel code. The documentation directory for Data Set #2 includes a file with the mapping between the new character channel code and the older *chanid*. Data Set #3 uses the character channel codes in the file names for the SAC beam files (Section 2.2). This difference is included in an updated version of the documentation for Data Set #3 in the *doc* directory.

*Static Data Directory.* The static data directory includes the short-period instrument response, individual array element locations and elevations, travel time curves for regional phases, and standard beam recipe files. Data Set #1 includes this data for the NORESS and ARCESS arrays in Norway, and Data Set #2 has updated beam recipe files to include a few beams that were not in Data Set #1. The *static* directory for Data Set #3 consists of the beam recipe file, the individual array element locations, and the short-period instrument response for GERESS. The travel time tables used in this version of the IMS are the same as the ones that are used for Fennoscandia. We are currently developing new tables for paths to GERESS under separate DARPA funding [Sereno *et al.*, 1992].

## DIRECTORY STRUCTURE / DATA SET #2

### Top-Level Directory

**DB1 doc static**

### Database Directory

#### **DB1**

<b>README</b>	<b>ExpSys</b>	<b>Analyst</b>	<b>EVID</b>	<b>SAC</b>
<i>ExpSys_Analyst.db1</i>	<i>IEB.orig</i>	<i>FEB.orig</i>	<i>README</i>	<i>oridXXXXXX</i>
	<i>IEB.det</i>	<i>FEB.det</i>	<i>EVID.db1</i>	<i>oridXXXXXX</i>
	<i>IEB.apma</i>	<i>FEB.distaz</i>	<i>Helsinki.orig</i>	<i>oridXXXXXX</i>
	<i>IEB.sbsnr</i>		<i>Helsinkiibul.db1</i>	<i>etc</i>
			<i>MSMP.db1</i>	
			<i>CEPPKS.db1</i>	
			<i>SPVAR.db1</i>	

### SAC Waveform Directory

#### **SAC/oridXXXXXX**

<i>ARA0.se.sac</i>	<i>ARC4.se.sac</i>	<i>ARD9.sz.sac</i>	<i>NRC3.sz.sac</i>	<i>NRD8.sz.sac</i>
<i>ARA0.sn.sac</i>	<i>ARC4.sn.sac</i>	<i>NRA0.se.sac</i>	<i>NRC4.se.sac</i>	<i>NRD9.sz.sac</i>
<i>ARA0.sz.sac</i>	<i>ARC4.sz.sac</i>	<i>NRA0.sn.sac</i>	<i>NRC4.sn.sac</i>	<i>ARC.cbxxx.sac</i>
<i>ARA1.sz.sac</i>	<i>ARC5.sz.sac</i>	<i>NRA0.sz.sac</i>	<i>NRC4.sz.sac</i>	<i>ARC.cbxxx.sac</i>
<i>ARA2.sz.sac</i>	<i>ARC6.sz.sac</i>	<i>NRA1.sz.sac</i>	<i>NRC5.sz.sac</i>	<i>ARC.cbxxx.sac</i>
<i>ARA3.sz.sac</i>	<i>ARC7.se.sac</i>	<i>NRA2.sz.sac</i>	<i>NRC6.sz.sac</i>	<i>ARC.cbxxx.sac</i>
<i>ARB1.sz.sac</i>	<i>ARC7.sn.sac</i>	<i>NRA3.sz.sac</i>	<i>NRC7.se.sac</i>	<i>ARC.cbxxx.sac</i>
<i>ARB2.sz.sac</i>	<i>ARC7.sz.sac</i>	<i>NRB1.sz.sac</i>	<i>NRC7.sn.sac</i>	<i>ARC.cbxxx.sac</i>
<i>ARB3.sz.sac</i>	<i>ARD1.sz.sac</i>	<i>NRB2.sz.sac</i>	<i>NRC7.sz.sac</i>	<i>ARC.cbxxx.sac</i>
<i>ARB4.sz.sac</i>	<i>ARD2.sz.sac</i>	<i>NRB3.sz.sac</i>	<i>NRD1.sz.sac</i>	<i>NOR.cbxxx.sac</i>
<i>ARB5.sz.sac</i>	<i>ARD3.sz.sac</i>	<i>NRB4.sz.sac</i>	<i>NRD2.sz.sac</i>	<i>NOR.cbxxx.sac</i>
<i>ARC1.sz.sac</i>	<i>ARD4.sz.sac</i>	<i>NRB5.sz.sac</i>	<i>NRD3.sz.sac</i>	<i>NOR.cbxxx.sac</i>
<i>ARC2.se.sac</i>	<i>ARD5.sz.sac</i>	<i>NRC1.sz.sac</i>	<i>NRD4.sz.sac</i>	<i>NOR.cbxxx.sac</i>
<i>ARC2.sn.sac</i>	<i>ARD6.sz.sac</i>	<i>NRC2.se.sac</i>	<i>NRD5.sz.sac</i>	<i>NOR.cbxxx.sac</i>
<i>ARC2.sz.sac</i>	<i>ARD7.sz.sac</i>	<i>NRC2.sn.sac</i>	<i>NRD6.sz.sac</i>	
<i>ARC3.sz.sac</i>	<i>ARD8.sz.sac</i>	<i>NRC2.sz.sac</i>	<i>NRD7.sz.sac</i>	

Figure 4. The directory structure is described for Data Set #2.

## DIRECTORY STRUCTURE / DATA SET #3

### Top-Level Directory

DB1 doc static

### Database Directory

DB1

<i>ExpSys_Analyst.db1</i>	<b>ExpSys</b>	<b>Analyst</b>	<b>EVID</b>	<b>SAC</b>
	<i>IEB.orig</i>	<i>FEB.orig</i>	<i>README</i>	<i>oridXXXXXX</i>
	<i>IEB.det</i>	<i>FEB.det</i>	<i>MSMP.db1</i>	<i>oridXXXXXX</i>
	<i>IEB.apma</i>	<i>FEB.distaz</i>	<i>CEPPKS.db1</i>	<i>oridXXXXXX</i>
	<i>IEB.sbsnr</i>		<i>SPVAR.db1</i>	<i>etc</i>

### SAC Waveform Directory

SAC/oridXXXXXX

<i>GEA0.sz.sac</i>	<i>GEC6.sz.sac</i>	<i>GED9.sz.sac</i>
<i>GEA1.sz.sac</i>	<i>GEC7.sz.sac</i>	<i>GER.CHAN.sac</i>
<i>GEA2.se.sac</i>	<i>GED1.se.sac</i>	<i>GER.CHAN.sac</i>
<i>GEA2.sn.sac</i>	<i>GED1.sn.sac</i>	<i>GER.CHAN.sac</i>
<i>GEA2.sz.sac</i>	<i>GED1.sz.sac</i>	<i>GER.CHAN.sac</i>
<i>GEA3.sz.sac</i>	<i>GED2.sz.sac</i>	<i>GER.CHAN.sac</i>
<i>GEB1.sz.sac</i>	<i>GED3.sz.sac</i>	<i>GER.CHAN.sac</i>
<i>GEB2.sz.sac</i>	<i>GED4.se.sac</i>	<i>GER.CHAN.sac</i>
<i>GEB3.sz.sac</i>	<i>GED4.sn.sac</i>	<i>GER.CHAN.sac</i>
<i>GEB4.sz.sac</i>	<i>GED4.sz.sac</i>	<i>GER.CHAN.sac</i>
<i>GEB5.sz.sac</i>	<i>GED5.sz.sac</i>	<i>GER.CHAN.sac</i>
<i>GEC1.sz.sac</i>	<i>GED6.sz.sac</i>	<i>GER.CHAN.sac</i>
<i>GEC2.sz.sac</i>	<i>GED7.se.sac</i>	<i>GER.CHAN.sac</i>
<i>GEC3.sz.sac</i>	<i>GED7.sn.sac</i>	
<i>GEC4.sz.sac</i>	<i>GED7.sz.sac</i>	
<i>GEC5.sz.sac</i>	<i>GED8.sz.sac</i>	

Figure 5. The directory structure is described for Data Set #3.

**Database Directory.** The general directory structure for the parametric data is shown in the middle of Figures 4 and 5. The database directory (DB1) includes four sub-directories, and one or two ASCII files. The *README* file gives information for a few specific events, and details regarding minor changes from Data Set #1. The *ExpSys\_Analyst.db1* file summarizes corrections made by the analyst to the results of the automated processing. For example, it includes the distance between the locations determined by the expert system and the analyst, the difference in their origin times, and the number of phases that were added or retimed by the analyst [see Appendix A; Sereno and Patnaik, 1991].

The *ExpSys* directory contains the results of the automated IMS processing (these data are not included in the Oracle database version at CSS). This includes the four files in Figures 4 and 5 with the prefix *IEB*, which stands for initial event bulletin. *IEB.orig* lists event origin data (latitude, longitude, depth, and origin time). *IEB.det* lists detection and association data such as phase identification, arrival time, azimuth and phase velocity estimated from  $f-k$  processing, amplitude, signal-to-noise ratio, and frequency. *IEB.apma* lists results from automated particle motion analysis [Jurkevics, 1988]. This includes estimates of rectilinearity, planarity, long- and short-axis incidence angles, and horizontal-to-vertical power ratio for each detection. *IEB.sbsnr* gives signal and noise amplitudes measured on a standard set of six beams.

The *Analyst* directory contains parametric data after review by a seismic analyst. The files *FEB.orig* and *FEB.det* are similar to the corresponding files under *ExpSys*, but they include changes made by the analyst (the *FEB* prefix stands for final event bulletin). *FEB.distaz* lists the epicentral distance and station-to-event azimuth for each event in *FEB.orig*. The *Analyst* directory does not include particle motion or standard-beam amplitude files since these attributes are not recalculated after analyst review.

The *EVID* directory in Data Set #2 contains the identification (e.g., earthquake or explosion) of each event in *FEB.orig*. This identification is based primarily on a regional seismic bulletin produced by the University of Helsinki. The *README* file gives information for a few specific events. *EVID.db1* gives the identification of each event, *Helsinki.orig* gives the origin information from the Helsinki Bulletin, and *Helsinki.bul.db1* gives the complete unedited listing from the Helsinki Bulletin. The events in Data Set #3 were not identified because independent bulletins were not available. The other three files in the *EVID* directory contain data that are relevant for event identification. *MSMP.db1* lists regional  $P$ -wave magnitudes computed from the amplitude of  $P_n$  and  $P_g$ , and regional  $S$ -wave magnitudes computed from the amplitude of  $S_n$  and  $L_g$  (note that these are computed using distance corrections that were developed for Fennoscandia, and probably are not accurate for paths to GERESS; Sereno et al., 1992). The difference between these magnitudes is a possible discriminant (high values of  $m_s - m_p$  indicate the event is an earthquake, low values are inconclusive). The two files called *CEPPKS.db1* and *SPVAR.db1* give the results of cepstral analysis, and are useful for identifying ripple-fired mining explosions

[Baumgardt and Ziegler, 1987]. These data are described in Appendix A of *Sereno and Patnaik* [1991].

## 2.2 Waveform Data

Data Set #2 includes all available short-period waveform data recorded at NORESS and ARCESS when the same event is detected by both arrays, and Data Set #3 includes short-period waveform data recorded at GERESS (the Oracle database at CSS has pointers to data recorded by all available IMS stations for each data set including the FINESA array in Finland and a single 3-component station in Poland called KSP). These data are stored under the SAC sub-directory shown in Figures 4 and 5. There is a separate directory for each event. These directories are labeled as *oridXXXXXX*, where *XXXXXX* refers to the unique integer origin identification in *FEB.orig*. There are separate SAC data files for each short-period channel in the arrays (33 channels/array). These waveform data files are 7-minute segments that start 30 seconds before the theoretical  $P_n$  arrival time (based on the final event origin). The files are named as *station.channel.sac* where *station* is the station code for each array element (e.g., *NRA0*, *NRA1*, *NRA2*, etc), and *channel* is the channel code (*sz* is short-period vertical, *se* is short-period east, and *sn* is short-period north).

In addition to the single-channel waveforms, each directory includes several coherent beams in SAC format. Coherent beams are formed by steering the single-channel waveforms using a specified velocity and azimuth, stacking, and filtering over a specified frequency band. These files are named as *array.cbxxx.sac* in Data Sets #1-2, where *array* is either *NOR* for NORESS or *ARC* for ARCESS, *cb* stands for coherent beam, and *xxx* is the *chanid*. The beam files are named as *array.CHAN.sac* for Data Set #3, where *CHAN* is the character channel code. The detecting beam is defined as the standard beam with the highest *snr*. This beam is included for each detection that is associated with a final origin. However, if the detecting beam is incoherent, then it is replaced by a coherent beam that uses the same beamforming parameters.

Coherent beams that are calculated using data from the four 3-component elements of each array are also included in each data set. Three of these beams are calculated for each detection that is associated with a final event origin (one for each component; vertical, north-south, and east-west). These 3-component beams use the same beamforming parameters as the detecting beam, except that the array subset only includes the four 3-component elements. For Data Sets #1-2, the number assigned to the beam formed from the vertical components is 200 plus the *chanid* of the detecting beam. Similarly, the numbers assigned to the beams formed from the north-south and east-west components are 400 and 600 plus the *chanid* of the detecting beam, respectively. For Data Set #3, the 3-component beams are identified as *CHANz* (vertical channels), *CHANew* (east-west channels), and *CHANns* (north-south channels), where *CHAN* is the character channel code of the detecting beam.

## 2.3 Documentation

The documentation for Data Set #1 includes a high-level description of the entire data set [Sereno and Patnaik, 1991], a report on the identification of the events [Sereno, 1991], and a 7-volume report that includes (for each event) a map showing station and event locations, a listing of event origin and detection data, waveform displays, and plots of each detecting and 3-component beam [Patnaik and Sereno, 1991a]. This section gives an example of the displays and information that are included in this 7-volume report. This example is for a mining explosion in western USSR. Figure 6 is a map showing the locations of NORESS and ARCESS, and the event epicenter. Table 2 lists detection data before analyst review (e.g., the results of the automated IMS processing), and Table 3 lists detection data after analyst review. Figure 7 shows the *display beams* for ARCESS (these beams are displayed to the analyst for review of the automated processing). Figure 8 plots the *detecting beam* for  $P_n$  at ARCESS, and the 3-component beams (vertical, north-south, and east-west). Similarly, Figure 9 plots the beams for  $S_n$  at ARCESS. Beams are not included for  $L_g$  since this phase was added by the analyst (e.g., it was not detected by the automated processing). Figure 10 shows the *display beams* for NORESS, and Figure 11 shows the *detecting* and 3-component beams for  $P_n$  at NORESS. Beams were not computed for  $S_n$  and  $L_g$  phases at NORESS because they were added by the analyst.

Similar documentation was developed for Data Sets #2-3. The high-level descriptions of these two data sets are given in Sections 3 and 4 of this final report, respectively. The database report for Data Set #2 is one volume, and it includes the event identification information from the Helsinki Bulletin [Mortell *et al.*, 1991]. The database report for Data Set #3 is 5-volumes [Mortell *et al.*, 1992]. There is no documentation on the identification of these events since independent bulletins were not available.



ORID=192093 90/02/14 10 16 5.013 LAT 61.70 LON 31.37 ML 2.2

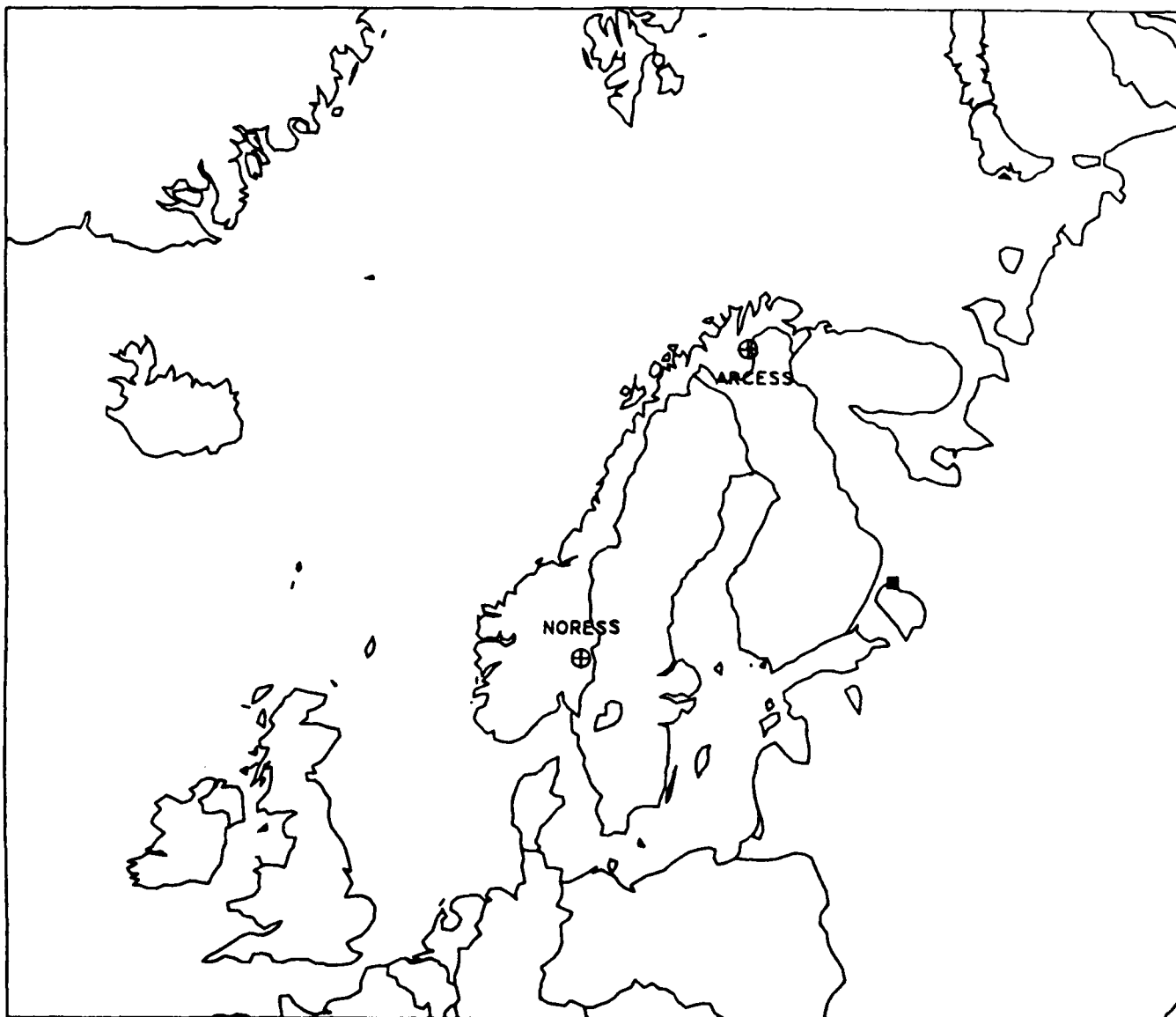


**Figure 6.** This map shows the NORESS and ARCESS station locations, and the epicenter of an event in Data Set #1 (after analyst review).

ECORID	ARID STA	CHAN	CHANID	YR	MM	DD	HR	MM	SS	MS	IPHASE	PHASE	AMP	FREQ	SNR	VELO	AZIMUTH Q
195318	129358 ARAO	zb	292	90	02	14	10:18:05.332	Pg			Pg		163.9	6.7	8.58	7.7	154.9 1
-1	129359 ARAO	zb	272	90	02	14	10:18:09.582	Pz					61.5	3.3	4.23	7.5	165.11 3
195318	129363 MRAO	zb	275	90	02	14	10:18:24.384	Pg			Pg		155.8	4.3	10.76	10.9	87.06 1
195319	129360 ARAO	zb	294	90	02	14	10:19:33.982	Lg			Lg		107.5	6.7	4.74	4.6	164.96 2
-1	129364 MRAO	zb	296	90	02	14	10:19:35.859	Sx					99.5	10.0	5.24	3.7	251.01 3
-1	129365 ARAO	zb	310	90	02	14	10:20:13.857	Pz					954.5	1.2	2.55	6.3	34.05 3
-1	129366 ARAO	zb	301	90	02	14	10:22:01.632	Sx					49.2	6.7	4.88	3.2	181.13 3
-1	129367 ARAO	zb	225	90	02	14	10:23:08.107	Sx					131.0	4.5	2.46	3.0	176.52 1

Table 2. This table gives parametric detection and phase association data before analyst review for the event plotted in Figure 6. Two phases were associated with this event by the expert system (arid 129358 is labeled Pg at ARCESS, and arid 129363 is labeled Pg at NORESS).

FORID	ARID STA	CHAN	CHANID	YR	MM	DD	HR	MM	SS	MS	IPHASE	PHASE	AMP	FREQ	SNR	VELO	AZIMUTH Q
192093	129358 ARAO	zb	292	90	02	14	10:18:02.514	Pn			Pn		163.9	6.7	8.58	7.7	154.9 1
-1	129359 ARAO	zb	272	90	02	14	10:18:09.582	Pz					61.5	3.3	4.23	7.5	165.11 3
192093	129363 NRAO	zb	275	90	02	14	10:18:23.871	Pn			Pn		155.8	4.3	10.76	10.9	87.06 1
192093	129360 ARAO	zb	294	90	02	14	10:19:33.982	Sn			Sn		107.5	6.7	4.74	4.6	164.96 2
-1	129364 NRAO	zb	296	90	02	14	10:19:35.859	Sz					99.5	10.0	5.24	3.7	251.01 3
192093	130563 NRAO	-	-1	90	02	14	10:20:04.312	Sn			Sn		-1.0	-1.0	-1	-1.0	-1
-1	129365 ARAO	zb	310	90	02	14	10:20:13.857	Pz					954.5	1.2	2.55	6.3	34.05 3
192093	130562 ARAO	-	-1	90	02	14	10:20:26.051	Lg			Lg		-1.0	-1.0	-1	-1.0	-1
192093	130564 NRAO	-	-1	90	02	14	10:21:05.305	Lg			Lg		-1.0	-1.0	-1	-1.0	-1
-1	129366 ARAO	zb	301	90	02	14	10:22:01.632	Sz					49.2	6.7	4.88	3.2	181.13 3
-1	129367 ARAO	zb	225	90	02	14	10:23:08.107	Sz					131.0	4.5	2.46	3.0	176.52 1

Table 3. This table gives parametric detection and phase association data after analyst review for the event plotted in Figure 6. The analyst made the following changes to the results of the expert system (see Table 2):

- (1) Rename *Pg* at ARCESS to *Pn*, and retime.
- (2) Rename *Lg* at ARCESS to *Sn*, and associate it with this event.
- (3) Add an *Lg* phase at ARCESS (signal processing is not recalled for phases that are added by analyst, so most of the detection fields are assigned N/A values).
- (4) Rename *Pg* at NORESS to *Pn*, and retime.
- (5) Add an *Sn* phase at NORESS.
- (6) Add an *Lg* phase at NORESS.

The location determined by the expert system is about 250 km from the by location determined by the analyst for this event.

# ORID = 192093 ARCESS

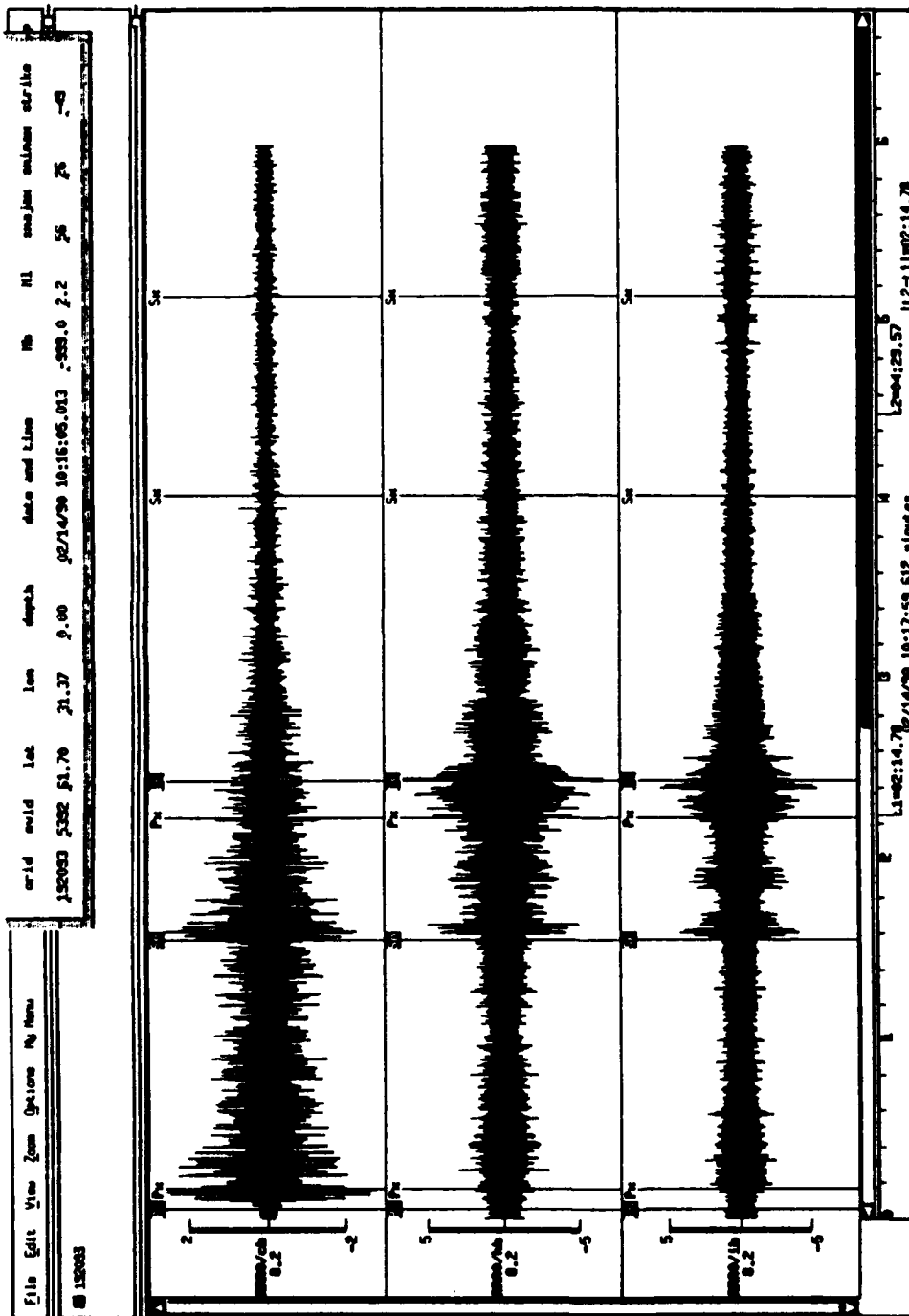


Figure 7. ARCESS display beams are plotted for the event in Figure 6. Associated  $P_n$ ,  $S_n$ , and  $L_g$  phases are highlighted. The top beam is a 4-8 Hz coherent beam (steered to the event using a velocity of 8 km/s), and it is intended to emphasize  $P_n$ . The middle beam is a 2-4 Hz incoherent beam formed from horizontal components intended to emphasize  $S_n$ . The lowest beam is also a 2-4 Hz incoherent beam, but it is formed from vertical components. It is intended to emphasize  $L_g$ .

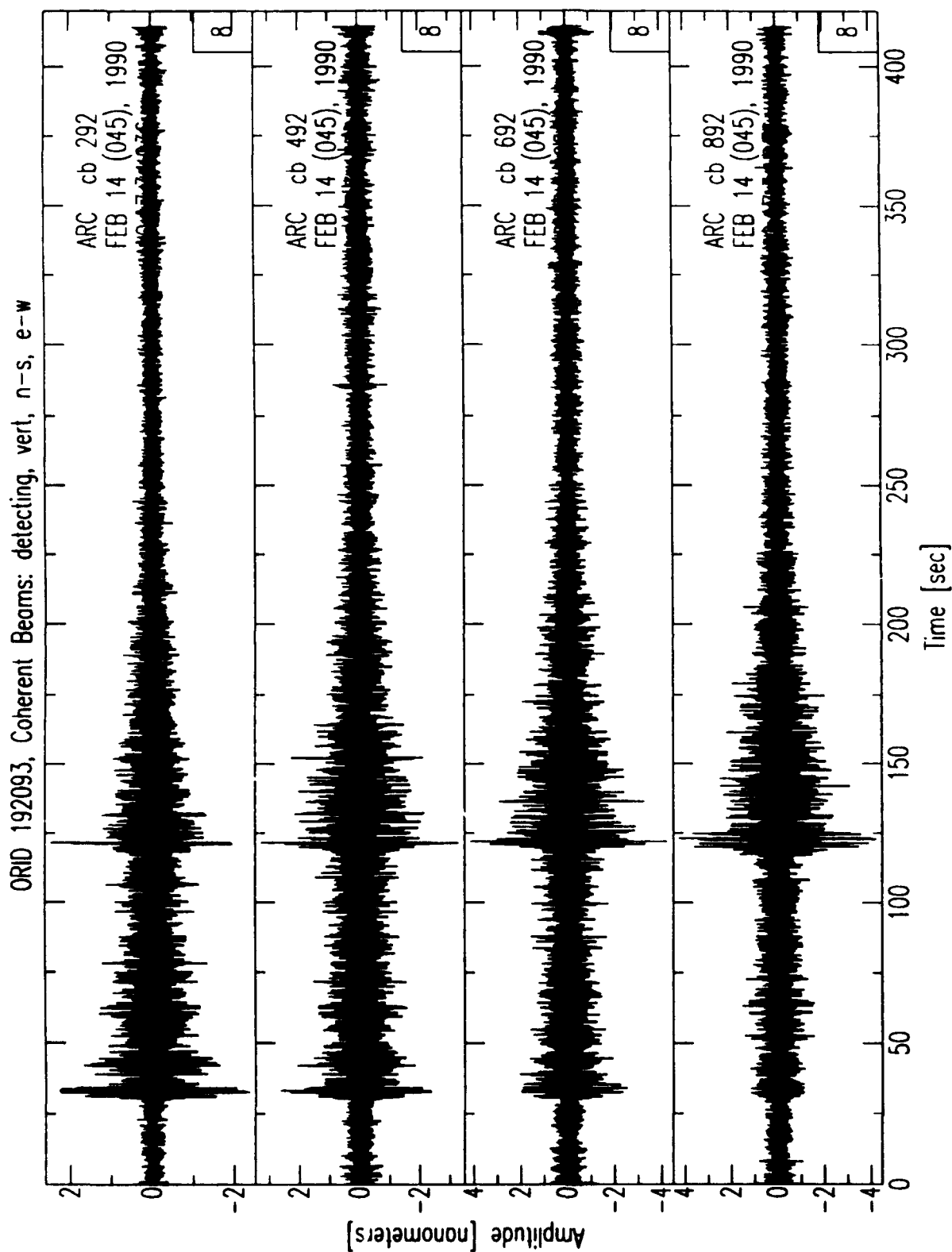


Figure 8. This figure shows the *detecting beam* for  $P_n$  at ARCESS in the top panel, and the beams formed from the 3-component array elements in the bottom panels (vertical, north-south, east-west).

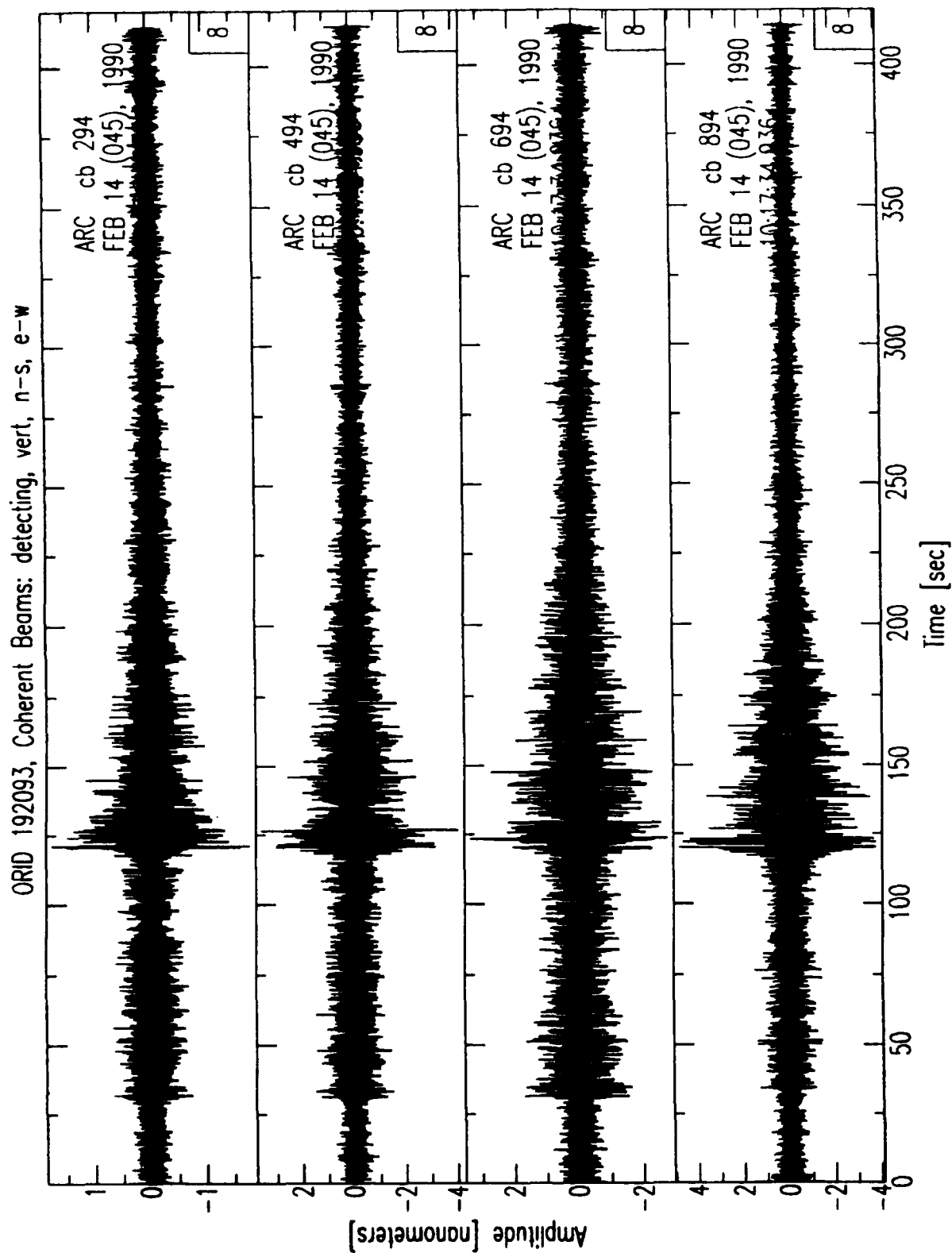
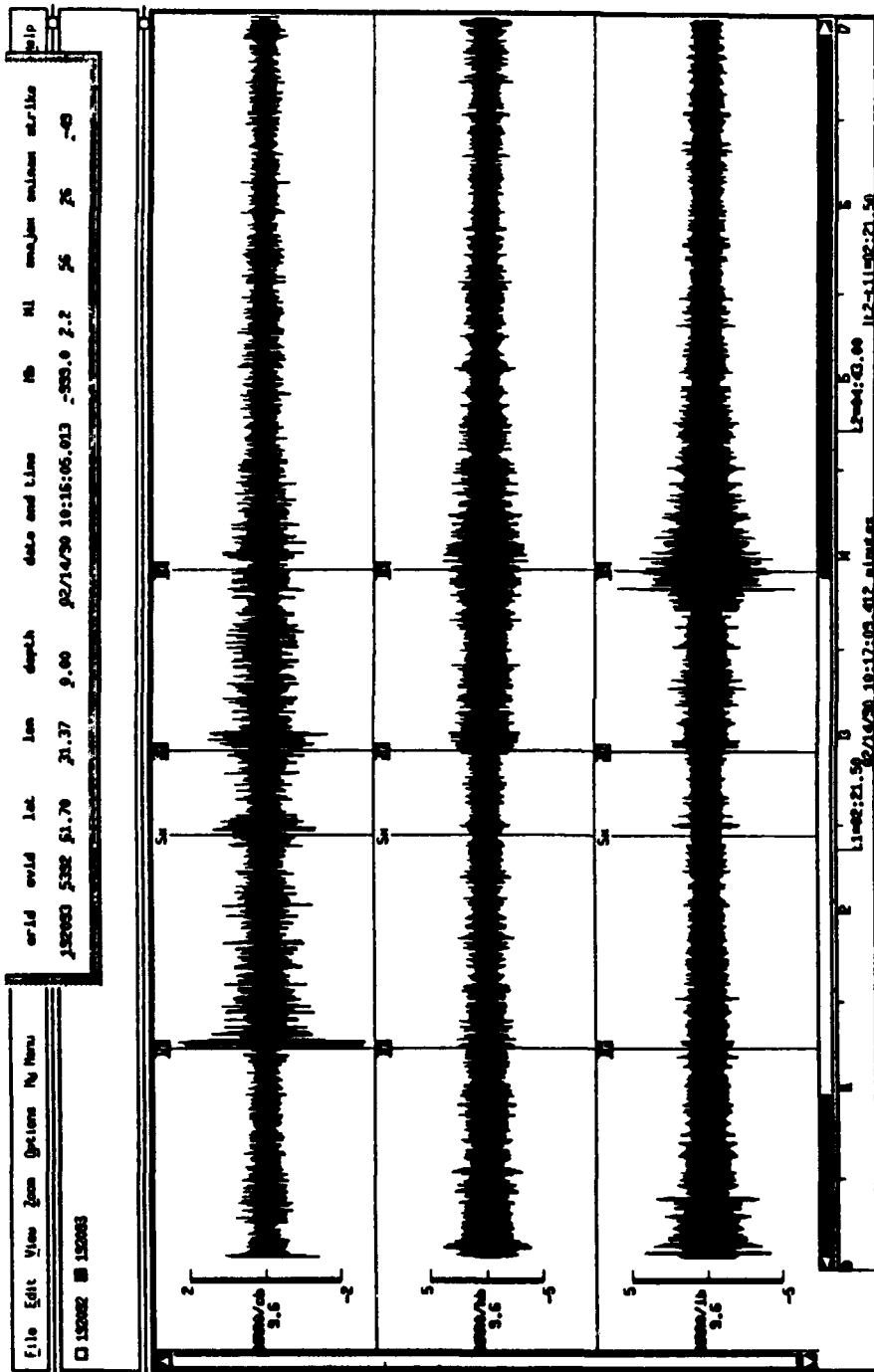


Figure 9. This figure shows the *detecting beam* for  $S_n$  at ARCESS in the top panel, and the beams formed from the 3-component array elements in the bottom panels (vertical, north-south, east-west).

# NORESS



**Figure 10.** NORESS *display beams* are plotted for the event in Figure 6. Associated  $Pn$ ,  $Sn$ , and  $Lg$  phases are highlighted (see caption for Figure 7).

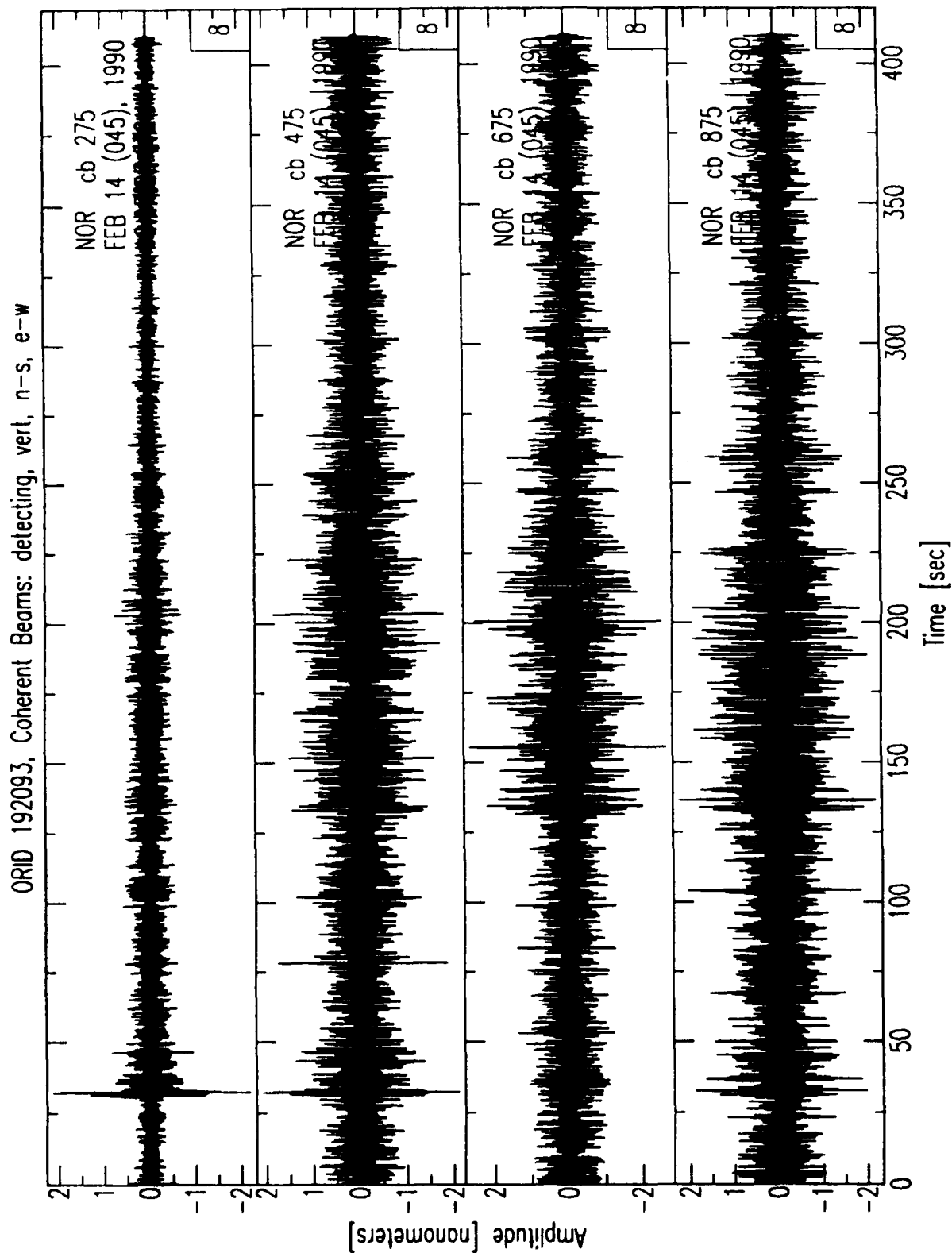


Figure 11. This figure shows the *detecting beam* for  $P_n$  at NORESS in the top panel, and the beams formed from the 3-component array elements in the bottom panels (vertical, north-south, east-west).



### 3. DATA SET #2

Data Set #2 includes single-channel waveform data, beams, and parametric data from 33 presumed earthquakes recorded at regional distances from the NORESS and ARCESS arrays in Norway. The purpose for assembling this data set is to use it to test the response of neural networks developed and trained with Data Set #1 to *novelty* signals (e.g., signals recorded at the same stations as the events in Data Set #1, but from different source types). Since over 90% of the events in Data Set #1 were explosions, earthquakes were selected for Data Set #2.

#### 3.1 NORESS/ARCESS Arrays

The NORESS and ARCESS arrays in Norway include 25 short-period instruments in four concentric rings with a maximum diameter of 3 km (Figure 12). The array configuration and sampling rate were designed to enhance the detection of regional signals [Mykkeltveit, *et al.*, 1983; Mykkeltveit and Ringdal, 1988]. The radius of the inner ring (called the A-ring) is about 150 m. The radii of the B-, C-, and D-rings are 300 m, 700 m, and 1500 m, respectively. The number of sensors on the A-, B-, C-, and D-rings are 3, 5, 7, and 9, respectively. The individual station locations for the NORESS and ARCESS arrays are given in Table 4 (locations are given relative to the reference locations listed at the bottom of this table). Four of the 25 array elements are equipped with 3-component seismometers. These are the center element (A0), and three sensors on the C-ring (C2, C4, and C7). The rest of the array elements only have vertical-component seismometers. Table 5 lists the standard beams used for IMS processing of NORESS and ARCESS data. The first column is the *chanid* (or beam number) that is used to identify the detecting beam.

The NORESS and ARCESS data are continuously recorded, and the short-period data are digitized at a rate of 40 samples/s. Figure 13 shows the short-period instrument response. This response applies to all elements of the NORESS and ARCESS arrays. The instrument response is approximately flat to velocity between 2 and 8 Hz. The digitization gain is  $10^5$  digital counts/volt.

#### 3.2 Regional Events

This section describes the events in Data Set #2. It gives the event locations, magnitudes, and epicentral distances from NORESS and ARCESS.

##### 3.2.1 Selection Criteria

All of the events in Data Set #2 are presumed to be earthquakes recorded at regional distances from NORESS and/or ARCESS. Of the 33 events, 27 were reported as presumed earthquakes in the regional bulletin produced by the University of Helsinki. Four others were reported as earthquakes by the University of Bergen, and these are included in the reports by Ahjos *et al.* [1990] or Uski and Pelkonen [1991]. The

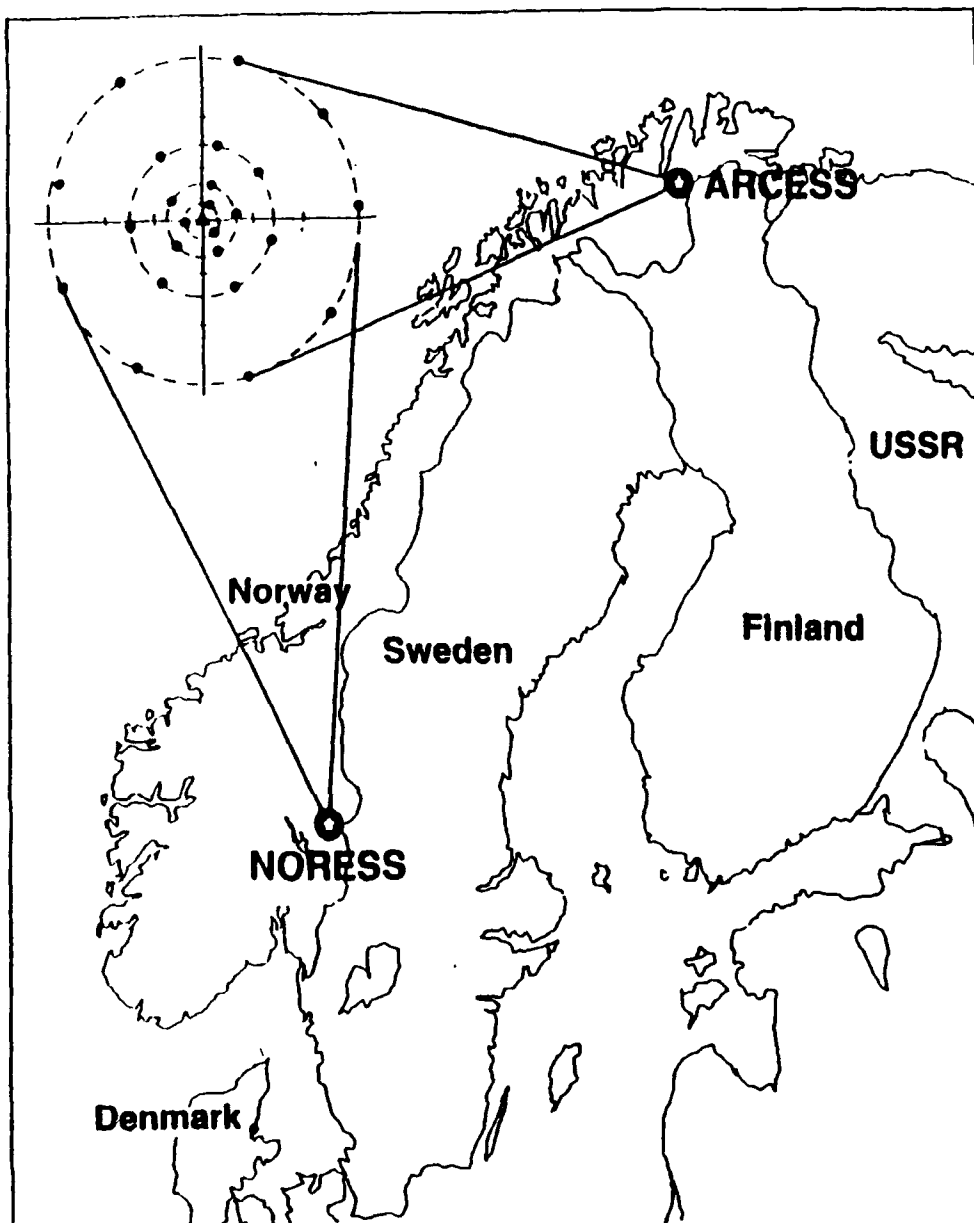


**Figure 12.** The location and array geometry are plotted for the NORESS and ARCESS arrays (Figure provided by Frode Ringdal, NORSAR).

**Table 4. Station Locations (NORESS and ARCESS)**

NORESS				ARCESS			
Station	Elevation (km)	dnorth <sup>1</sup> (km)	deast <sup>1</sup> (km)	Station	Elevation (km)	dnorth <sup>2</sup> (km)	deast <sup>2</sup> (km)
NRA0	.3020	.0030	.0040	ARA0	.4030	.0010	-.0003
NRA1	.2910	.1460	.0490	ARA1	.4110	.1600	.0530
NRA2	.3110	-.1030	.1080	ARA2	.3920	-.1210	.0770
NRA3	.2960	-.0300	-.1430	ARA3	.4020	-.0300	-.1490
NRB1	.2990	.3210	.0700	ARB1	.4140	.3360	.0820
NRB2	.3150	.0300	.3340	ARB2	.3970	.0970	.2940
NRB3	.3140	-.2980	.1430	ARB3	.3760	-.2690	.1890
NRB4	.2990	-.2170	-.2280	ARB4	.3780	-.2250	-.2310
NRB5	.2890	.1630	-.2720	ARB5	.4050	.1580	-.2830
NRC1	.2990	.6870	.1090	ARC1	.3810	.6900	.0810
NRC2	.3390	.3410	.6030	ARC2	.3950	.3863	.6657
NRC3	.3520	-.2380	.6470	ARC3	.3760	-.2140	.6730
NRC4	.3110	-.6570	.2080	ARC4	.3770	-.6167	.2287
NRC5	.2990	-.5690	-.3960	ARC5	.3740	-.5380	-.2960
NRC6	.3030	-.0480	-.6870	ARC6	.3950	-.0810	-.6830
NRC7	.2750	.5480	-.4470	ARC7	.3620	.5300	-.4700
NRD1	.3050	1.4800	.1920	ARD1	.3950	1.4910	.1350
NRD2	.3720	1.0150	1.0980	ARD2	.3660	1.1430	.9720
NRD3	.4530	.0760	1.4930	ARD3	.3310	.1880	1.6510
NRD4	.3790	-.9010	1.1890	ARD4	.3710	-.8580	1.1810
NRD5	.3480	-1.4510	.3350	ARD5	.3510	-1.4940	.2330
NRD6	.3520	-1.3260	-.6810	ARD6	.4130	-1.3470	-.6130
NRD7	.3370	-.5660	-1.3680	ARD7	.4130	-.6070	-1.3600
NRD8	.3010	.4140	-1.3360	ARD8	.3680	.3920	-1.4430
NRD9	.2780	1.2570	-.8020	ARD9	.3590	1.1730	-.7780

1. Relative to the reference location: 60.735°N, 11.541°E.

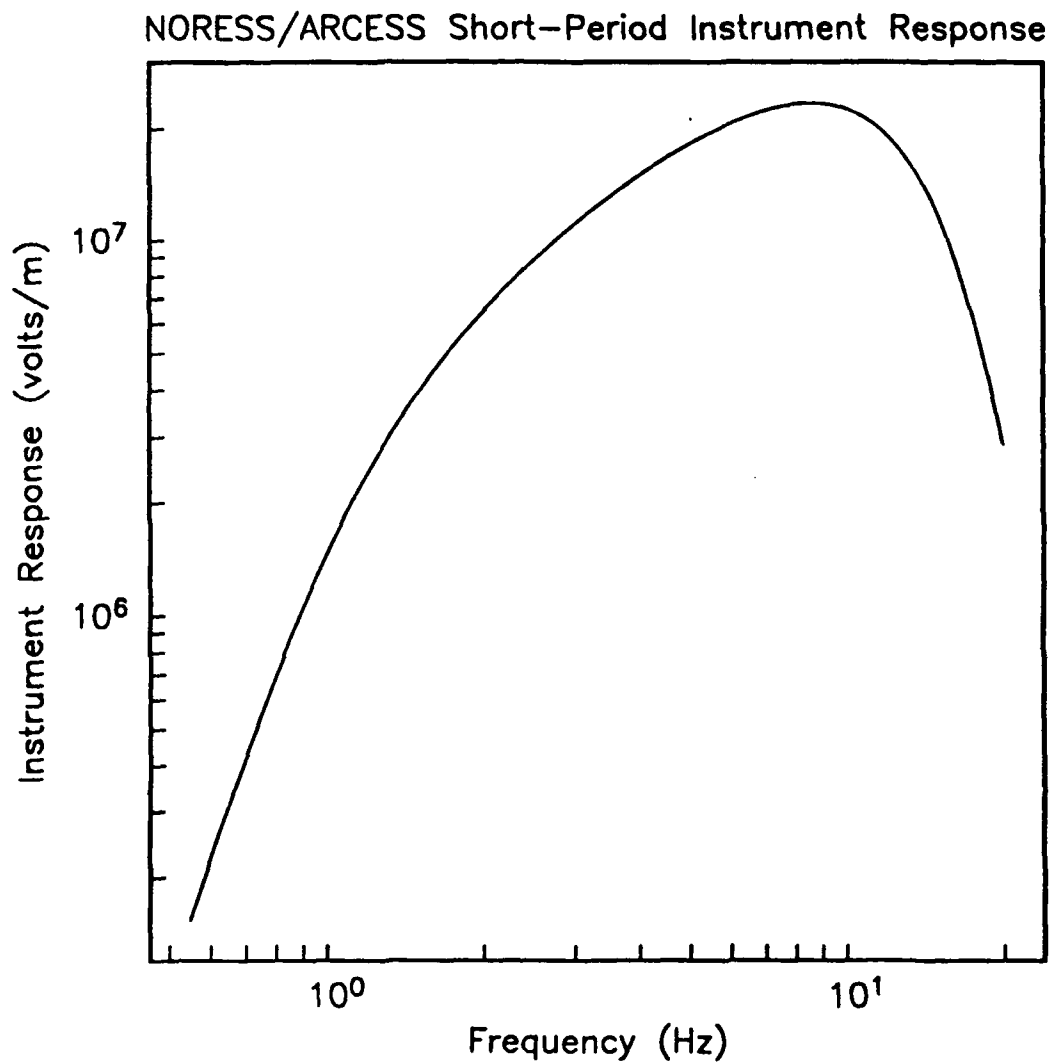
2. Relative to the reference location: 69.535°N, 25.506°E.

Table 5. IMS Standard Beams for NORESS and ARCESS

Beam	Velocity (km/s)	Filter (Hz)	Filter Order	Azimuth (degrees)	Beam Type <sup>1</sup>	Ring Subset			
201	∞	1.0-3.0	3	0.0	C	A0		C	D
202	∞	1.5-3.5	3	0.0	C	A0		C	D
207	∞	8.0-16.0	3	0.0	C	A0	A	B	
220	∞	1.5-2.5	2	0.0	I	A0		C	
221	∞	2.0-4.0	3	0.0	H	A0		C	
223	∞	5.0-10.0	3	0.0	H	A0		C	
225	∞	3.5-5.5	3	0.0	I	A0		C	
226	∞	3.5-5.5	3	0.0	H	A0		C	
228	∞	8.0-16.0	3	0.0	H	A0		C	
248	11.0	1.5-3.5	3	30.0	C	A0		C	D
249	11.0	1.5-3.5	3	90.0	C	A0		C	D
250	11.0	1.5-3.5	3	150.0	C	A0		C	D
251	11.0	1.5-3.5	3	210.0	C	A0		C	D
252	11.0	1.5-3.5	3	270.0	C	A0		C	D
253	11.0	1.5-3.5	3	330.0	C	A0		C	D
254	∞	2.0-4.0	3	0.0	C	A0		C	D
255	10.1	2.0-4.0	3	30.0	C	A0		C	D
256	10.1	2.0-4.0	3	90.0	C	A0		C	D
257	10.1	2.0-4.0	3	150.0	C	A0		C	D
258	10.1	2.0-4.0	3	210.0	C	A0		C	D
259	10.1	2.0-4.0	3	270.0	C	A0		C	D
260	10.1	2.0-4.0	3	330.0	C	A0		C	D
261	∞	2.5-4.5	3	0.0	C	A0	B	C	D
262	8.8	2.5-4.5	3	30.0	C	A0	B	C	D
263	8.8	2.5-4.5	3	90.0	C	A0	B	C	D
264	8.8	2.5-4.5	3	150.0	C	A0	B	C	D
265	8.8	2.5-4.5	3	210.0	C	A0	B	C	D
266	8.8	2.5-4.5	3	270.0	C	A0	B	C	D
267	8.8	2.5-4.5	3	330.0	C	A0	B	C	D
268	∞	3.0-5.0	3	0.0	C	A0	B	C	D
269	10.5	3.0-5.0	3	30.0	C	A0	B	C	D
270	10.5	3.0-5.0	3	90.0	C	A0	B	C	D
271	10.5	3.0-5.0	3	150.0	C	A0	B	C	D
272	10.5	3.0-5.0	3	210.0	C	A0	B	C	D
273	10.5	3.0-5.0	3	270.0	C	A0	B	C	D
274	10.5	3.0-5.0	3	330.0	C	A0	B	C	D
275	∞	3.5-5.5	3	0.0	C	A0	B	C	
276	11.1	3.5-5.5	3	30.0	C	A0	B	C	
277	11.1	3.5-5.5	3	90.0	C	A0	B	C	
278	11.1	3.5-5.5	3	150.0	C	A0	B	C	
279	11.1	3.5-5.5	3	210.0	C	A0	B	C	
280	11.1	3.5-5.5	3	270.0	C	A0	B	C	
281	11.1	3.5-5.5	3	330.0	C	A0	B	C	
282	∞	4.0-8.0	3	0.0	C	A0	B	C	
283	9.4	4.0-8.0	3	30.0	C	A0	B	C	
284	9.4	4.0-8.0	3	90.0	C	A0	B	C	
285	9.4	4.0-8.0	3	150.0	C	A0	B	C	
286	9.4	4.0-8.0	3	210.0	C	A0	B	C	
287	9.4	4.0-8.0	3	270.0	C	A0	B	C	
288	9.4	4.0-8.0	3	330.0	C	A0	B	C	

Beam	Velocity (km/s)	Filter (Hz)	Filter Order	Azimuth (degrees)	Beam Type <sup>1</sup>	Ring Subset			
289	∞	5.0-10.0	3	0.0	C	A0	B	C	
290	10.4	5.0-10.0	3	30.0	C	A0	B	C	
291	10.4	5.0-10.0	3	90.0	C	A0	B	C	
292	10.4	5.0-10.0	3	150.0	C	A0	B	C	
293	10.4	5.0-10.0	3	210.0	C	A0	B	C	
294	10.4	5.0-10.0	3	270.0	C	A0	B	C	
295	10.4	5.0-10.0	3	330.0	C	A0	B	C	
296	9.9	8.0-16.0	3	30.0	C	A0	A	B	
297	9.9	8.0-16.0	3	90.0	C	A0	A	B	
298	9.9	8.0-16.0	3	150.0	C	A0	A	B	
299	9.9	8.0-16.0	3	210.0	C	A0	A	B	
300	9.9	8.0-16.0	3	270.0	C	A0	A	B	
301	9.9	8.0-16.0	3	330.0	C	A0	A	B	
302	15.9	1.5-3.5	3	80.0	C	A0			C D
303	15.9	2.0-4.0	3	80.0	C	A0			C D
304	15.9	2.5-4.5	3	80.0	C	A0	B	C	D
305	15.9	3.0-5.0	3	80.0	C	A0	B	C	D
306	10.0	1.5-3.5	3	30.0	C	A0			C D
307	10.0	2.0-4.0	3	30.0	C	A0			C D
308	10.0	2.5-4.5	3	30.0	C	A0	B	C	D
309	10.0	3.0-5.0	3	30.0	C	A0	B	C	D
310	∞	1.0-2.0	2	0.0	I	A0			C
312	∞	2.0-4.0	3	0.0	I	A0			C
313	∞	2.0-3.0	2	0.0	I	A0			C
314	∞	0.5-1.5	3	0.0	I	A0			C D

1. C = Coherent, I = Incoherent (vertical channels), H = Incoherent (horizontal channels)



**Figure 13.** The short-period instrument response is plotted for NORESS and ARCESS.

other two events in Data Set #2 were identified as earthquakes by SAIC on the basis of location, origin time, *S/P* amplitude ratios, cepstral analysis, and past seismicity. All of the events are located between 50°N and 80°N, and between -10°E and 40°E.

### 3.2.2 Event Description

Table 6 lists the 33 events in Data Set #2. The first column lists the *orid*, which is a unique positive integer that identifies each event in the CSS database [Anderson *et al.*, 1990]. The rest of the columns list the event origin time, latitude, longitude, local magnitude ( $M_L$ ), number of detecting stations, and number of defining phases.

The event locations are plotted in Figure 14. Of the 33 events, 25 were recorded at both NORESS and ARCESS, and 29 had at least 3 defining phases. The epicentral distances are primarily between 200 and 2000 km (Figure 15). The magnitude distribution is plotted in Figure 16. This magnitude is computed from the short-term average amplitude of regional phases (*Pn*, *Pg*, *Sn*, and *Lg*) measured on a 2–4 Hz incoherent beam [Bache *et al.*, 1991]. The magnitudes of the events in Data Set #2 are primarily between 1.0 and 2.9.

### 3.2.3 Sample Waveforms

This section shows some samples of the waveform data. Figure 17 is a map with epicenters of 6 events in Data Set #2 (the events are labeled by the *orid* in Table 6). Figures 18–23 display the 3-component waveforms recorded by the center element of the closest array to each event. The waveforms for the other events in Data Set #2 are of similar quality.

Table 6. Events in Data Set #2

orid	Origin Time		Latitude	Longitude	$M_L$	nsta <sup>1</sup>	ndef <sup>2</sup>
129581	89 10 19	02:49:12.486	61.93	7.14	.86	1	2
140781	89 10 28	01:36:35.681	54.83	16.51	2.75	2	3
152076	89 11 03	20:11:43.862	73.18	6.06	1.96	2	4
152950	89 11 04	18:04:03.898	72.35	1.17	2.85	2	4
152953	89 11 04	18:17:16.057	72.25	1.23	2.82	2	4
161045	89 11 11	03:12:43.839	80.11	21.33	2.59	2	3
167872	89 11 13	17:57:46.185	77.51	19.38	2.85	1	2
175129	89 11 16	13:22:37.823	64.20	20.99	1.66	2	6
178823	89 11 19	22:19:08.942	69.76	17.46	1.57	2	3
189645	89 11 25	05:12:40.420	60.35	5.66	.32	1	2
191216	90 01 13	03:56:22.534	64.58	7.73	.00	2	6
197884	90 05 02	13:24:42.971	57.58	5.70	1.47	2	4
198078	90 05 12	07:27:06.386	73.04	12.19	1.74	2	4
200221	90 05 28	04:43:41.075	74.95	10.00	2.09	2	4
200342	90 06 14	11:37:05.777	80.18	4.81	2.38	2	3
201814	90 07 25	02:35:42.874	74.59	10.42	2.24	2	3
202414	90 08 22	04:08:30.471	63.86	20.81	2.12	2	6
206832	90 10 13	03:58:59.733	70.77	5.31	2.51	2	6
207992	90 10 18	00:30:34.609	61.49	5.21	2.40	1	3
208137	90 10 25	04:52:11.131	76.49	11.29	2.02	2	4
208529	90 10 28	20:47:08.657	58.57	.95	1.84	1	2
208583	90 10 30	23:08:10.908	67.65	15.41	2.29	2	7
8256	90 12 16	00:58:27.571	71.11	28.36	2.26	3	8
7795	91 01 15	17:00:03.429	71.53	13.92	2.18	3	5
8013	91 01 20	01:56:14.748	71.62	14.89	2.03	3	6
8527	91 01 23	15:45:36.910	62.07	4.85	2.79	1	3
13838	91 03 12	07:23:20.456	66.86	22.84	1.82	3	7
14662	91 03 16	00:01:39.114	68.21	10.80	2.46	3	6
15982	91 03 28	17:54:39.426	66.60	8.52	2.71	3	5
18644	91 04 17	17:47:29.072	67.11	24.16	2.11	3	8
23957	91 05 23	19:24:54.759	61.50	24.99	1.39	2	5
25522	91 06 05	09:05:53.049	64.40	21.92	1.71	2	4
25748	91 06 06	12:46:11.596	65.50	22.90	3.22	3	8

1. The number of detecting stations.

2. The number of defining phases (number of phases used to locate the event).



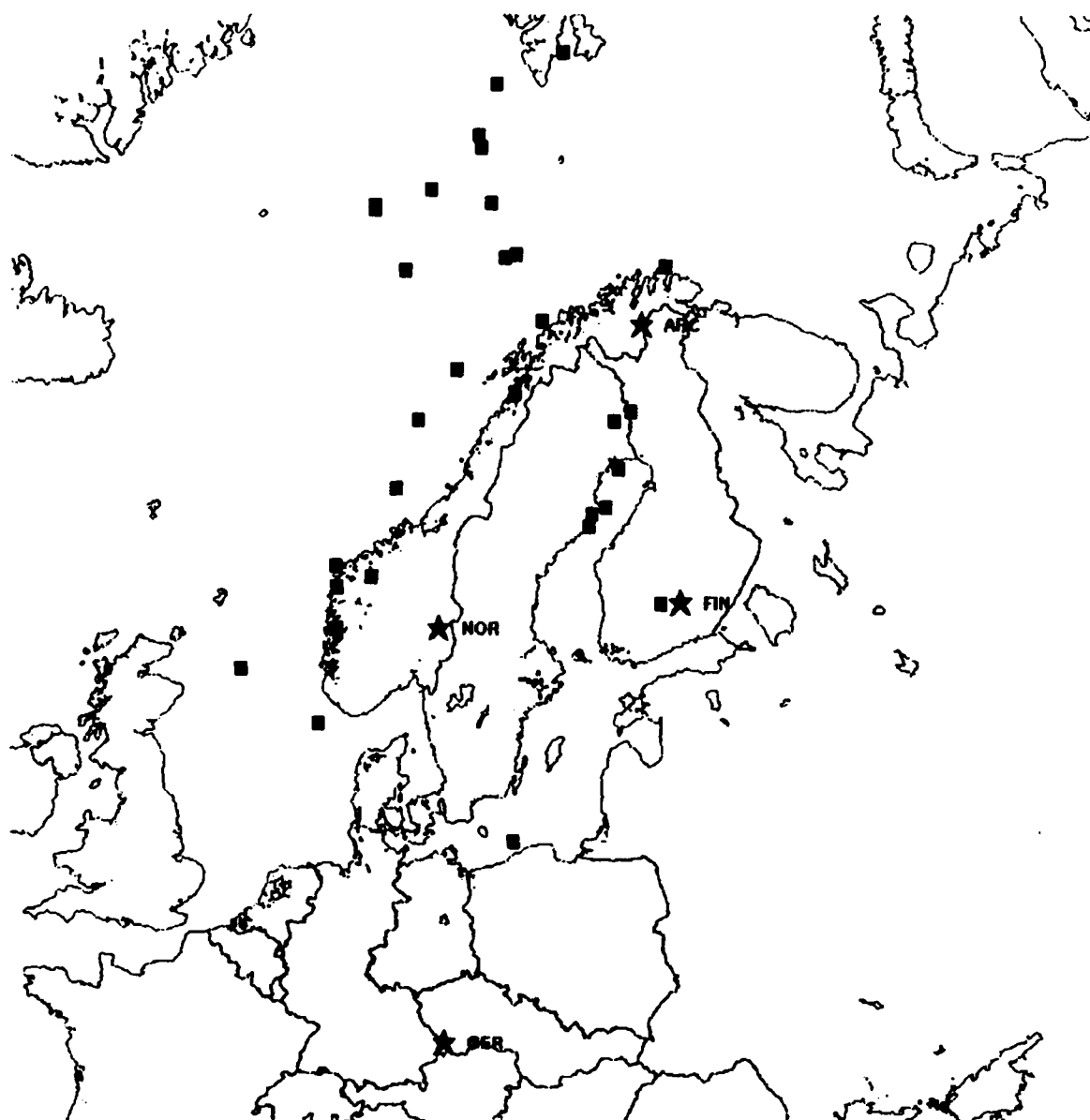


**Figure 14.** Epicenters are plotted for the 33 events in Data Set #2.

## DATA SET #2

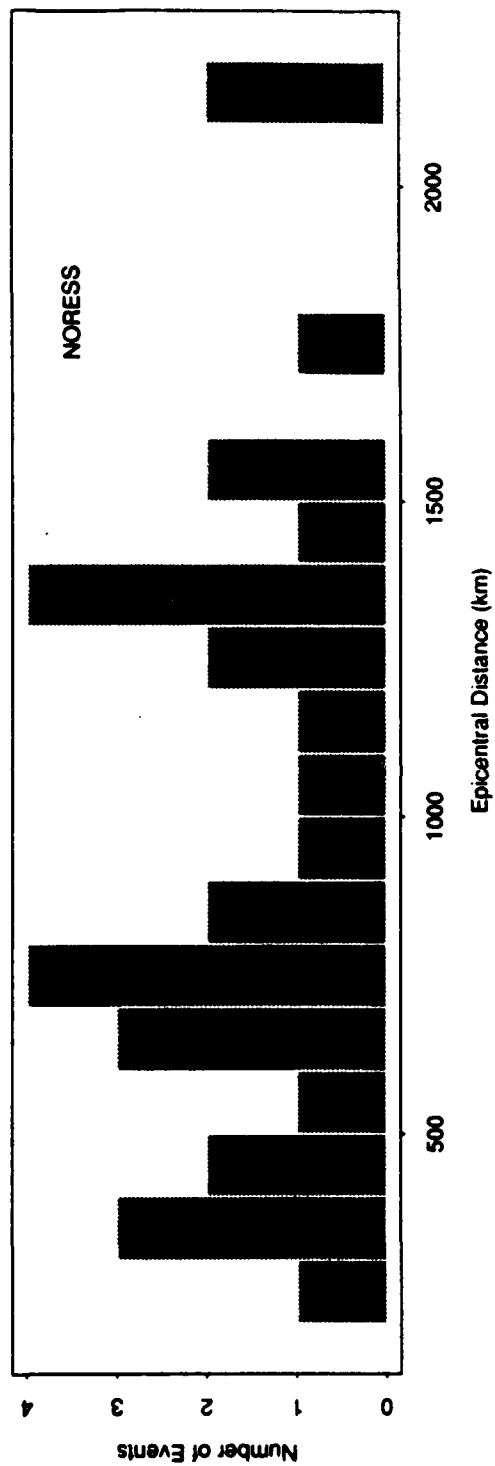
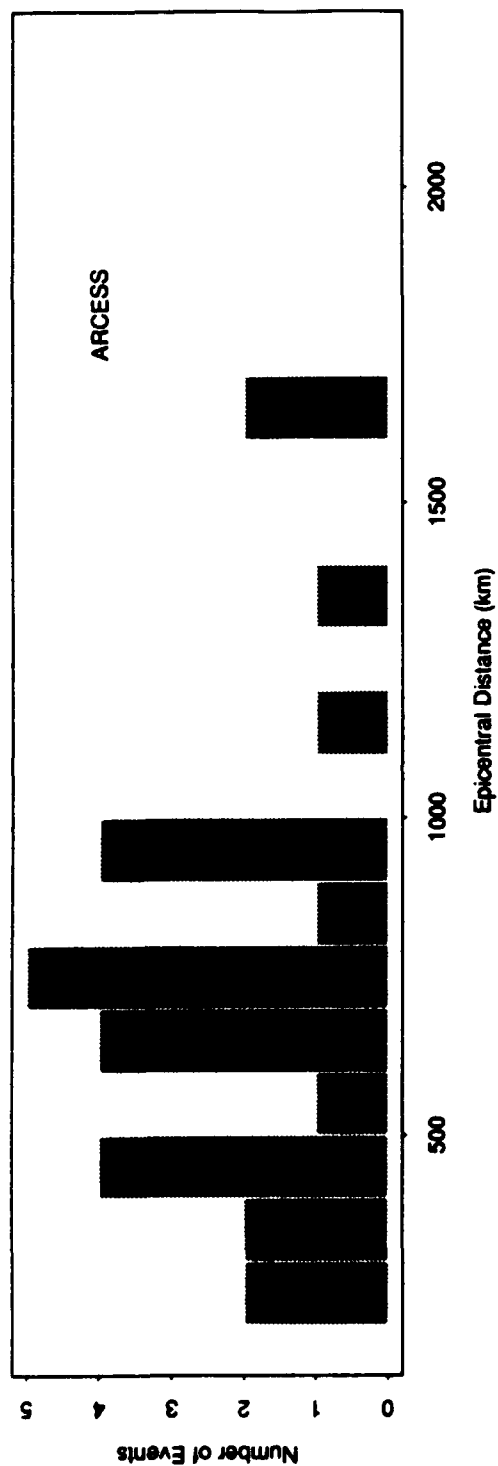


Figure 15. Histograms of epicentral distance to the events in Data Set #2 are plotted for ARCESS (top) and NORESS (bottom).

## DATA SET #2

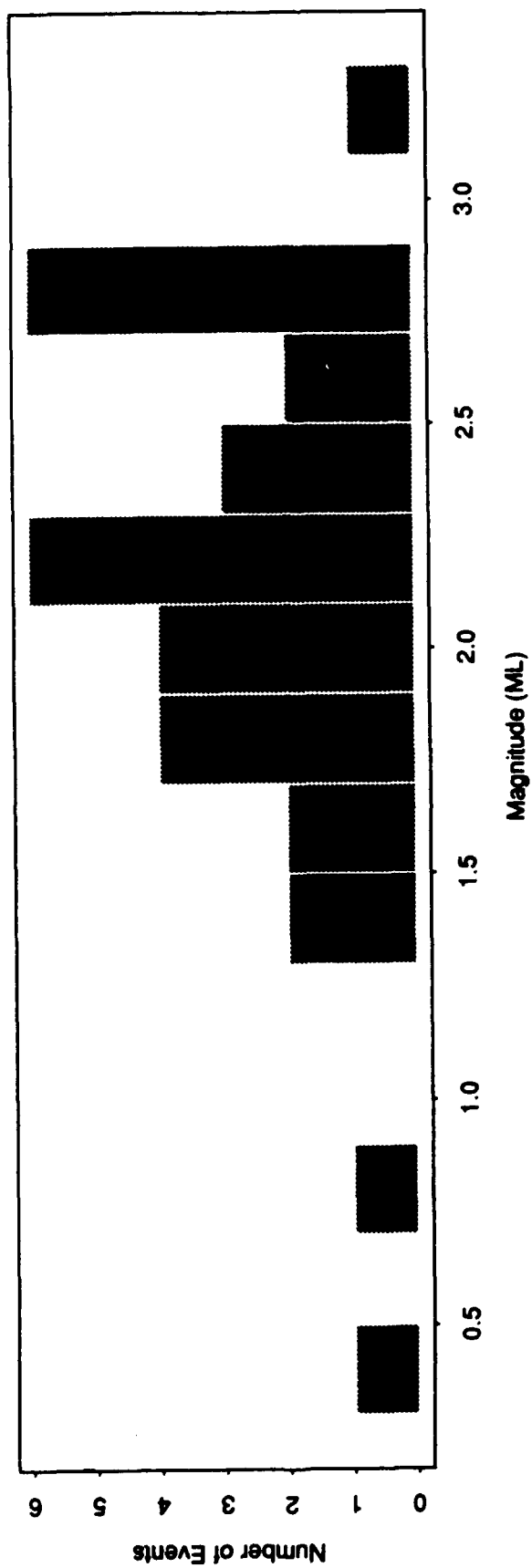
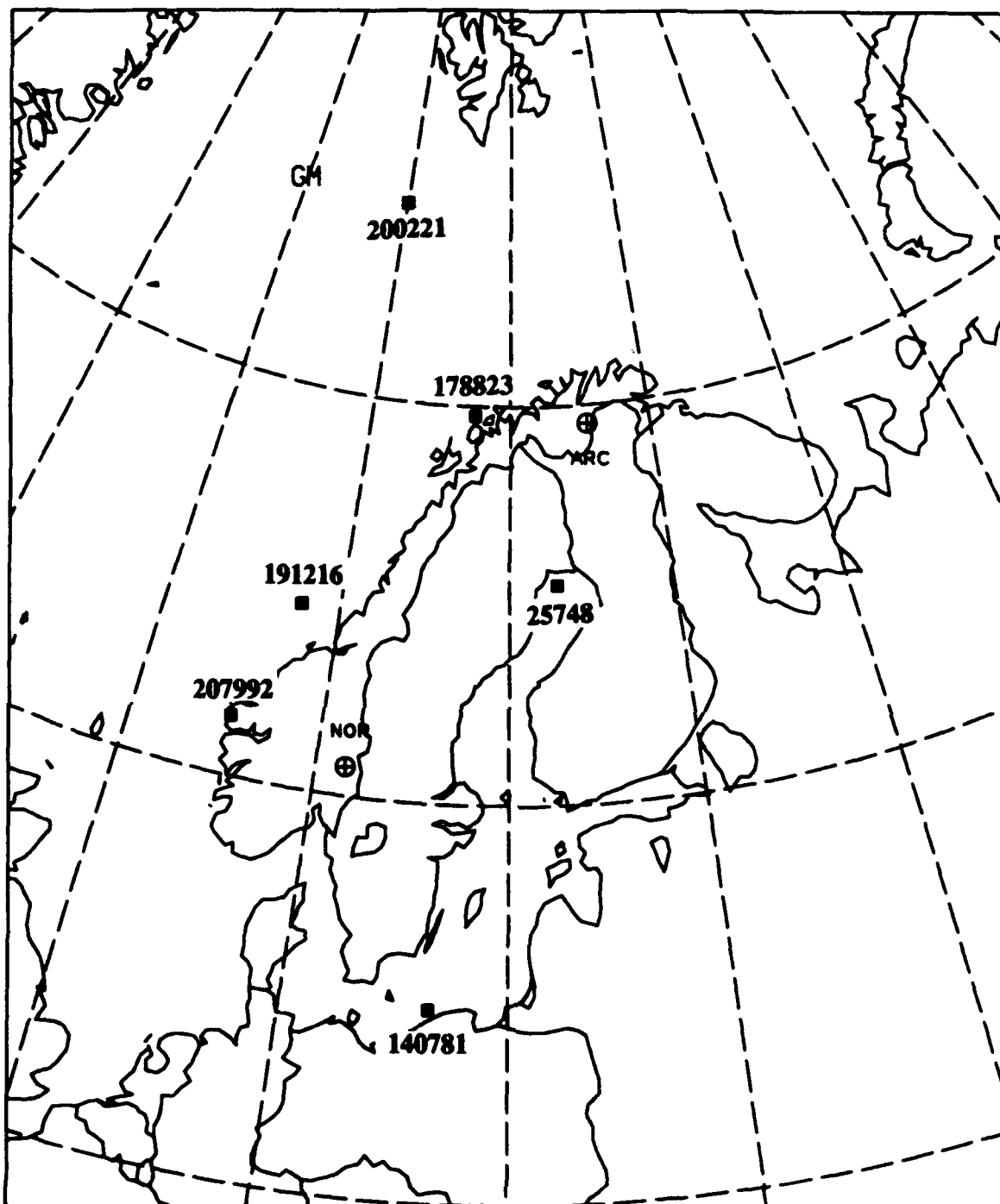
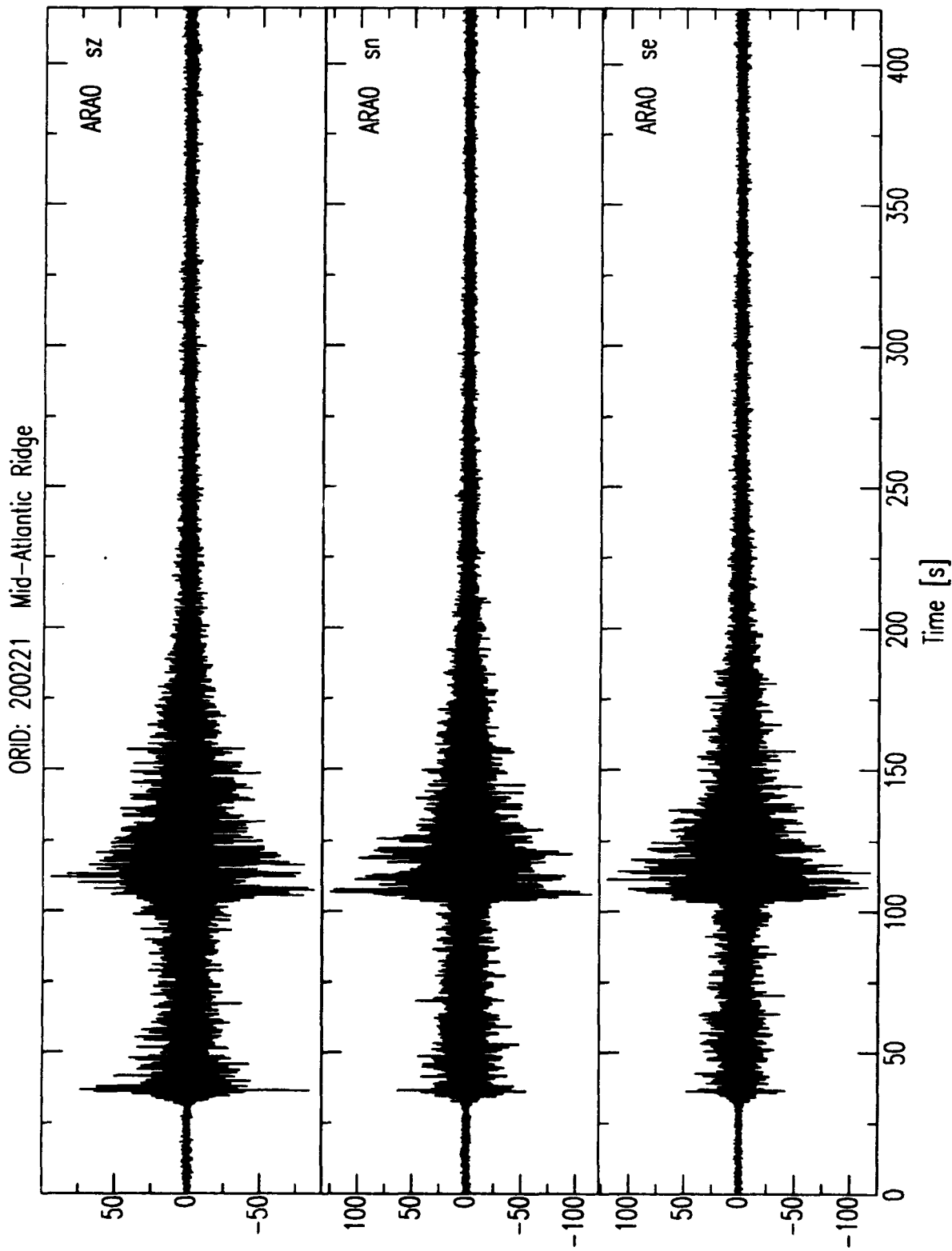


Figure 16. A histogram of local magnitude is shown for events in Data Set #2.



**Figure 17.** The locations of six events in Data Set #2 are plotted. Sample waveforms for these events are plotted in Figures 18–23. The events are labeled by the *orid* in Table 6.



**Figure 18.** Seismograms recorded by the 3-component center element of the ARCESS array for an event on the Mid-Atlantic Ridge. The seismograms are bandpassed from 1 to 15 Hz.

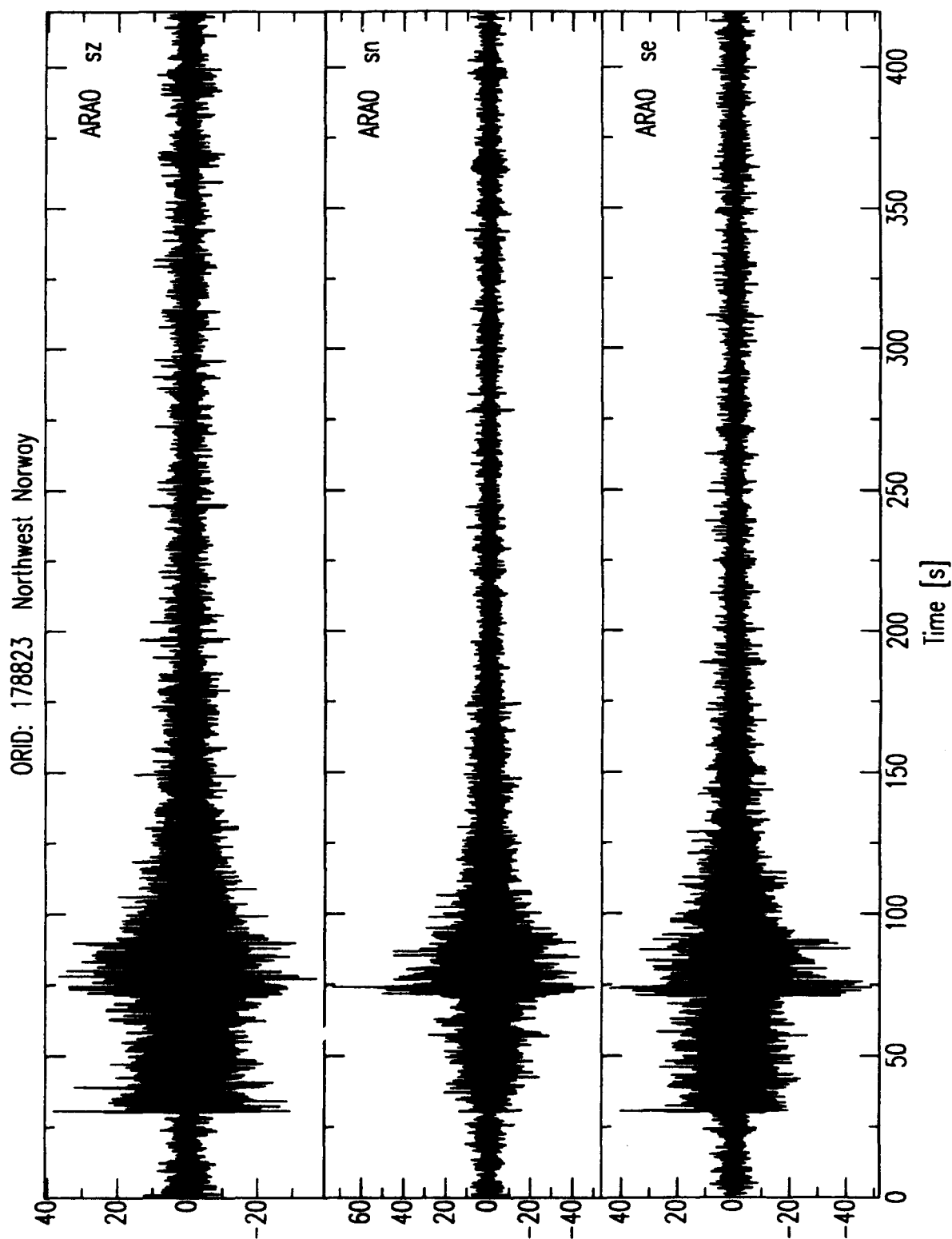


**Figure 19.** Seismograms recorded by the 3-component center element of the ARCESS array for an event near the northwest coast of Norway. The seismograms are bandpassed from 1 to 15 Hz.

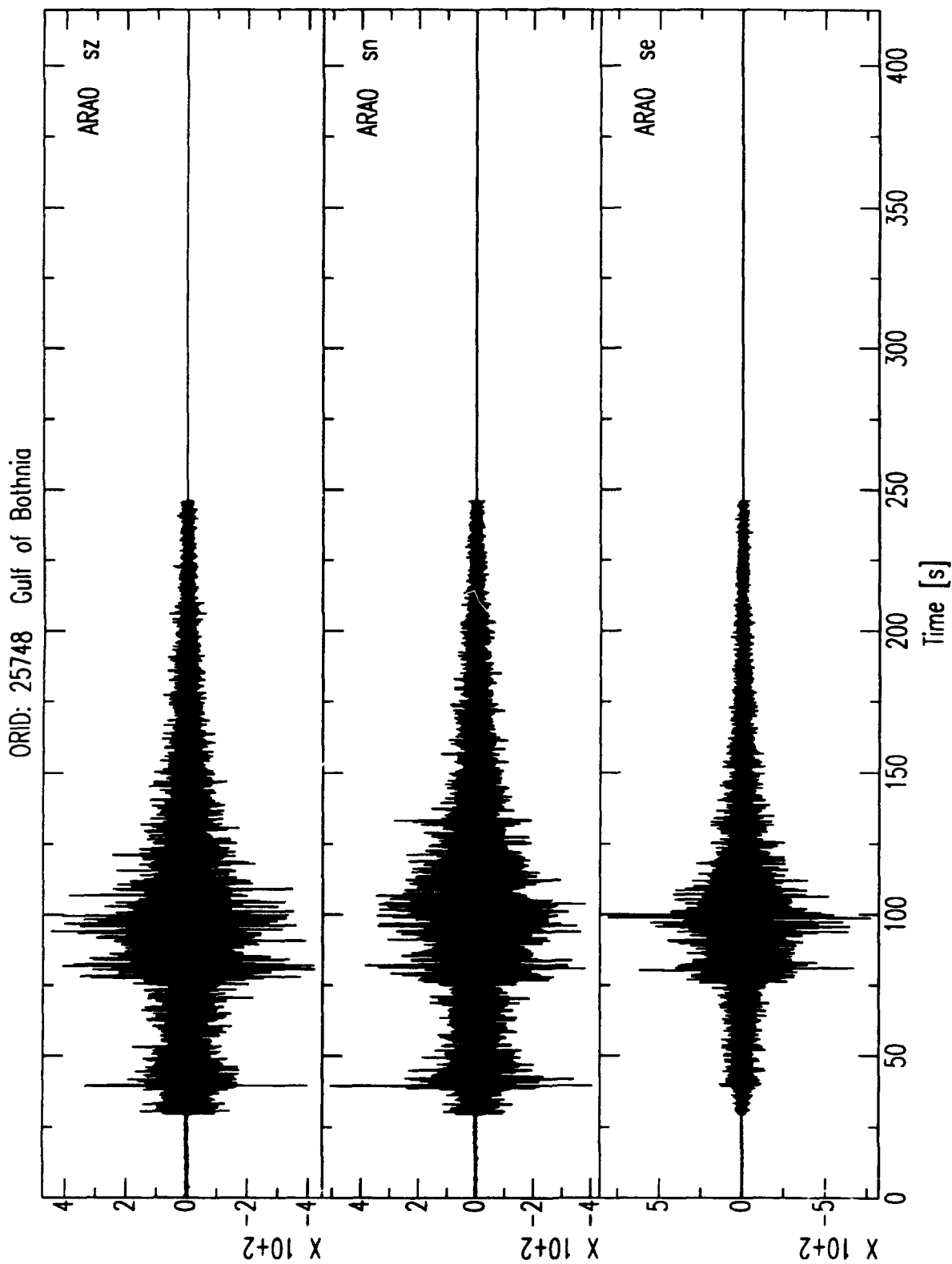


**Figure 20.** Seismograms recorded by the 3-component center element of the ARCESS array for an event in the Gulf of Bothnia. The seismograms are bandpassed from 1 to 15 Hz.

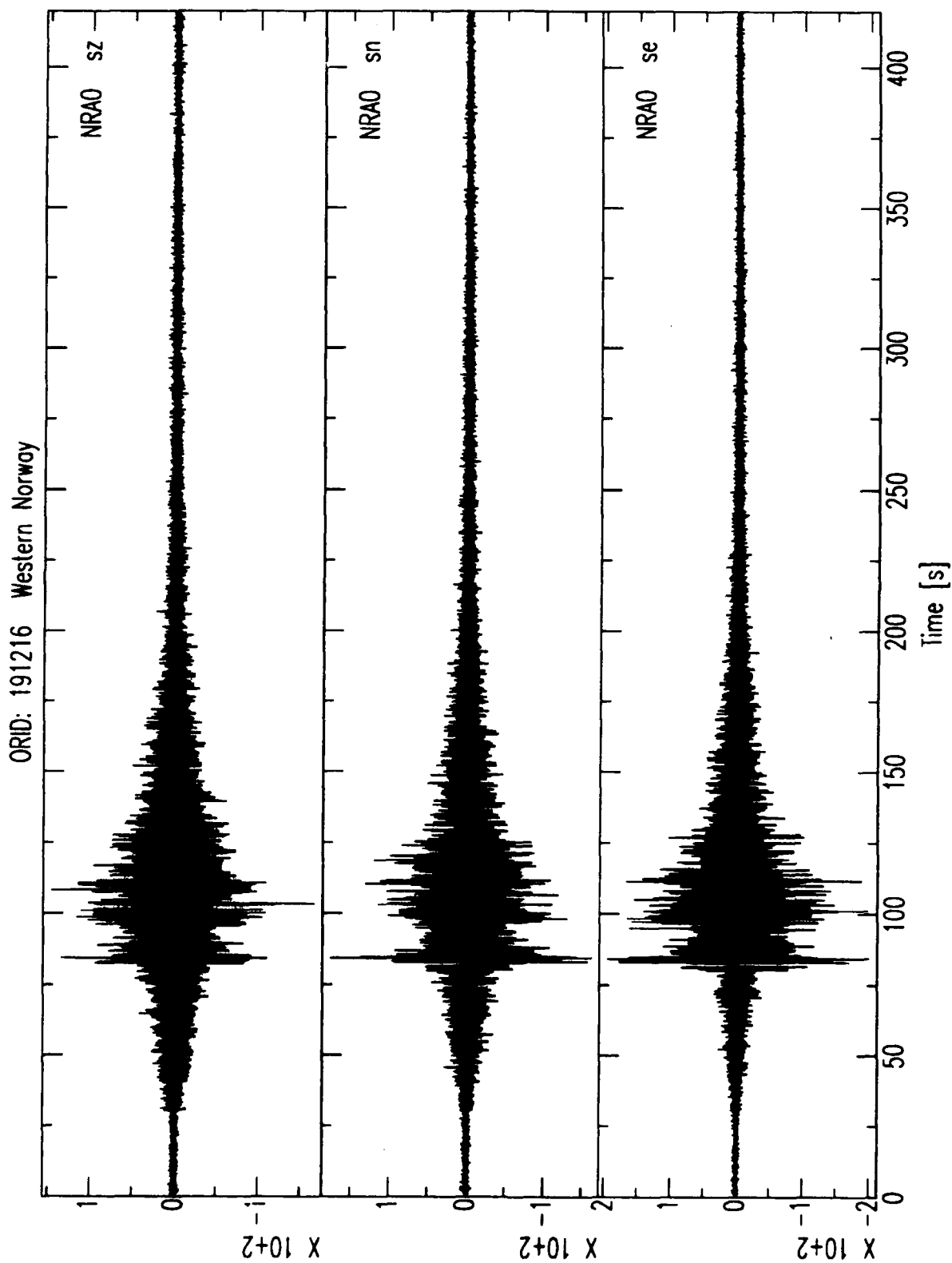


**Figure 21.** Seismograms recorded by the 3-component center element of the NORESS array for an event off the west coast of Norway. The seismograms are bandpassed from 1 to 15 Hz.



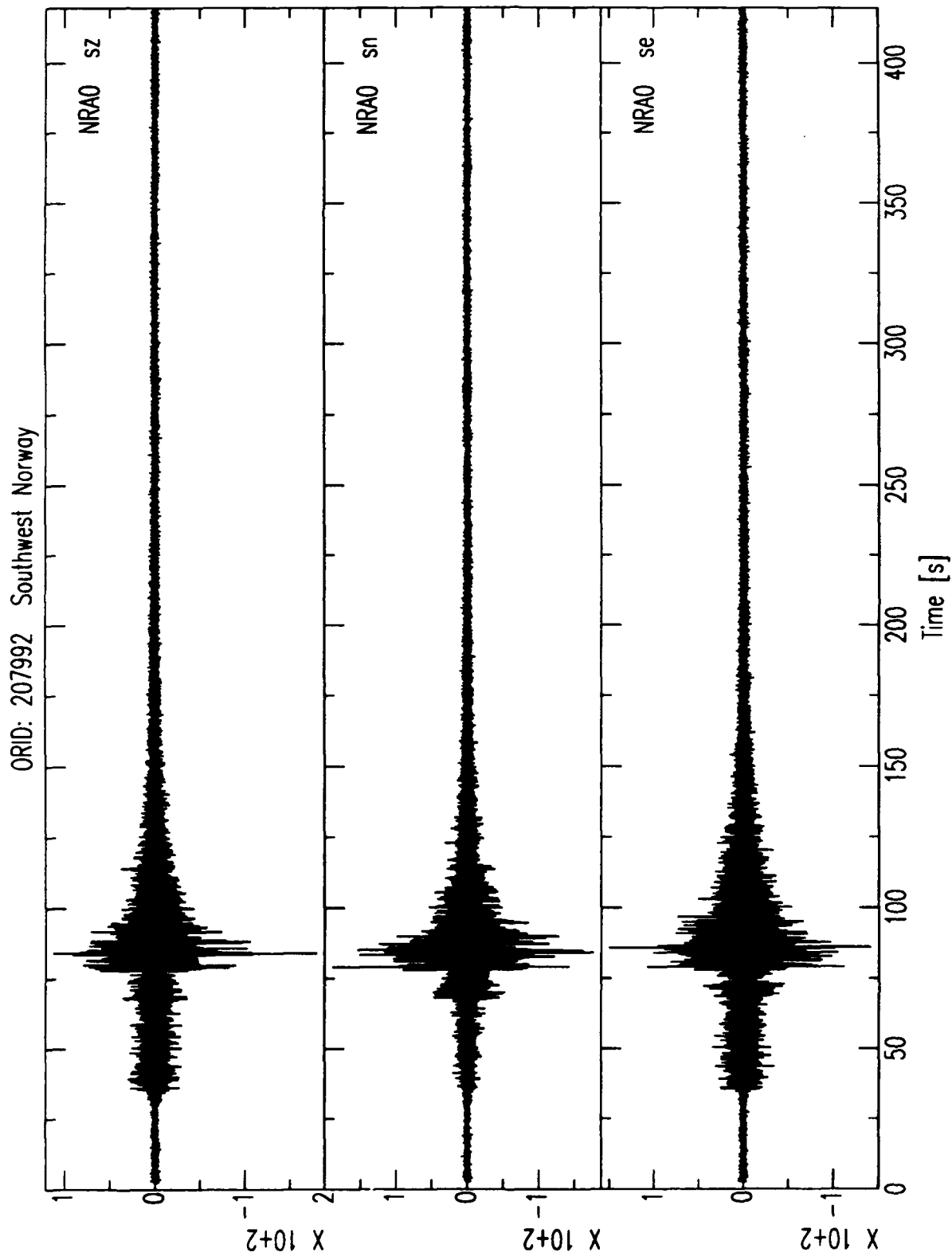


**Figure 22.** Seismograms recorded by the 3-component center element of the NORESS array for an event near the southwest coast of Norway. The seismograms are bandpassed from 1 to 15 Hz.

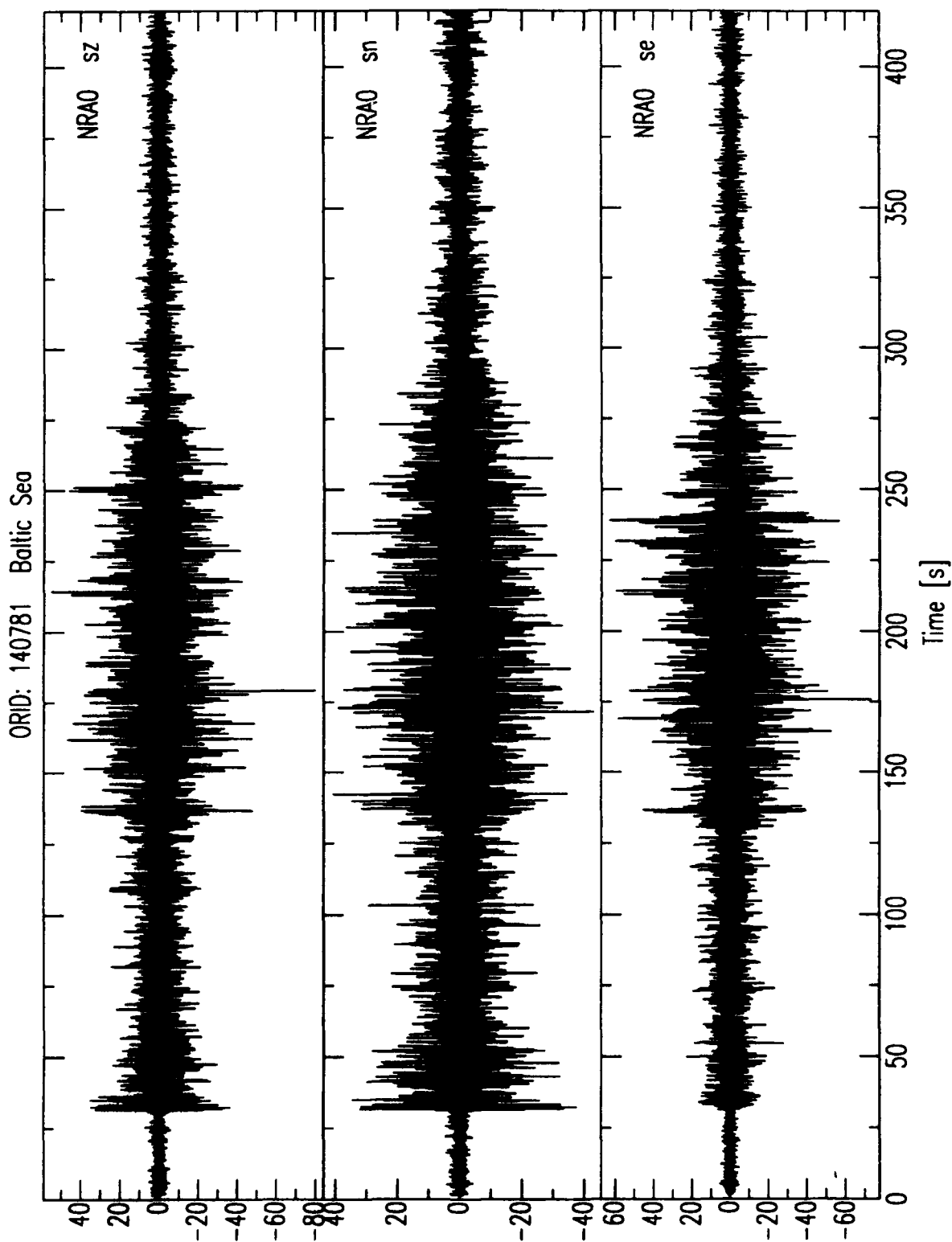


**Figure 23.** Seismograms recorded by the 3-component center element of the NORESS array for an event in the Baltic Sea. The seismograms are bandpassed from 1 to 15 Hz.

## 4. DATA SET #3

Data Set #3 includes single-channel waveform data, beams, and parametric data from 255 regional events recorded at the GERESS array in Germany. GERESS is in a much different geologic and tectonic environment than the arrays in Norway, and this data set was developed to test the generality and adaptability of the neural networks that were trained with NORESS and ARCESS data (Data Set #1).

### 4.1 GERESS Array

The GERESS array in Germany includes 25 short-period seismometers in four concentric rings with a maximum diameter of about 4 km (Figure 24). The array configuration and sampling rate were designed to enhance the detection of regional signals, and were based on the design of the arrays in Fennoscandia [Mykkeltveit, *et al.*, 1983; Mykkeltveit and Ringdal, 1988; Harjes, 1990; Harjes *et al.*, 1991]. The radius of the inner ring (called the A-ring) is about 200 m. The radii of the B-, C-, and D-rings are 430 m, 925 m, and 1988 m, respectively. The number of sensors on the A-, B-, C-, and D-rings are 3, 5, 7, and 9, respectively. The individual station locations for the GERESS array are given in Table 7 (locations are given relative to the reference location listed at the bottom of this table). Four of the 25 array elements are equipped with 3-component seismometers. One is on the A-ring (A2), and three are on the D-ring (D1, D4, and D7). The rest of the short-period array elements only have vertical-component seismometers. Table 8 lists the standard beams used for IMS processing of GERESS data. The first column is the *chan* (or channel name) that is used to identify the detecting beam.

The GERESS data are continuously recorded, and the short-period data are digitized at a rate of 40 samples/s. Figure 25 shows the short-period instrument response. This response applies to all short-period elements of the GERESS array. The instrument response is approximately flat to velocity beyond about 1 Hz. The total sensitivity is 26.53 counts/(nm/s) at 5 Hz [Harjes *et al.*, 1991]. Figure 25 does not include the digital filtering and resampling stages which cannot be conveniently expressed in terms of poles and zeroes. The FIR filters (applied in the time domain) produce a sharp cut-off near 20 Hz. The complete response (analog and digital) is given by Harjes *et al.* [1991].

### 4.2 Regional Events

This section describes the events in Data Set #3. It gives the event locations, magnitudes, and epicentral distances from GERESS.

#### 4.2.1 Selection Criteria

The events in Data Set #3 were required to have latitudes between 35°N and 62°N and longitudes between -10°E and 35°E (regional distance to GERESS), origin

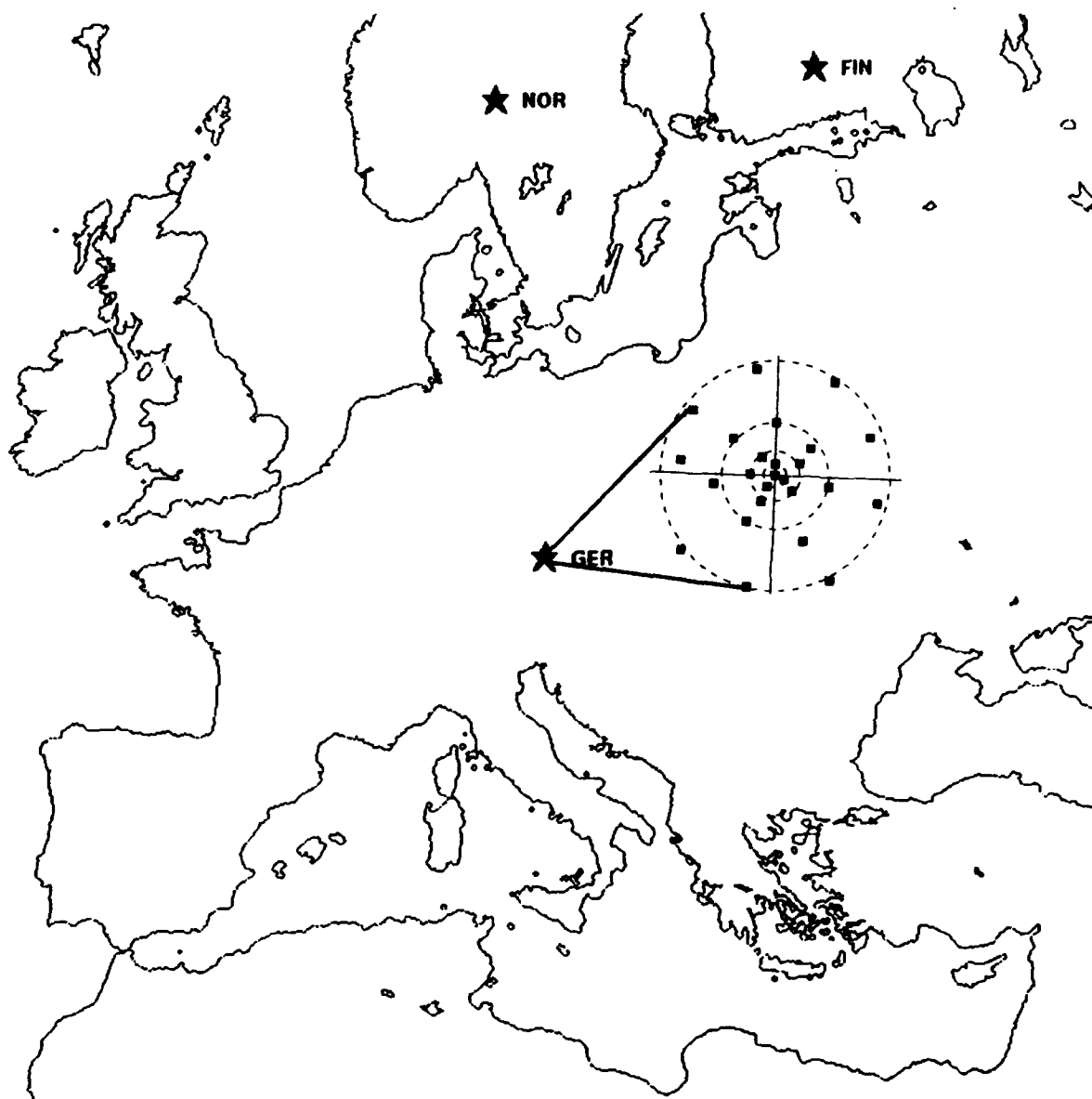


**Figure 24.** The location and array geometry are plotted for the GERESS array.

**Table 7. GERESS Station Locations**

Station	GERESS		
	Elevation (km)	dnorth <sup>1</sup> (km)	deast <sup>1</sup> (km)
GEA0	1.022	-.923	.008
GEA1	1.004	-.984	.157
GEA2	1.056	-.722	.007
GEA3	1.012	-1.120	-.131
GEB1	1.010	-.699	.427
GEB2	1.089	-.615	-.227
GEB3	1.054	-.899	-.425
GEB4	1.001	-1.372	-.222
GEB5	.972	-1.177	.302
GEC1	1.023	-.441	.606
GEC2	1.132	.000	.000
GEC3	1.070	-.292	-.730
GEC4	1.098	-1.084	-1.051
GEC5	1.004	-1.716	-.460
GEC6	.937	-2.048	.515
GEC7	.981	-1.090	.930
GED1	1.057	.729	.982
GED2	.994	.909	-.361
GED3	.945	.180	-1.447
GED4	1.035	-.698	-1.621
GED5	1.080	-2.252	-1.571
GED6	1.079	-2.851	-.410
GED7	.955	-2.706	1.009
GED8	.933	-1.358	1.777
GED9	.982	-.214	1.628

1. Relative to the reference location: 48.8451°N, 13.7016°E.

Table 8. IMS Standard Beams for GERESS

Chan	Velocity (km/s)	Filter (Hz)	Filter Order	Azimuth (degrees)	Beam Type <sup>1</sup>	N	Ring Subset			
Current IMS Beam Deployment										
GA01	12.00	1.0- 3.0	3	0.0	C	21	A	B	C	D
GA02	12.00	1.0- 3.0	3	30.0	C	21	A	B	C	D
GA03	12.00	1.0- 3.0	3	60.0	C	21	A	B	C	D
GA04	12.00	1.0- 3.0	3	90.0	C	21	A	B	C	D
GA05	12.00	1.0- 3.0	3	120.0	C	21	A	B	C	D
GA06	12.00	1.0- 3.0	3	150.0	C	21	A	B	C	D
GA07	12.00	1.0- 3.0	3	180.0	C	21	A	B	C	D
GA08	12.00	1.0- 3.0	3	210.0	C	21	A	B	C	D
GA09	12.00	1.0- 3.0	3	240.0	C	21	A	B	C	D
GA10	12.00	1.0- 3.0	3	270.0	C	21	A	B	C	D
GA11	12.00	1.0- 3.0	3	300.0	C	21	A	B	C	D
GA12	12.00	1.0- 3.0	3	330.0	C	21	A	B	C	D
GC01	4.00	0.7- 3.0	3	0.0	C	21	A	B	C	D
GC02	4.00	0.7- 3.0	3	30.0	C	21	A	B	C	D
GC03	4.00	0.7- 3.0	3	60.0	C	21	A	B	C	D
GC04	4.00	0.7- 3.0	3	90.0	C	21	A	B	C	D
GC05	4.00	0.7- 3.0	3	120.0	C	21	A	B	C	D
GC06	4.00	0.7- 3.0	3	150.0	C	21	A	B	C	D
GC07	4.00	0.7- 3.0	3	180.0	C	21	A	B	C	D
GC08	4.00	0.7- 3.0	3	210.0	C	21	A	B	C	D
GC09	4.00	0.7- 3.0	3	240.0	C	21	A	B	C	D
GC10	4.00	0.7- 3.0	3	270.0	C	21	A	B	C	D
GC11	4.00	0.7- 3.0	3	300.0	C	21	A	B	C	D
GC12	4.00	0.7- 3.0	3	330.0	C	21	A	B	C	D
GF01	6.50	2.5- 4.5	3	0.0	C	16	A	B	C	D
GF02	6.50	2.5- 4.5	3	30.0	C	16	A	B	C	D
GF03	6.50	2.5- 4.5	3	60.0	C	16	A	B	C	D
GF04	6.50	2.5- 4.5	3	90.0	C	16	A	B	C	D
GF05	6.50	2.5- 4.5	3	120.0	C	16	A	B	C	D
GF06	6.50	2.5- 4.5	3	150.0	C	16	A	B	C	D
GF07	6.50	2.5- 4.5	3	180.0	C	16	A	B	C	D
GF08	6.50	2.5- 4.5	3	210.0	C	16	A	B	C	D
GF09	6.50	2.5- 4.5	3	240.0	C	16	A	B	C	D
GF10	6.50	2.5- 4.5	3	270.0	C	16	A	B	C	D
GF11	6.50	2.5- 4.5	3	300.0	C	16	A	B	C	D
GF12	6.50	2.5- 4.5	3	330.0	C	16	A	B	C	D
GF13	6.50	6.0-10.0	3	0.0	C	16	A	B	C	D
GF14	6.50	6.0-10.0	3	30.0	C	16	A	B	C	D
GF15	6.50	6.0-10.0	3	60.0	C	16	A	B	C	D
GF16	6.50	6.0-10.0	3	90.0	C	16	A	B	C	D
GF17	6.50	6.0-10.0	3	120.0	C	16	A	B	C	D
GF18	6.50	6.0-10.0	3	150.0	C	16	A	B	C	D
GF19	6.50	6.0-10.0	3	180.0	C	16	A	B	C	D
GF20	6.50	6.0-10.0	3	210.0	C	16	A	B	C	D
GF21	6.50	6.0-10.0	3	240.0	C	16	A	B	C	D
GF22	6.50	6.0-10.0	3	270.0	C	16	A	B	C	D
GF23	6.50	6.0-10.0	3	300.0	C	16	A	B	C	D

Chan	Velocity (km/s)	Filter (Hz)	Filter Order	Azimuth (degrees)	Beam Type <sup>1</sup>	N	Ring Subset			
GF24	6.50	6.0-10.0	3	330.0	C	16		A	B	C D
GF77	0.33	8.0-16.0	3	305.0	C	11	A0	A	B	C D
GF88	0.33	8.0-16.0	3	99.0	C	11	A0	A	B	C D
GF99	∞	0.7- 2.0	3	0.0	C	17	A0			C D
GG01	8.50	1.0- 4.0	3	0.0	C	16		A	B	C D
GG02	8.50	1.0- 4.0	3	30.0	C	16		A	B	C D
GG03	8.50	1.0- 4.0	3	60.0	C	16		A	B	C D
GG04	8.50	1.0- 4.0	3	90.0	C	16		A	B	C D
GG05	8.50	1.0- 4.0	3	120.0	C	16		A	B	C D
GG06	8.50	1.0- 4.0	3	150.0	C	16		A	B	C D
GG07	8.50	1.0- 4.0	3	180.0	C	16		A	B	C D
GG08	8.50	1.0- 4.0	3	210.0	C	16		A	B	C D
GG09	8.50	1.0- 4.0	3	240.0	C	16		A	B	C D
GG10	8.50	1.0- 4.0	3	270.0	C	16		A	B	C D
GG11	8.50	1.0- 4.0	3	300.0	C	16		A	B	C D
GG12	8.50	1.0- 4.0	3	330.0	C	16		A	B	C D
GG13	8.50	6.0-10.0	3	0.0	C	16		A	B	C D
GG14	8.50	6.0-10.0	3	30.0	C	16		A	B	C D
GG15	8.50	6.0-10.0	3	60.0	C	16		A	B	C D
GG16	8.50	6.0-10.0	3	90.0	C	16		A	B	C D
GG17	8.50	6.0-10.0	3	120.0	C	16		A	B	C D
GG18	8.50	6.0-10.0	3	150.0	C	16		A	B	C D
GG19	8.50	6.0-10.0	3	180.0	C	16		A	B	C D
GG20	8.50	6.0-10.0	3	210.0	C	16		A	B	C D
GG21	8.50	6.0-10.0	3	240.0	C	16		A	B	C D
GG22	8.50	6.0-10.0	3	270.0	C	16		A	B	C D
GG23	8.50	6.0-10.0	3	300.0	C	16		A	B	C D
GG24	8.50	6.0-10.0	3	330.0	C	16		A	B	C D
GHI1	∞	1.0- 4.0	3	0.0	I	16		A	B	C D
GHI2	∞	8.0-16.0	3	0.0	I	13		A	B	C
GHI3	∞	0.7- 2.0	3	0.0	I	20	A0	A		C D
GVI1	∞	0.7- 2.0	3	0.0	I	25	A0	A	B	C D
GVI2	∞	1.0- 4.0	3	0.0	I	21		A	B	C D
Initial IMS Beam Deployment (before May 3, 1991)										
G011	∞	0.5- 1.5	3	0.0	C	10	A0			D
G021	∞	1.0- 3.0	3	0.0	C	17	A0			C D
G031	∞	1.5- 3.5	3	0.0	C	17	A0			C D
G032	11.00	1.5- 3.5	3	30.0	C	17	A0			C D
G033	11.00	1.5- 3.5	3	90.0	C	17	A0			C D
G034	11.00	1.5- 3.5	3	150.0	C	17	A0			C D
G035	11.00	1.5- 3.5	3	210.0	C	17	A0			C D
G036	11.00	1.5- 3.5	3	270.0	C	17	A0			C D
G037	11.00	1.5- 3.5	3	330.0	C	17	A0			C D
G038	15.80	1.5- 3.5	3	80.0	C	17	A0			C D
G039	10.00	1.5- 3.5	3	30.0	C	17	A0			C D
G041	∞	2.0- 4.0	3	0.0	C	17	A0			C D
G042	10.20	2.0- 4.0	3	30.0	C	17	A0			C D
G043	10.20	2.0- 4.0	3	90.0	C	17	A0			C D
G044	10.20	2.0- 4.0	3	150.0	C	17	A0			C D
G045	10.20	2.0- 4.0	3	210.0	C	17	A0			C D

Chan	Velocity (km/s)	Filter (Hz)	Filter Order	Azimuth (degrees)	Beam Type <sup>1</sup>	N	Ring Subset			
G046	10.20	2.0- 4.0	3	270.0	C	17	A0		C	D
G047	10.20	2.0- 4.0	3	330.0	C	17	A0		C	D
G048	15.80	2.0- 4.0	3	80.0	C	17	A0		C	D
G049	10.00	2.0- 4.0	3	30.0	C	17	A0		C	D
G051	∞	2.5- 4.5	3	0.0	C	22	A0	B	C	D
G052	8.90	2.5- 4.5	3	30.0	C	22	A0	B	C	D
G053	8.90	2.5- 4.5	3	90.0	C	22	A0	B	C	D
G054	8.90	2.5- 4.5	3	150.0	C	22	A0	B	C	D
G055	8.90	2.5- 4.5	3	210.0	C	22	A0	B	C	D
G056	8.90	2.5- 4.5	3	270.0	C	22	A0	B	C	D
G057	8.90	2.5- 4.5	3	330.0	C	22	A0	B	C	D
G058	15.80	2.5- 4.5	3	80.0	C	22	A0	B	C	D
G059	10.00	2.5- 4.5	3	30.0	C	22	A0	B	C	D
G061	∞	3.0- 5.0	3	0.0	C	22	A0	B	C	D
G062	10.50	3.0- 5.0	3	30.0	C	22	A0	B	C	D
G063	10.50	3.0- 5.0	3	90.0	C	22	A0	B	C	D
G064	10.50	3.0- 5.0	3	150.0	C	22	A0	B	C	D
G065	10.50	3.0- 5.0	3	210.0	C	22	A0	B	C	D
G066	10.50	3.0- 5.0	3	270.0	C	22	A0	B	C	D
G067	10.50	3.0- 5.0	3	330.0	C	22	A0	B	C	D
G068	15.80	3.0- 5.0	3	80.0	C	22	A0	B	C	D
G069	10.00	3.0- 5.0	3	30.0	C	22	A0	B	C	D
G071	∞	3.5- 5.5	3	0.0	C	13	A0	B	C	
G072	11.10	3.5- 5.5	3	30.0	C	13	A0	B	C	
G073	11.10	3.5- 5.5	3	90.0	C	13	A0	B	C	
G074	11.10	3.5- 5.5	3	150.0	C	13	A0	B	C	
G075	11.10	3.5- 5.5	3	210.0	C	13	A0	B	C	
G076	11.10	3.5- 5.5	3	270.0	C	13	A0	B	C	
G077	11.10	3.5- 5.5	3	330.0	C	13	A0	B	C	
G081	∞	4.0- 8.0	3	0.0	C	13	A0	B	C	
G082	9.50	4.0- 8.0	3	30.0	C	13	A0	B	C	
G083	9.50	4.0- 8.0	3	90.0	C	13	A0	B	C	
G084	9.50	4.0- 8.0	3	150.0	C	13	A0	B	C	
G085	9.50	4.0- 8.0	3	210.0	C	13	A0	B	C	
G086	9.50	4.0- 8.0	3	270.0	C	13	A0	B	C	
G087	9.50	4.0- 8.0	3	330.0	C	13	A0	B	C	
G091	∞	5.0-10.0	3	0.0	C	13	A0	B	C	
G092	10.50	5.0-10.0	3	30.0	C	13	A0	B	C	
G093	10.50	5.0-10.0	3	90.0	C	13	A0	B	C	
G094	10.50	5.0-10.0	3	150.0	C	13	A0	B	C	
G095	10.50	5.0-10.0	3	210.0	C	13	A0	B	C	
G096	10.50	5.0-10.0	3	270.0	C	13	A0	B	C	
G097	10.50	5.0-10.0	3	330.0	C	13	A0	B	C	
G101	∞	8.0-16.0	3	0.0	C	9	A0	A	B	
G102	9.90	8.0-16.0	3	30.0	C	9	A0	A	B	
G103	9.90	8.0-16.0	3	90.0	C	9	A0	A	B	
G104	9.90	8.0-16.0	3	150.0	C	9	A0	A	B	
G105	9.90	8.0-16.0	3	210.0	C	9	A0	A	B	
G106	9.90	8.0-16.0	3	270.0	C	9	A0	A	B	
G107	9.90	8.0-16.0	3	330.0	C	9	A0	A	B	
GH01	∞	2.0- 4.0	3	0.0	H	8		A		D
GH02	∞	3.5- 5.5	3	0.0	H	8		A		D



Chan	Velocity (km/s)	Filter (Hz)	Filter Order	Azimuth (degrees)	Beam Type <sup>1</sup>	N	Ring Subset	
GH03	∞	5.0-10.0	3	0.0	H	8	A	D
GH04	∞	8.0-16.0	3	0.0	H	8	A	D
GV01	∞	0.5- 1.5	3	0.0	I	10	A0	D
GV02	∞	1.0- 2.0	3	0.0	I	8	A0	C
GV03	∞	1.5- 2.5	3	0.0	I	8	A0	C
GV04	∞	2.0- 3.0	3	0.0	I	8	A0	C
GV05	∞	2.0- 4.0	3	0.0	I	8	A0	C
GV06	∞	3.5- 5.5	3	0.0	I	8	A0	C

1. C = Coherent, I = Incoherent (vertical channels), H = Incoherent (horizontal channels)

GA01-GV12 are the current beams used for IMS processing (since May 3, 1991). A different naming convention was used when this beam set was initially deployed. Some arrivals at GERESS in the IMS database between May 3, 1991 and May 5, 1991 have channel names that are not listed in Table 8. The mapping between the old names and the new names (in Table 8) is:

*GA01-GA12 are also called GF101-GF112*

*GC01-GC12 are also called GF301-GF312*

*GF01-GF24 are also called GF601-GF624*

*GF77 is also called GF777*

*GF88 is also called GF888*

*GF99 is also called GF999*

*GG01-GG24 is also called GF701-GF724*

A0 is the center element of the array, but it is currently excluded from most beams. Beams GA01-GC12 and GV12 use 21 array elements on the A-, B-, C- and D-rings (A3, B3 and D5 are excluded). Beams GF01-GF24 and GG01-GHI1 use 16 elements on the A-, B-, C-, and D-rings (A3, B3, C1, C3, C5, D2, D5, D8 and D9 are excluded). Beams GF77 and GF88 use 11 array elements: A0, A3, B3, B5, C1, C3, C5, D2, D5, D8, and D9. GF99 uses all 16 elements on the C- and D-rings plus A0. GHI2 uses all elements on the A-, B-, and C-rings except A3 and B3. GHI3 uses all elements on the A-, C-, and D-rings plus A0, and GVI1 uses all 25 short-period elements.

The initial GERESS beam deployment (before May 3, 1991) is listed in the bottom half of Table 8 (beams G011-GV06). These use all short-period vertical elements on the rings that are indicated (except GH01-GH04 which only use the horizontal components).

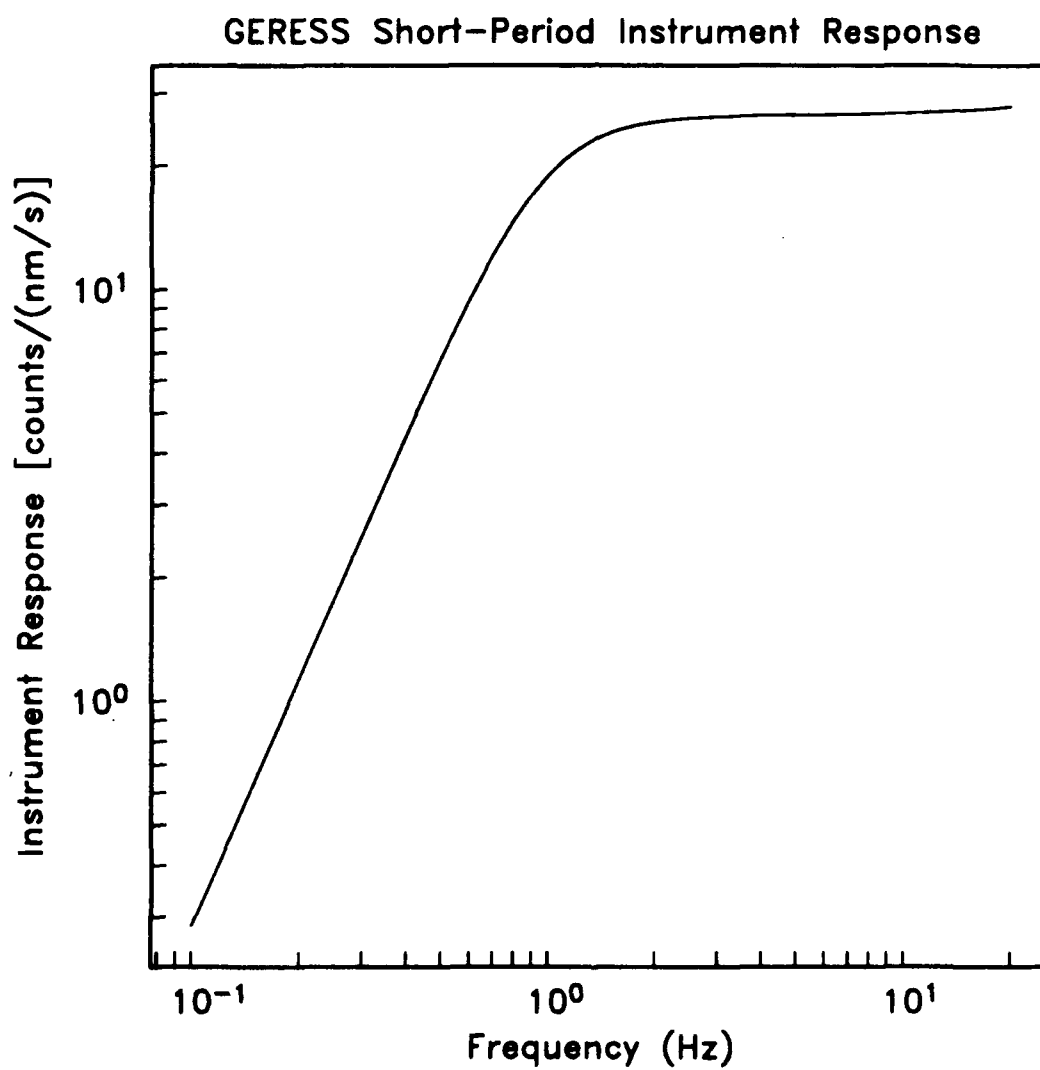


**Figure 25.** The short-period instrument response is plotted for GERESS.

times after 31 March 1991, at least 3 defining phases, and at least one associated phase at GERESS. The restriction on origin time was to ensure that a stable version of IMS was used. IMS became operational in November, 1990, and the rules and processing parameters were modified frequently to improve performance until the end of March, 1991.

#### 4.2.2 Event Description

Table 9 lists the 255 events in Data Set #3. The first column lists the *orid*, which is a unique positive integer that identifies each event in the CSS database [Anderson *et al.*, 1990]. The rest of the columns list the event origin time, latitude, longitude, local magnitude ( $M_L$ ), number of detecting stations, and number of defining phases.

The event locations are plotted in Figure 26. The epicentral distances are primarily between 50 and 1700 km (Figure 27). The magnitude distribution is plotted in Figure 28. This magnitude is computed from the short-term average amplitude of regional phases ( $P_n$ ,  $P_g$ ,  $S_n$ , and  $L_g$ ) measured on a 2–4 Hz incoherent beam [Bache *et al.*, 1991]. The magnitudes of the events in Data Set #3 are primarily between 2.0 and 5.0. The correction tables used to calculate these magnitudes were developed by Sereno *et al.* [1992], who find that the magnitude bias between GERESS and the arrays in Fennoscandia is approximately 1.0  $M_L$ .

The events in Data Set #3 were not identified because independent bulletins were not available. However, most of the events to the south of GERESS are probably earthquakes. For example, over 60% of these are also in the PDE bulletin. In contrast, most of the events to the north of GERESS are mining explosions (Figure 29). For example, Data Set #3 includes about 55 events from an active copper mining region in Lubin, Poland [e.g., Gibowicz, 1987; Gestermann, 1992], and about 15 events near the *Dubna Skala* mine near Cracow, Poland (this mine was included in a list provided to CSS by Klaus-G. Hinzen at BGR in Germany). There are also 10 events that are close to two mines that are about 100 km southwest of Berlin called *Dubring* and *Schwarzkollm* (these were also reported by Klaus-G. Hinzen). Unfortunately, we don't have details regarding the activities of these mines, so it is difficult to associate the events recorded at GERESS with them. Both earthquakes and chemical explosions occur in the Volgtland area, about 180 km to the northwest of GERESS [Wuster, 1992].

#### 4.2.3 Sample Waveforms

This section shows some samples of the waveform data. Figure 30 is a map with epicenters of 8 events in Data Set #3. Figures 31–38 display waveforms for these events recorded by one of the 3-component elements of the GERESS array. The data drop-outs are common for the horizontal channels, and also occur occasionally on the vertical channels. It is uncertain whether these occur as part of the GERESS instrumentation, or if they occur during transmission of the data to the NORSAR Data

Table 9. Events in Data Set #3

orid	Origin Time		Latitude	Longitude	$M_L$	nsta <sup>1</sup>	ndef <sup>2</sup>
16193	91 04 01	01:40:39.919	51.38	16.73	2.20	3	4
16290	91 04 01	11:40:18.399	56.40	22.54	1.58	3	7
16201	91 04 04	19:03:41.358	43.66	18.84	3.01	3	4
16202	91 04 04	20:43:05.067	45.92	16.55	3.27	1	3
16736	91 04 05	05:37:08.553	50.23	6.67	2.54	2	3
17185	91 04 07	08:35:12.681	51.64	15.96	2.27	4	8
17286	91 04 08	00:19:58.861	51.35	16.38	2.21	2	4
17301	91 04 08	09:45:59.715	51.43	16.13	2.53	2	3
17536	91 04 10	01:31:23.321	35.89	21.05	4.04	4	4
17627	91 04 10	11:01:34.217	50.35	14.04	2.15	2	3
17565	91 04 11	08:37:21.954	42.35	24.92	2.91	4	4
17654	91 04 11	18:02:29.675	51.53	16.15	2.43	2	5
17658	91 04 11	19:31:13.357	51.59	16.52	2.42	4	6
17874	91 04 12	08:23:10.529	50.88	16.16	2.55	1	3
17976	91 04 13	14:14:14.269	51.44	16.57	3.23	1	3
18594	91 04 16	10:04:51.709	52.12	13.80	3.15	2	4
18742	91 04 18	04:37:39.429	51.63	15.87	2.81	3	5
19192	91 04 18	18:51:13.180	50.50	18.56	2.86	1	3
19237	91 04 18	19:24:06.566	40.19	16.02	3.94	4	5
19450	91 04 20	09:23:12.897	50.15	13.55	2.24	2	3
22454	91 04 23	09:24:30.708	59.27	26.99	2.28	3	4
19060	91 04 24	13:21:53.893	36.89	14.98	4.01	4	4
19717	91 04 25	00:19:18.117	50.48	18.01	2.72	1	3
19813	91 04 25	08:49:18.372	61.17	22.84	1.58	2	3
19827	91 04 25	11:17:39.151	44.48	13.74	3.39	1	3
19831	91 04 25	11:51:42.375	51.56	16.13	2.88	4	7
19843	91 04 25	12:18:33.383	51.49	16.50	3.43	1	3
20061	91 04 27	04:25:26.887	51.51	16.16	1.97	2	3
20199	91 04 27	15:54:57.353	39.59	20.01	4.04	4	5
20202	91 04 27	16:35:33.324	56.25	12.01	1.96	4	8
20205	91 04 27	18:44:56.809	46.62	14.87	3.38	4	4
20209	91 04 27	19:54:26.095	42.81	17.53	3.08	3	4
20249	91 04 28	21:24:18.962	45.72	27.37	3.38	4	4
21325	91 04 29	18:16:48.887	50.74	31.20	2.14	3	3
21392	91 04 29	21:38:12.061	43.50	18.56	3.20	4	5
20297	91 04 30	03:40:36.346	51.55	16.33	2.97	4	5
20077	91 04 30	10:55:59.746	51.38	15.95	3.17	2	3
21329	91 05 02	11:19:11.556	47.90	16.44	2.87	1	3
21353	91 05 02	18:39:47.471	51.58	16.48	2.35	4	5
21362	91 05 02	22:27:43.955	47.96	16.46	3.34	1	3
21848	91 05 03	23:26:24.863	50.07	18.76	2.51	3	4
22152	91 05 06	11:16:55.268	50.25	12.41	2.31	1	3
20932	91 05 07	01:45:52.602	51.44	16.60	2.27	2	5
20935	91 05 07	03:02:44.265	51.48	16.44	2.74	4	7
22298	91 05 08	11:14:38.279	50.24	12.60	2.33	1	3
22299	91 05 08	11:43:12.122	54.60	20.04	2.39	3	4
21209	91 05 08	11:58:11.333	60.56	17.30	1.56	2	3
22467	91 05 09	08:57:16.530	39.13	15.66	3.37	2	3
22469	91 05 09	09:47:07.031	39.03	15.62	3.34	2	3
22482	91 05 09	19:37:23.882	51.59	15.99	2.65	1	3
22800	91 05 10	20:45:30.086	49.85	17.99	2.74	1	3

orid	Origin Time		Latitude	Longitude	$M_L$	nsta <sup>1</sup>	ndef <sup>2</sup>
22856	91 05 11	03:11:02.688	49.60	6.39	3.19	1	3
22913	91 05 11	10:02:03.302	51.53	16.72	2.33	3	4
21712	91 05 12	10:05:23.762	46.78	34.52	2.26	3	3
21911	91 05 13	10:46:40.273	45.37	11.26	2.82	1	3
22086	91 05 14	01:18:21.481	50.31	18.95	2.59	2	4
22859	91 05 16	10:44:51.266	49.58	6.58	3.37	1	3
23112	91 05 17	11:02:52.851	50.24	12.64	2.31	1	3
23190	91 05 18	01:44:40.065	38.61	19.92	4.01	3	3
23217	91 05 18	11:15:39.930	51.52	16.23	2.50	3	6
23275	91 05 19	03:22:10.519	50.28	12.09	2.44	2	3
23287	91 05 19	17:21:32.481	35.42	18.38	3.71	3	3
23406	91 05 20	11:03:53.555	50.29	12.35	2.47	1	3
23209	91 05 21	11:02:22.196	50.41	12.80	2.51	1	3
23231	91 05 21	16:49:23.537	50.50	18.05	2.49	2	4
23249	91 05 21	23:15:56.114	51.54	16.70	2.61	3	5
23615	91 05 23	11:01:06.643	50.21	12.75	2.43	1	3
23958	91 05 23	19:42:53.502	51.59	16.07	2.79	4	6
24348	91 05 26	12:26:04.754	40.68	15.76	4.97	3	4
24522	91 05 27	19:22:28.255	51.22	17.03	2.47	3	5
24533	91 05 27	23:49:55.250	35.60	27.39	2.37	3	3
24129	91 05 28	03:52:47.874	51.50	16.33	2.71	4	9
24140	91 05 28	09:28:46.199	42.38	28.66	4.20	3	3
23897	91 05 28	12:41:26.130	51.10	15.21	2.42	1	3
24177	91 05 28	18:27:08.040	42.39	26.46	3.37	4	4
24180	91 05 28	18:58:31.274	35.15	22.71	2.44	4	4
24215	91 05 29	01:27:53.829	51.15	16.59	2.60	1	4
24054	91 05 29	07:52:49.760	47.05	15.29	2.62	1	3
24390	91 05 29	20:24:59.883	45.99	9.70	3.72	1	3
24551	91 05 30	07:54:02.861	59.45	27.31	1.46	4	5
24554	91 05 30	09:23:43.536	50.12	12.79	2.41	1	3
24593	91 05 30	21:18:22.627	51.62	16.24	2.38	4	5
24924	91 06 01	05:41:56.513	36.26	21.88	4.26	4	5
25117	91 06 03	11:02:10.313	50.17	12.67	2.54	1	3
25351	91 06 04	11:05:30.958	50.21	12.33	2.60	1	3
25365	91 06 04	13:08:02.809	50.16	13.32	2.34	1	3
25499	91 06 05	01:18:18.933	45.87	27.20	3.03	4	4
25534	91 06 05	11:02:16.032	50.52	12.32	2.52	2	3
25274	91 06 06	12:04:39.583	54.87	21.01	2.17	2	3
25749	91 06 06	13:50:18.952	50.07	31.89	2.65	3	3
25974	91 06 08	07:40:21.877	51.40	16.61	2.23	2	3
25975	91 06 08	08:09:26.614	37.96	10.25	3.57	3	3
26144	91 06 09	00:34:05.115	46.28	1.72	3.56	1	3
26145	91 06 09	00:57:46.151	45.13	16.84	2.52	2	3
26660	91 06 14	02:34:54.127	50.58	18.85	2.67	3	3
26680	91 06 14	10:42:38.354	50.34	18.13	1.56	1	3
26846	91 06 14	14:08:05.024	49.70	6.44	3.05	1	3
27379	91 06 15	12:51:27.682	51.54	16.39	2.62	2	6
27398	91 06 15	18:30:07.573	51.51	16.65	2.26	3	6
27419	91 06 15	20:58:10.857	36.66	16.41	3.98	3	3
27463	91 06 16	05:53:15.915	51.44	16.18	2.23	2	4
27569	91 06 16	17:20:58.142	37.57	21.70	4.36	3	5
27688	91 06 17	03:06:43.886	49.84	33.02	2.49	3	3
27704	91 06 17	12:47:54.608	51.36	16.27	2.71	1	4

orid	Origin Time		Latitude	Longitude	$M_L$	nsta <sup>1</sup>	ndef <sup>2</sup>
26563	91 06 17	21:34:56.382	41.00	19.67	3.95	2	3
27169	91 06 20	12:10:11.489	50.68	14.31	2.46	1	3
27074	91 06 24	01:36:32.675	39.23	21.10	4.44	2	3
27982	91 06 25	13:24:20.515	46.26	13.52	2.44	1	3
28036	91 06 25	16:20:42.882	55.28	9.69	2.08	3	6
28293	91 06 26	11:43:40.505	39.37	22.46	4.84	4	8
28326	91 06 26	15:57:20.459	46.50	30.79	2.99	4	3
28335	91 06 26	20:01:30.838	40.57	19.24	3.67	4	3
27886	91 06 27	22:11:23.032	54.54	19.12	2.85	5	10
28063	91 06 28	02:32:56.449	51.56	16.13	2.31	3	6
28338	91 06 28	16:43:01.721	48.23	15.15	2.15	1	4
28186	91 06 29	08:12:28.896	39.15	20.59	3.80	3	4
28437	91 06 30	08:24:22.693	50.16	18.93	3.01	2	4
28467	91 06 30	18:36:16.336	51.52	16.07	2.65	2	7
28364	91 07 01	07:52:55.631	47.64	15.13	2.21	1	3
28543	91 07 01	22:24:24.598	44.68	28.78	2.41	3	4
28206	91 07 02	21:05:39.849	49.37	6.53	2.84	1	3
28555	91 07 03	03:31:49.435	43.16	27.39	3.21	3	4
28756	91 07 04	01:29:32.225	50.25	19.04	2.65	2	6
28762	91 07 04	06:44:38.513	51.44	16.31	2.90	1	3
28979	91 07 05	03:24:58.753	51.48	16.10	2.24	3	8
29081	91 07 05	15:30:50.155	50.57	18.84	2.03	3	6
29268	91 07 06	14:45:46.525	50.21	18.58	2.67	2	4
29348	91 07 10	05:55:47.984	43.31	23.38	2.90	3	3
29367	91 07 10	11:33:22.039	51.54	16.11	3.03	4	10
29396	91 07 10	23:57:20.093	51.55	16.20	2.20	4	9
29719	91 07 11	09:10:59.855	50.43	12.72	2.51	2	4
30016	91 07 12	03:44:47.927	47.06	11.26	2.83	1	3
30073	91 07 12	10:42:22.973	45.50	21.09	4.51	4	10
30096	91 07 12	16:29:23.605	45.83	19.82	3.07	4	6
30097	91 07 12	17:20:32.767	44.74	19.02	2.70	2	3
29428	91 07 12	18:58:01.090	44.19	28.17	2.85	4	3
29431	91 07 12	19:21:45.784	45.31	11.33	2.57	1	3
30111	91 07 12	21:13:30.954	48.05	20.43	2.60	2	4
30386	91 07 14	23:59:46.739	46.35	20.22	2.97	4	5
30408	91 07 15	15:45:26.919	46.52	19.16	2.77	4	7
30933	91 07 17	00:22:22.603	36.65	21.02	3.74	4	5
30934	91 07 17	20:05:46.099	36.76	20.80	3.78	4	5
30701	91 07 18	11:56:40.019	45.80	22.62	4.31	4	7
30709	91 07 18	12:03:38.196	45.35	21.93	3.00	2	3
30718	91 07 18	14:04:16.129	46.66	20.24	2.42	2	4
30844	91 07 19	01:19:53.660	45.44	21.32	3.77	4	6
30846	91 07 19	01:27:31.753	45.46	21.47	4.00	4	8
30848	91 07 19	02:43:26.717	45.22	20.70	2.98	4	5
30854	91 07 19	07:00:02.234	50.39	13.96	2.21	2	3
30422	91 07 19	08:06:42.268	45.52	20.53	2.68	2	3
31002	91 07 20	03:23:35.140	51.54	16.08	3.06	2	5
31015	91 07 20	03:36:53.656	46.55	19.52	2.89	4	5
31346	91 07 21	01:56:27.366	35.20	22.60	4.04	4	5
31364	91 07 21	13:07:07.938	51.51	16.11	1.71	3	9
31384	91 07 21	15:03:31.674	37.05	20.11	3.85	3	3
31388	91 07 21	17:10:50.781	51.43	16.06	1.91	3	6
31389	91 07 21	18:15:47.437	51.01	15.99	4.23	2	3

orid	Origin Time		Latitude	Longitude	$M_L$	nsta <sup>1</sup>	ndef <sup>2</sup>
31409	91 07 21	21:34:26.818	39.18	22.73	3.50	3	3
31416	91 07 21	22:50:41.171	51.60	16.22	1.79	4	8
31258	91 07 22	09:58:20.710	50.05	12.74	2.31	2	4
31399	91 07 23	08:40:50.255	42.73	14.07	3.10	3	4
31473	91 07 23	23:14:01.328	50.28	19.35	2.55	5	8
31610	91 07 24	03:17:45.260	51.64	16.02	2.66	5	8
31675	91 07 24	10:39:39.997	51.35	10.39	3.08	1	3
31686	91 07 24	11:00:38.272	50.33	12.49	2.36	2	4
31648	91 07 25	00:17:34.203	51.66	7.06	2.03	2	6
31685	91 07 25	04:41:06.715	49.20	6.48	2.85	1	3
31692	91 07 25	07:53:04.502	47.51	14.87	2.21	2	3
31729	91 07 25	08:26:28.351	43.51	31.55	3.95	5	7
32237	91 07 27	03:05:04.988	51.51	16.08	1.62	4	8
32247	91 07 27	11:38:13.803	37.50	30.67	4.39	5	5
32252	91 07 27	14:05:59.267	51.55	16.08	1.65	4	8
32254	91 07 27	14:44:25.286	40.18	31.03	3.94	3	3
32255	91 07 27	15:04:33.535	37.15	30.80	4.12	4	4
32441	91 07 28	23:32:43.213	51.52	16.13	2.34	5	7
32593	91 07 29	14:29:19.751	48.99	12.99	2.23	2	4
32597	91 07 29	17:00:52.855	35.26	29.70	2.39	3	3
32757	91 07 30	15:03:53.429	50.34	18.88	3.70	2	5
32766	91 07 31	07:28:39.391	51.50	15.99	2.56	5	10
33878	91 08 04	21:00:14.844	39.45	17.12	2.69	3	3
33811	91 08 05	09:18:28.586	50.45	13.57	2.31	2	4
34098	91 08 06	11:00:47.773	50.50	13.70	2.46	2	4
34118	91 08 06	15:04:40.125	44.92	21.97	3.04	5	6
34083	91 08 07	03:14:25.351	45.17	15.10	2.87	1	4
34105	91 08 07	09:17:40.023	46.54	26.42	3.43	5	9
34107	91 08 07	09:34:51.792	51.47	14.16	2.80	3	7
34121	91 08 07	09:59:33.443	50.59	13.97	2.66	2	4
34129	91 08 07	10:40:37.738	50.55	13.42	2.32	2	4
34139	91 08 07	12:16:20.669	51.47	16.28	2.76	3	5
34297	91 08 07	19:24:04.173	45.30	20.78	2.91	5	6
34702	91 08 08	20:02:42.161	51.62	16.22	3.08	2	5
34948	91 08 09	07:10:06.365	46.40	13.86	3.25	1	3
34955	91 08 09	08:08:10.420	50.50	14.04	2.51	2	4
35393	91 08 11	21:26:15.930	46.98	19.41	2.61	3	4
35399	91 08 12	04:59:45.332	45.72	20.82	3.45	4	4
35458	91 08 12	19:26:09.176	50.21	18.97	2.57	3	6
34695	91 08 13	11:30:00.091	49.98	12.80	2.10	2	3
34938	91 08 14	11:43:56.196	49.17	14.06	2.33	1	3
34970	91 08 14	21:51:06.307	50.34	18.50	2.72	2	4
34980	91 08 14	23:35:56.997	45.06	21.25	3.65	4	7
34993	91 08 15	01:34:53.859	46.42	19.55	3.26	4	6
34998	91 08 15	04:44:37.377	45.46	21.46	3.33	2	3
34999	91 08 15	04:58:57.212	40.93	22.56	4.38	4	5
35050	91 08 15	19:35:23.016	45.24	21.09	3.03	3	4
35230	91 08 16	07:59:49.435	50.29	13.29	2.42	2	4
35308	91 08 18	23:02:08.726	46.73	19.27	3.05	2	4
35524	91 08 19	11:23:32.350	46.69	10.79	3.40	1	3
35595	91 08 20	10:29:10.244	50.53	15.66	4.20	1	3
35793	91 08 20	16:59:43.019	48.04	24.58	3.29	1	3
36111	91 08 23	10:04:07.763	50.22	12.36	2.33	2	3

orid	Origin Time		Latitude	Longitude	$M_L$	nsta <sup>1</sup>	ndef <sup>2</sup>
36122	91 08 23	12:11:23.461	51.60	16.04	2.65	4	8
36918	91 08 27	22:02:59.829	38.74	15.73	3.43	4	5
36561	91 08 28	00:03:37.872	44.57	15.34	3.47	2	5
37053	91 08 29	13:14:52.107	50.53	14.59	2.74	2	4
37668	91 09 03	05:52:45.022	45.19	14.97	2.86	1	3
37672	91 09 03	07:36:45.481	54.64	19.13	2.38	3	5
37704	91 09 03	12:13:23.324	61.62	-5.05	2.41	5	6
38119	91 09 04	12:34:49.683	51.21	14.20	2.85	2	5
38188	91 09 06	07:00:10.851	50.41	13.94	2.41	2	4
38296	91 09 06	10:43:59.122	51.43	14.07	2.97	2	4
38301	91 09 06	11:32:53.503	51.56	16.18	2.78	5	8
38411	91 09 06	20:25:29.833	50.87	18.99	2.95	2	3
38419	91 09 06	23:17:48.659	49.95	11.81	2.64	2	3
38575	91 09 07	06:11:04.143	45.54	-21	2.49	2	3
38617	91 09 07	12:01:45.496	46.55	19.36	2.86	1	3
38618	91 09 07	14:00:22.884	44.80	12.98	2.73	1	3
38789	91 09 08	19:45:16.211	41.28	18.94	3.84	5	7
38937	91 09 09	10:33:32.233	51.58	14.08	2.47	3	6
39286	91 09 10	11:26:30.715	51.42	14.23	2.99	2	4
39339	91 09 10	18:59:31.516	41.92	27.83	3.35	3	4
39510	91 09 11	10:09:55.255	50.62	13.55	2.38	2	4
39518	91 09 11	11:02:36.369	48.17	15.15	2.04	1	3
39519	91 09 11	11:05:58.863	51.58	14.03	3.19	2	5
39700	91 09 11	16:24:20.401	51.59	16.06	2.31	5	9
39743	91 09 12	09:36:33.962	51.59	14.02	3.18	2	5
39787	91 09 12	11:13:50.639	50.29	12.51	2.29	2	4
39452	91 09 13	02:23:19.482	51.57	16.36	2.12	5	9
39461	91 09 13	08:38:27.730	51.02	15.93	2.63	2	5
39888	91 09 14	10:27:53.040	50.48	30.26	2.54	3	3
39732	91 09 15	11:03:32.055	35.37	27.52	2.56	5	4
41640	91 09 25	11:58:50.281	51.01	13.69	1.86	2	3
41650	91 09 25	13:21:22.543	37.04	16.12	3.88	4	4
41656	91 09 25	14:53:25.760	36.30	14.83	4.09	4	4
41671	91 09 25	21:21:32.634	36.81	15.03	3.65	4	4
41694	91 09 26	10:26:26.087	50.58	13.64	2.50	2	4
41721	91 09 26	13:29:50.771	50.54	14.52	2.48	2	4
41757	91 09 27	09:30:40.755	51.67	14.03	3.26	2	5
41769	91 09 27	11:31:05.590	51.61	16.21	2.99	2	4
41772	91 09 27	11:41:23.661	45.98	11.42	2.85	1	4
41791	91 09 27	16:05:04.348	51.59	16.05	2.26	5	10
41892	91 09 27	19:30:08.057	36.19	21.07	4.14	5	4
41792	91 09 28	00:37:52.142	51.51	16.25	2.53	5	9
41796	91 09 28	04:00:14.608	50.31	18.78	2.45	2	4
41829	91 09 29	04:37:26.677	47.74	15.55	2.46	2	4
41850	91 09 29	21:41:23.667	51.30	24.53	2.96	5	5

1. The number of detecting stations.

2. The number of defining phases (number of phases used to locate the event).



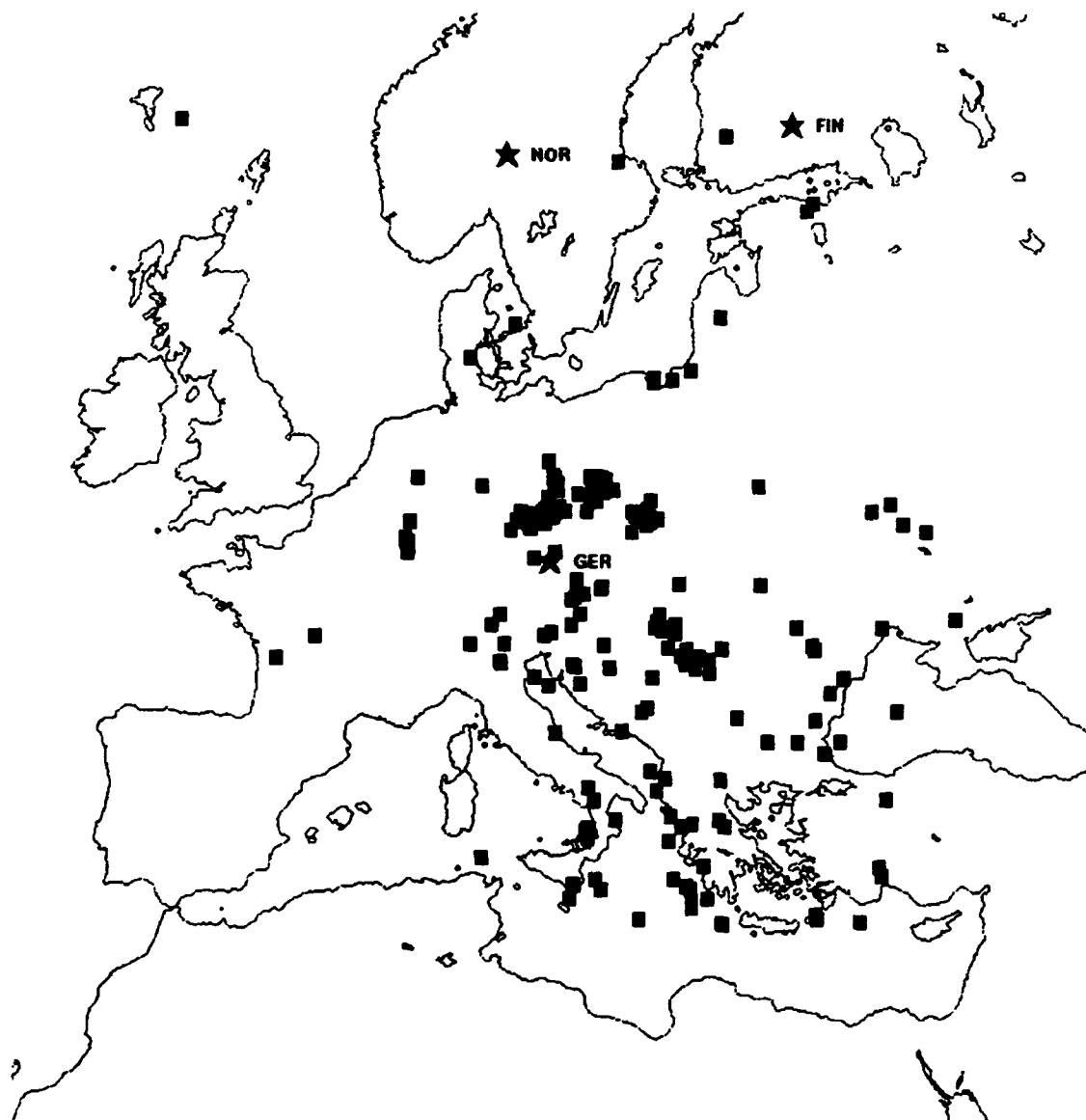


**Figure 26.** Epicenters are plotted for the 255 events in Data Set #3.

### DATA SET #3

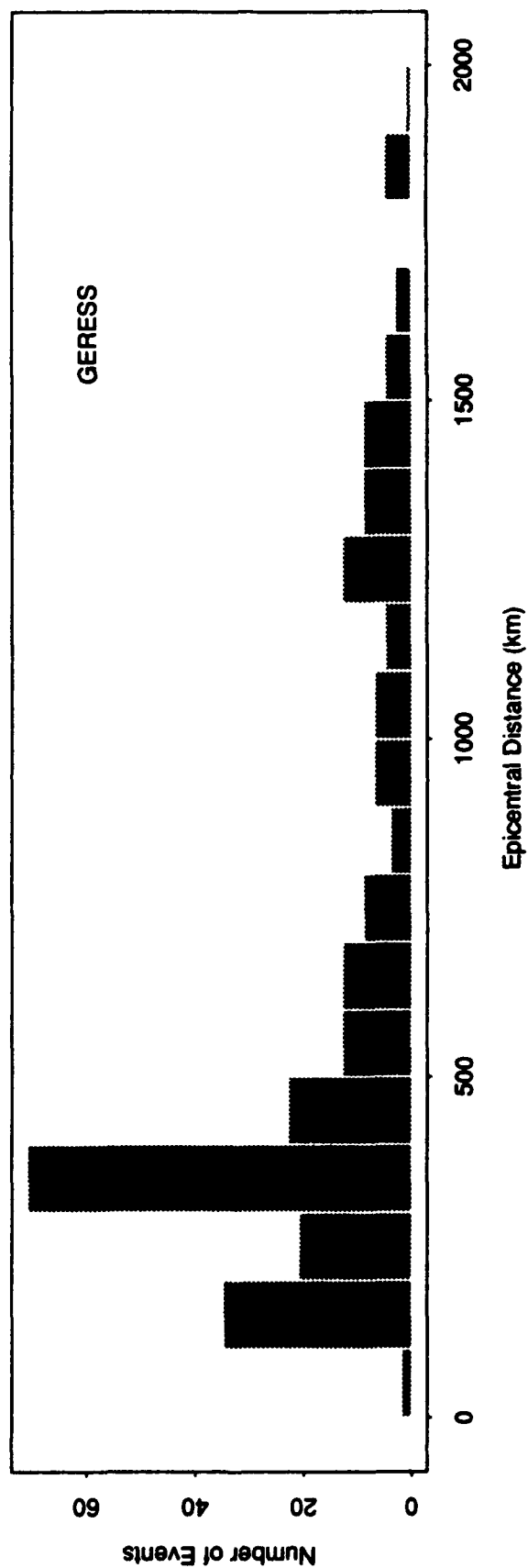


Figure 27. Histograms of epicentral distance to the events in Data Set #3 are plotted for GERESS.

### DATA SET #3

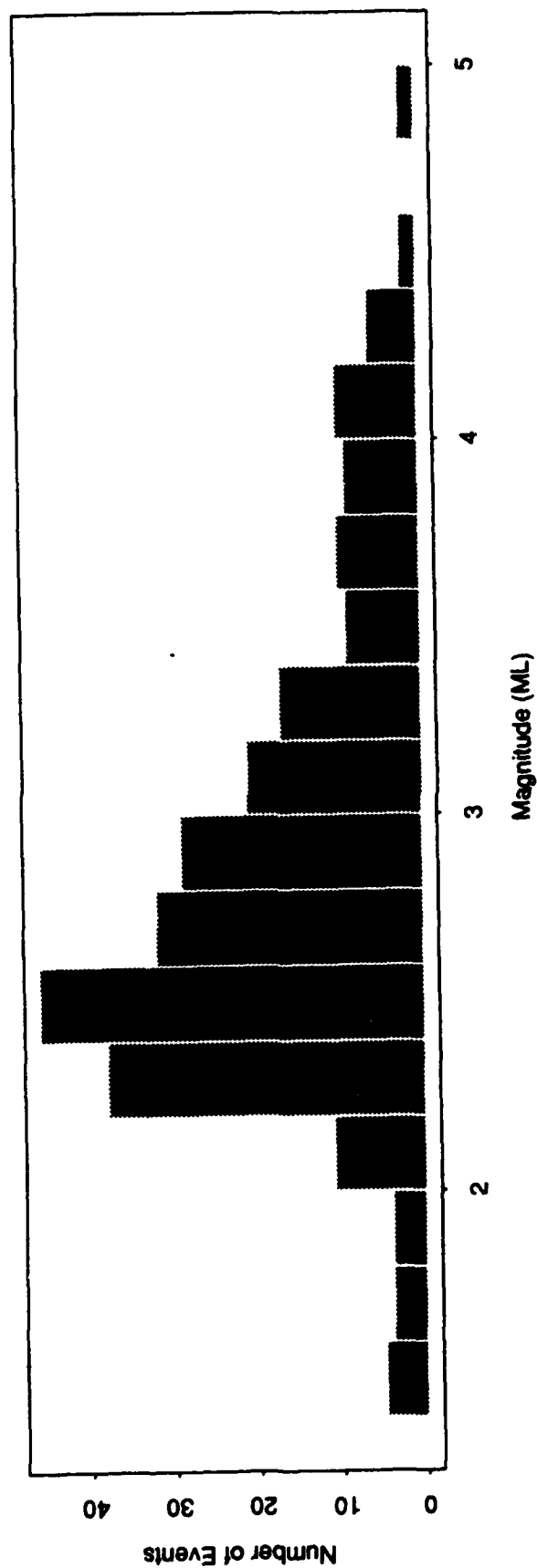
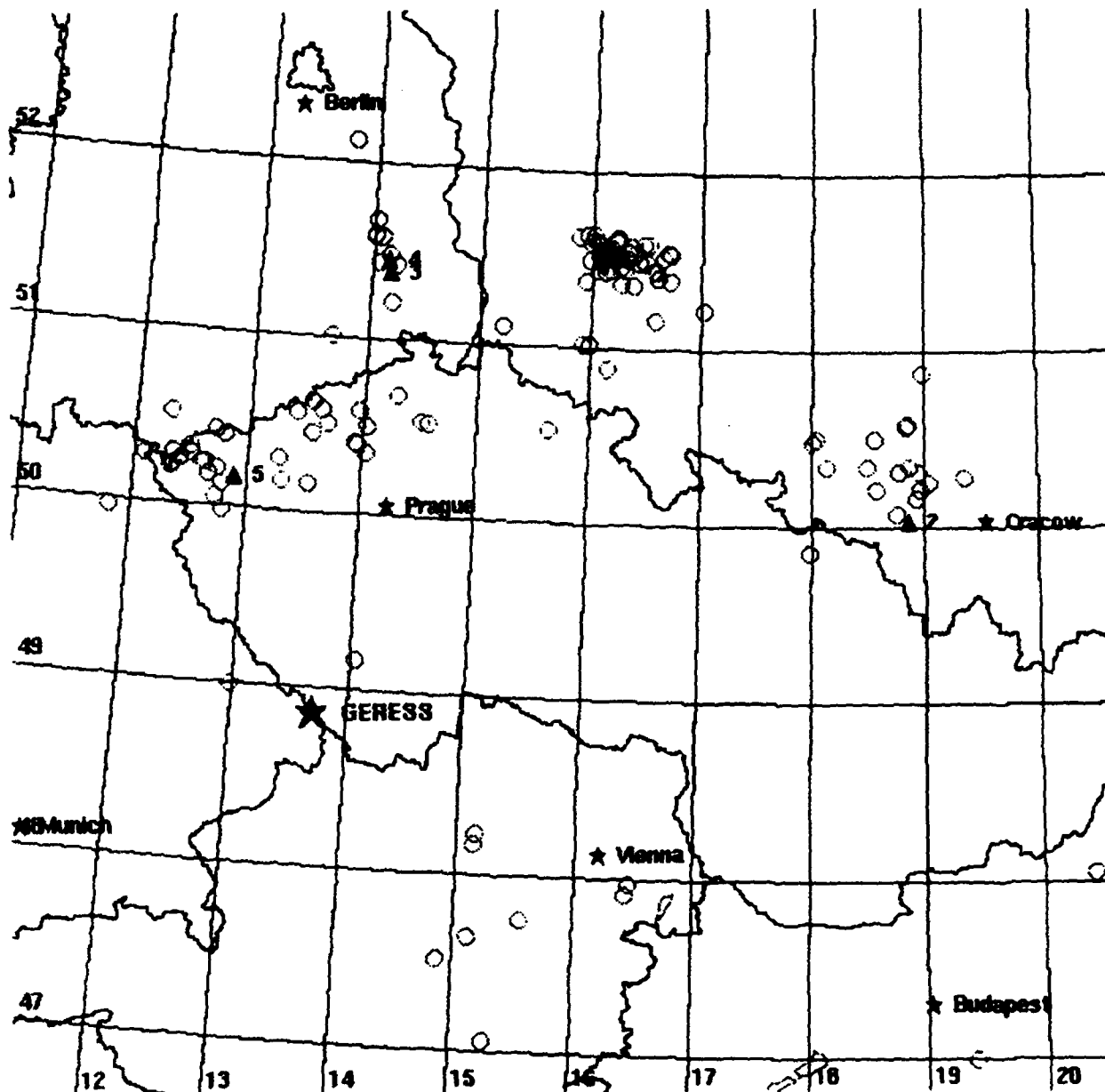
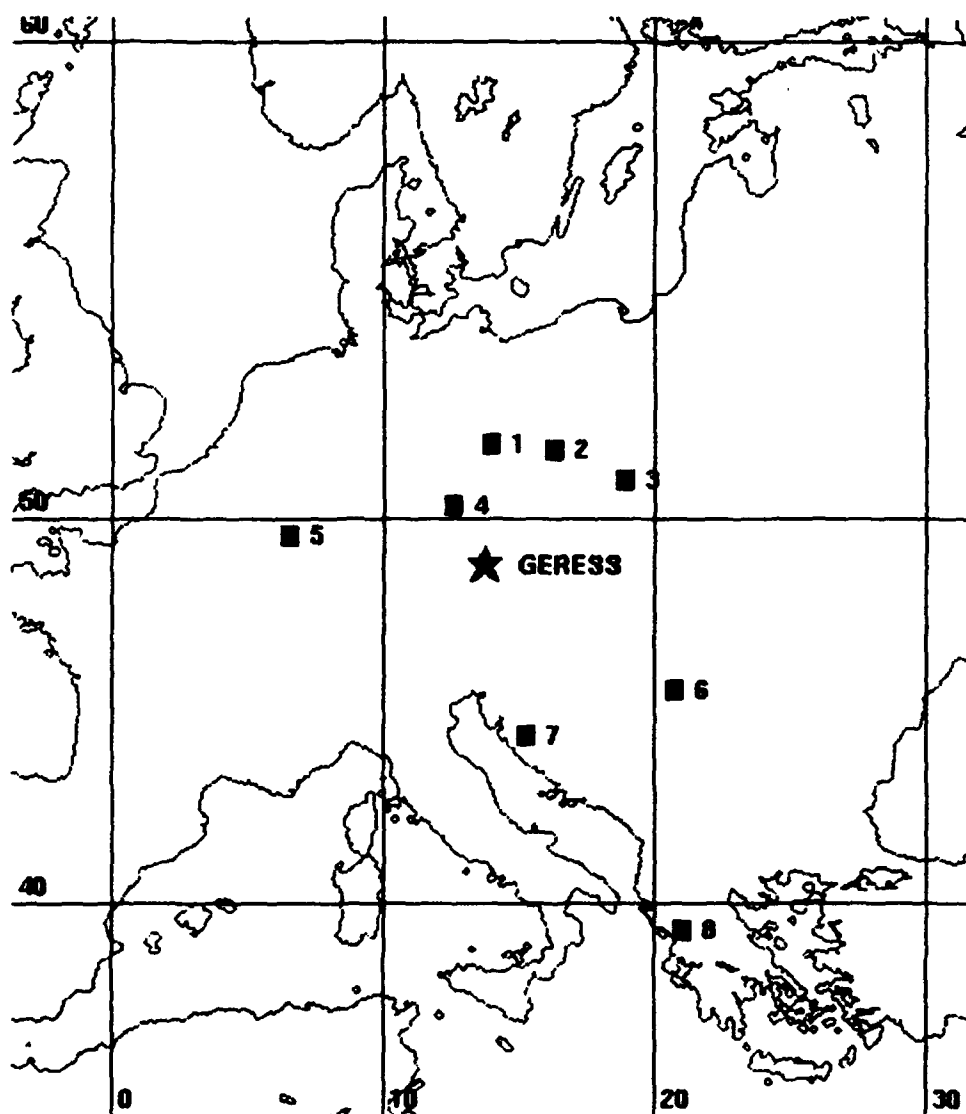


Figure 28. A histogram of local magnitude is shown for events in Data Set #3.



**Figure 29.** This map shows the locations of the events in Data Set #3 that are within approximately 300–400 km of GERESE (open circles). The solid triangles indicate the location of known mines in this area: (1) copper mine in Lubin, Poland; (2) *Dubna Skala*; (3) *Dubring*; (4) *Schwarzkolm*; (5) a mine in the Volgtland area [Wuster, 1992]. There are many other mines in this region (e.g., along the border between Germany and Czechoslovakia), but more information regarding the activities of these mines is needed to accurately associate events recorded at GERESE with them.



**Figure 30.** The locations of eight events in Data Set #3 are plotted. Sample waveforms for these events are plotted in Figures 31–38. The *orids* in Table 9 are (1) 41757, (2) 39452, (3) 38411, (4) 22298, (5) 22859, (6) 35399, (7) 36561, and (8) 27074.

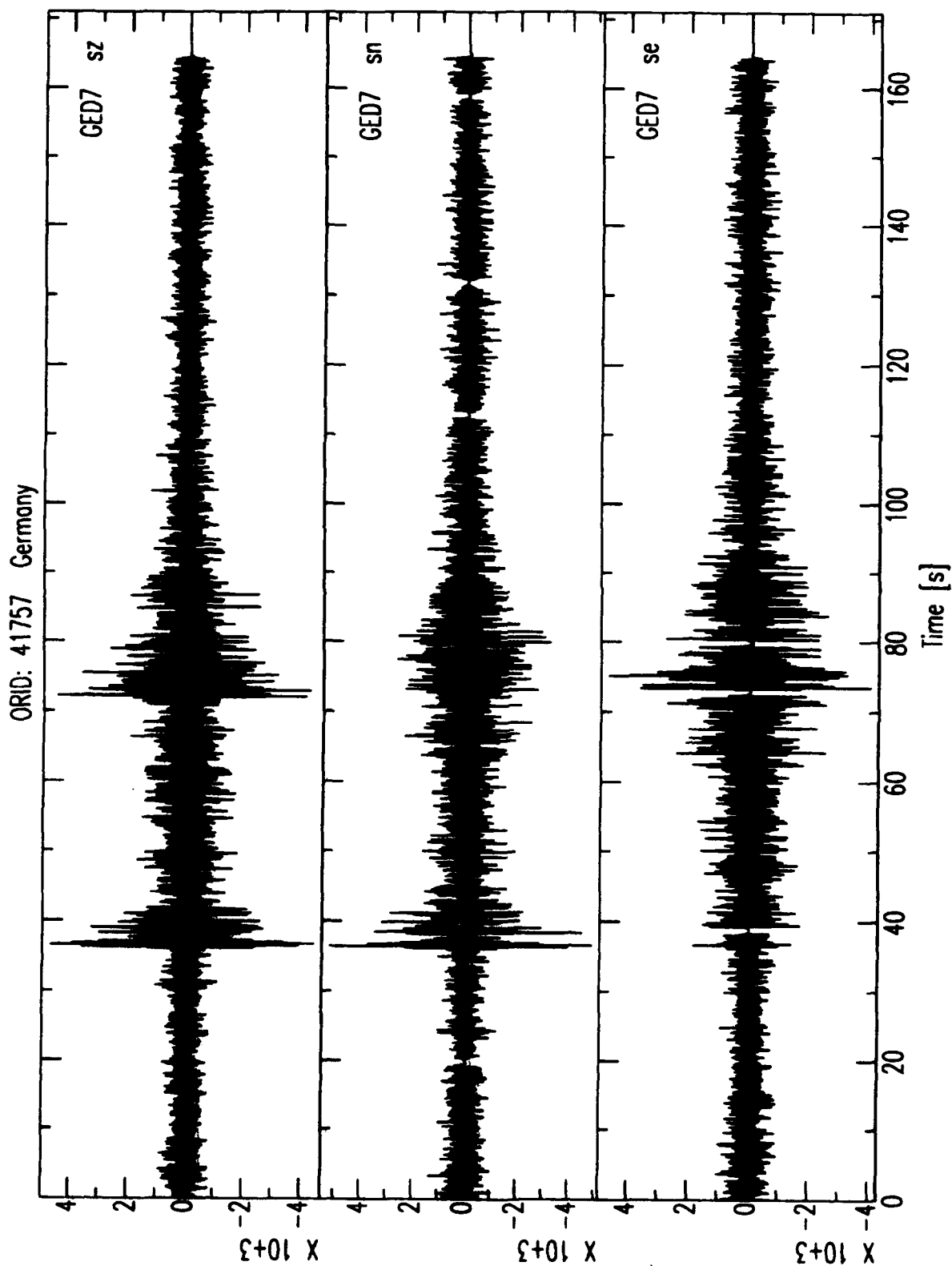


**Figure 31.** Seismograms recorded by a 3-component element of the GERESS array for an event in Germany about 100 km southeast of Berlin (event 1 in Figure 30). The seismograms are bandpassed from 1 to 15 Hz.

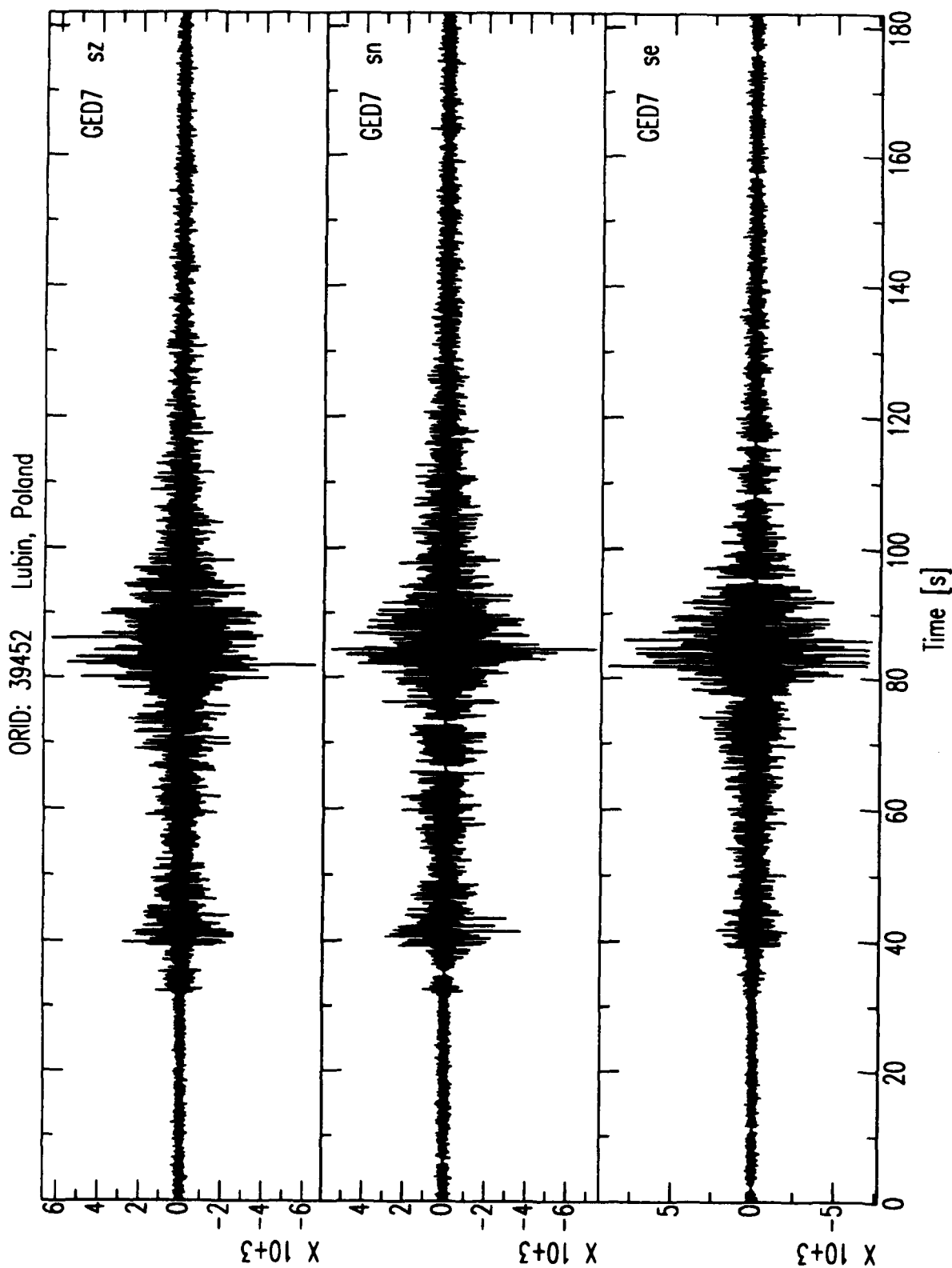


Figure 32. Seismograms recorded by a 3-component element of the GERESS array for a probable mining explosion in Lubin, Poland (event 2 in Figure 30). The seismograms are bandpassed from 1 to 15 Hz.

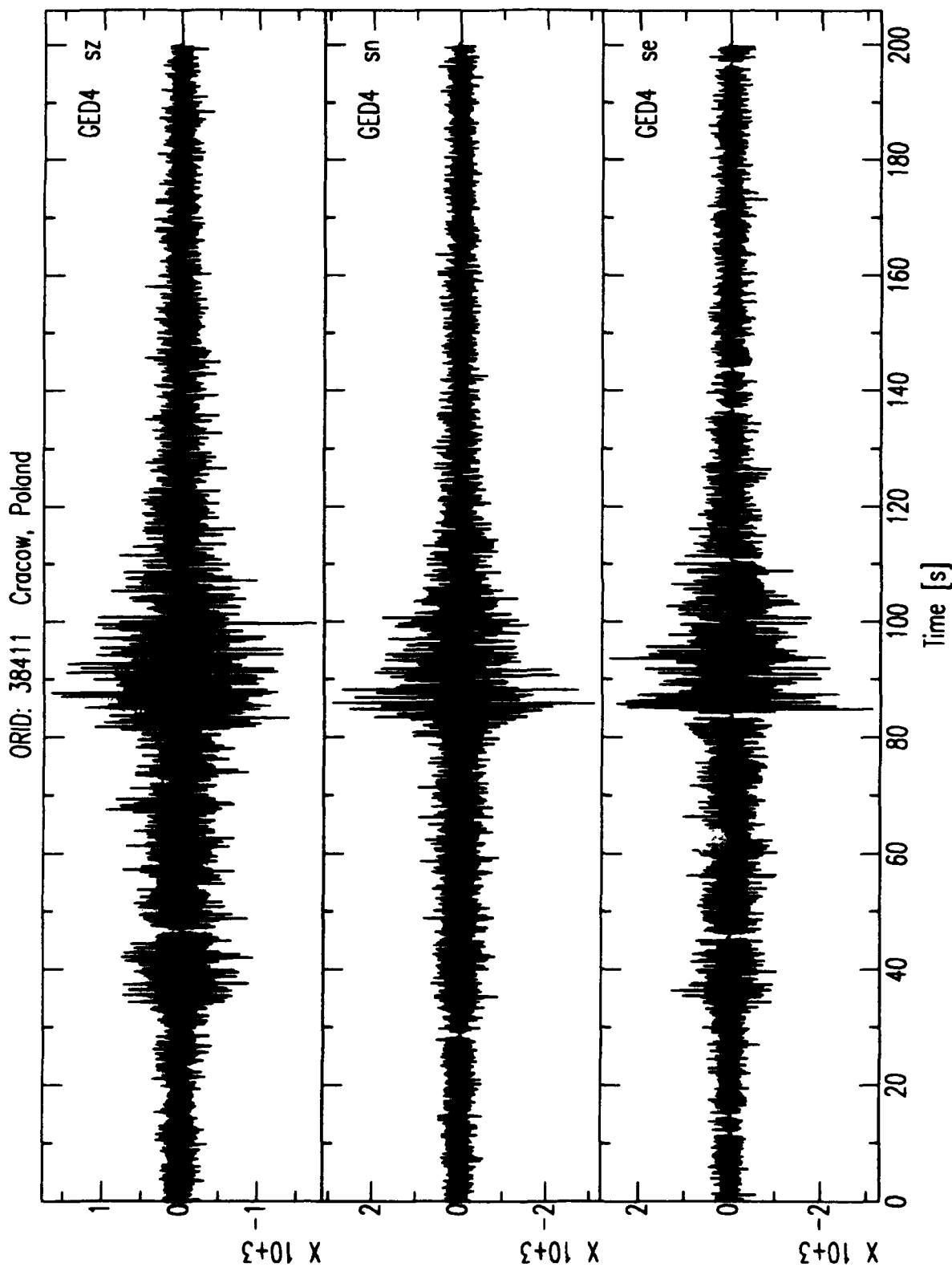
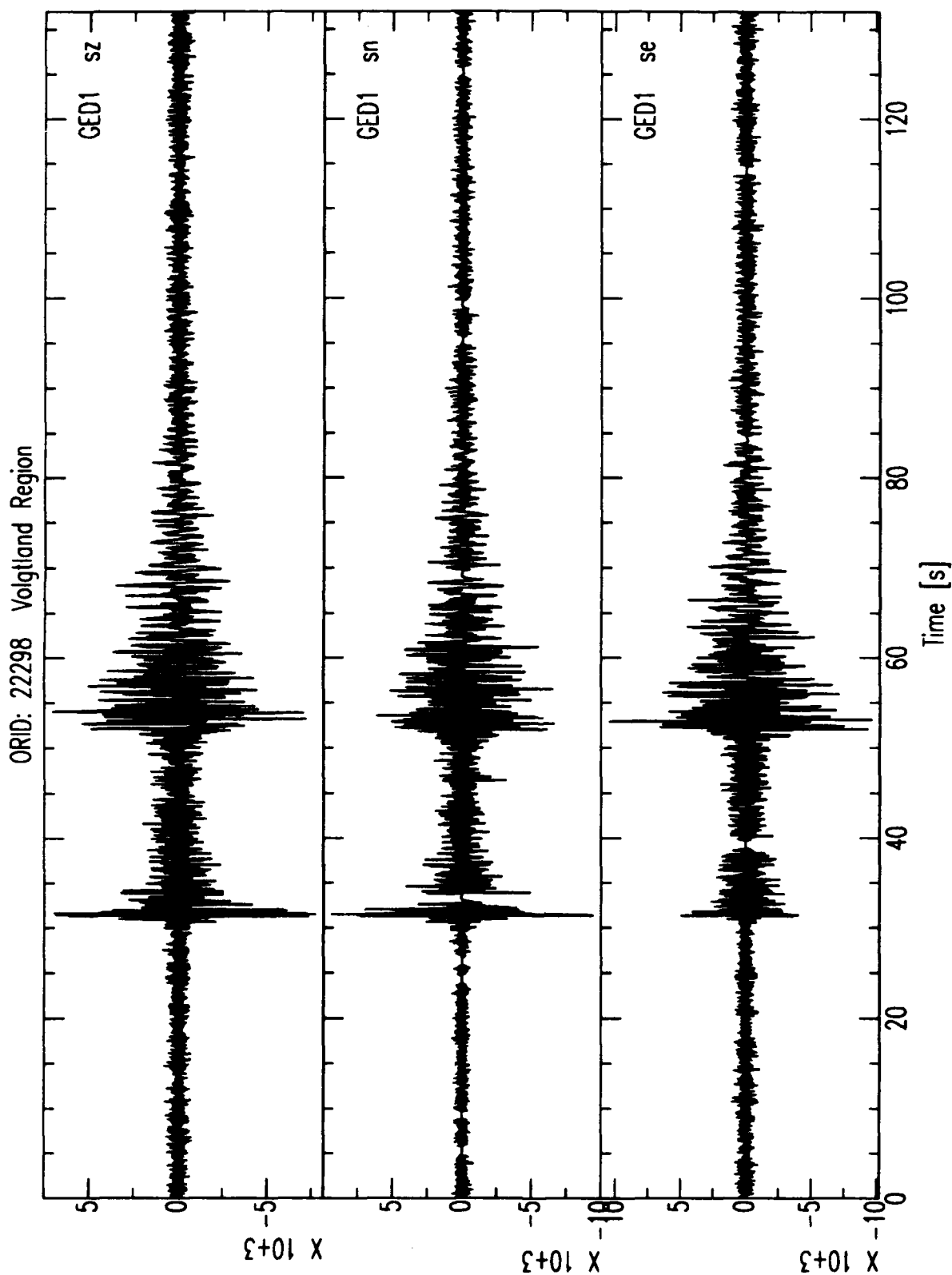
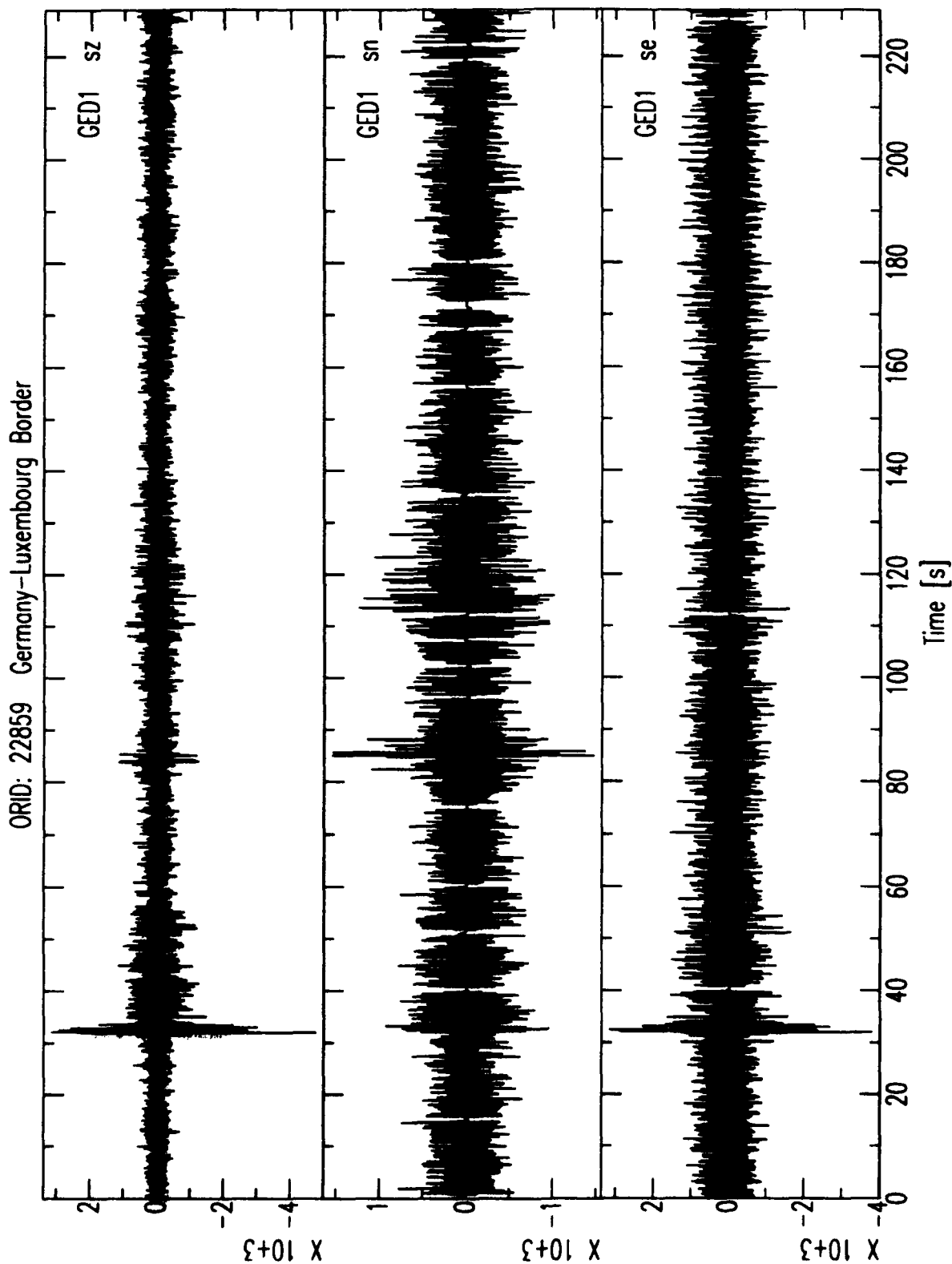


Figure 33. Seismograms recorded by a 3-component element of the GERESS array for an event near the *Dubna Skala* mine in Poland (event 3 in Figure 30). The seismograms are bandpassed from 1 to 15 Hz.





**Figure 34.** Seismograms recorded by a 3-component element of the GERESS array for a probable mining explosion in the Volgtland area (event 4 in Figure 30). The seismograms are bandpassed from 1 to 15 Hz.



**Figure 35.** Seismograms recorded by a 3-component element of the GERESS array for an event near the border between Germany and Luxembourg (event 5 in Figure 30). The seismograms are bandpassed from 1 to 15 Hz.

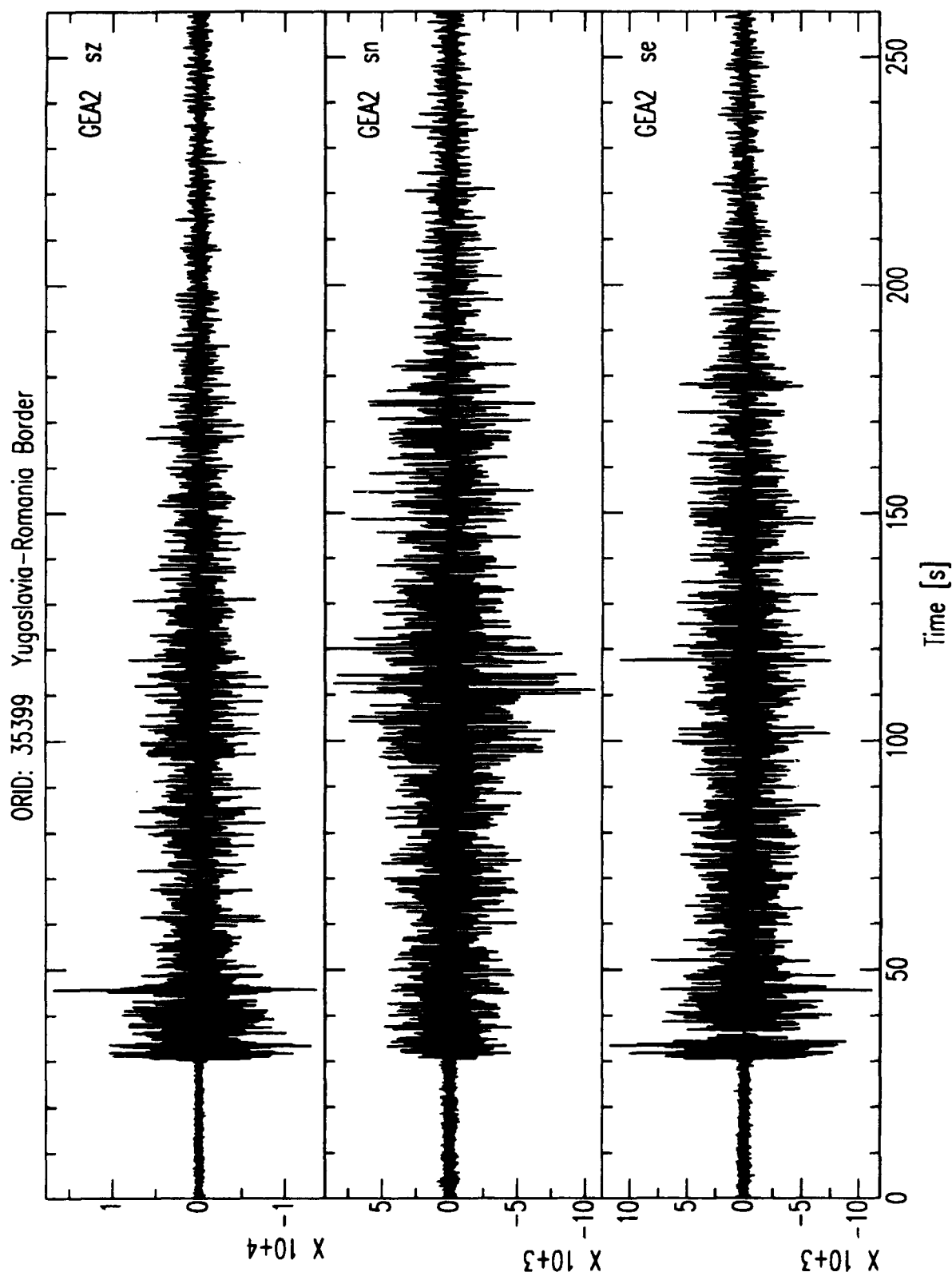


**Figure 36.** Seismograms recorded by a 3-component element of the GERESS array for an event near the border between Yugoslavia and Romania (event 6 in Figure 30). The seismograms are bandpassed from 1 to 15 Hz.

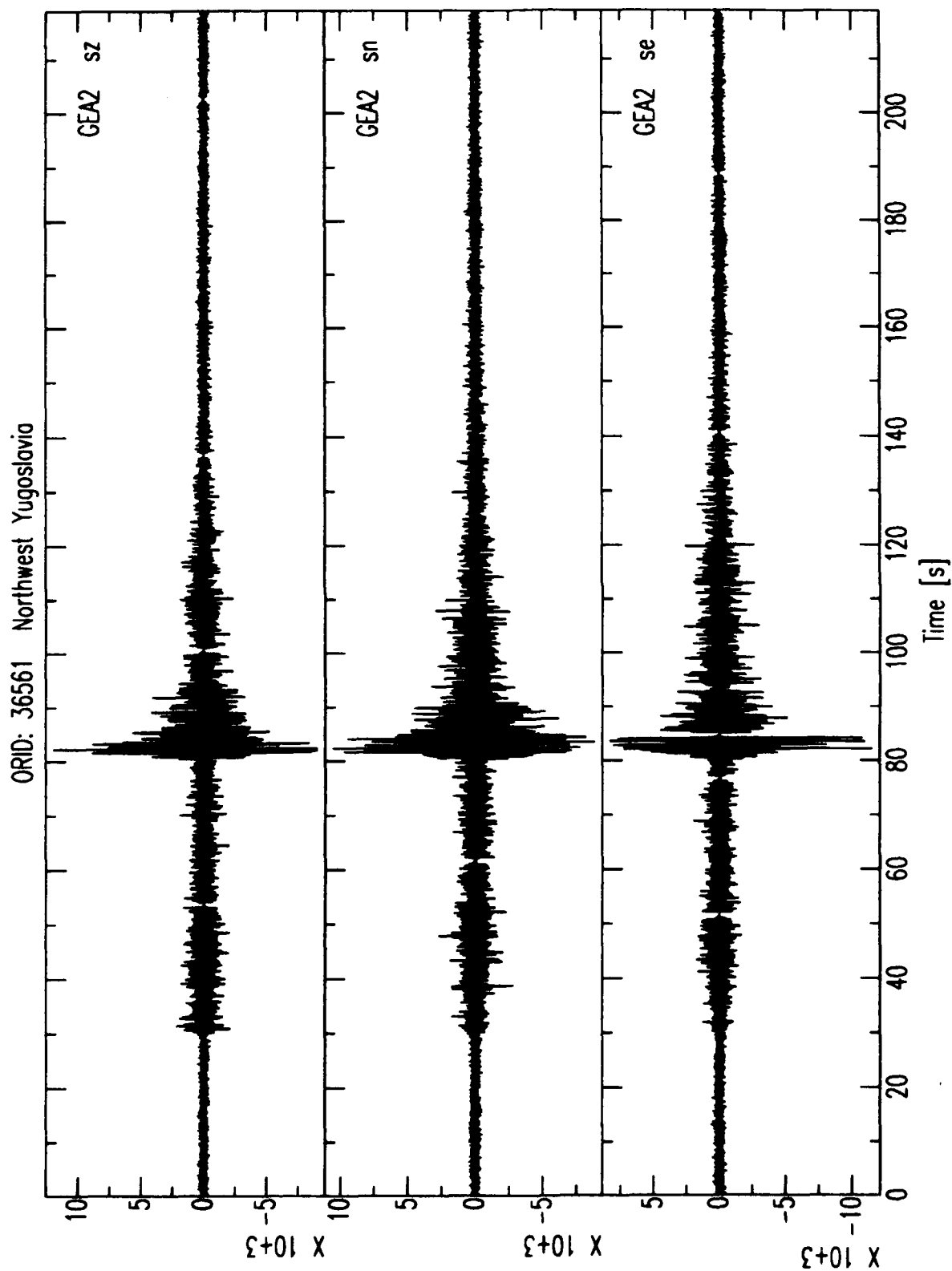
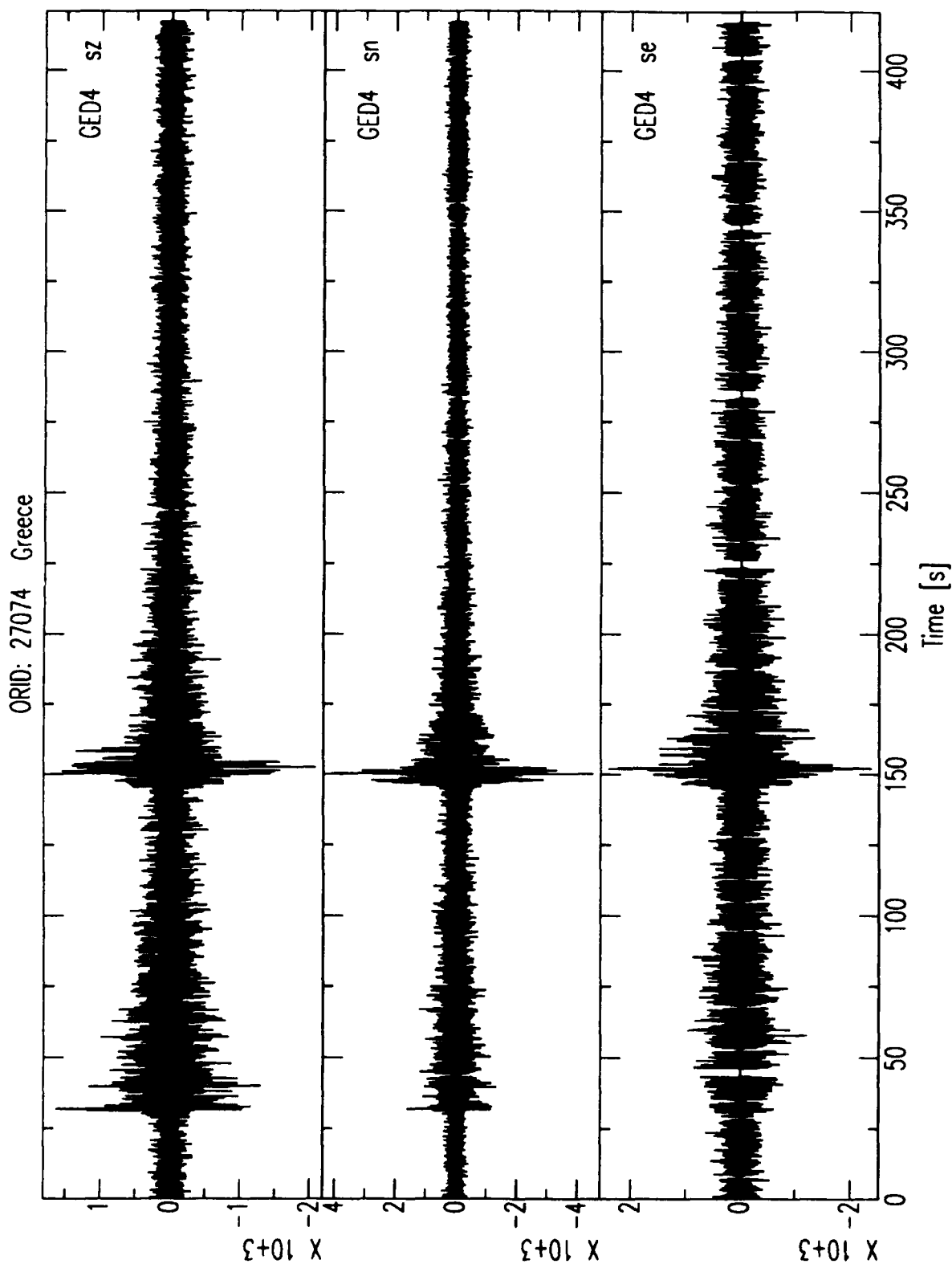


Figure 37. Seismograms recorded by a 3-component element of the GERESS array for an event in northwest Yugoslavia (event 7 in Figure 30). The seismograms are bandpassed from 1 to 15 Hz.



**Figure 38.** Seismograms recorded by a 3-component element of the GERESS array for an event near the northwest coast of Greece (event 8 in Figure 30). The seismograms are bandpassed from 1 to 15 Hz.

Analysis Center in Norway. Waveforms for the other events in Data Set #3 are of similar quality.

## 5. CONCLUSIONS

We developed a data set to test and evaluate the performance of neural networks for automated processing and interpretation of regional seismic data. This data set may also be valuable for other applications related to seismic monitoring at regional distances, and it is available at the Center for Seismic Studies (CSS) in an Oracle database or in UNIX tar format on exabyte tapes. It consists of waveform and parametric data from >500 regional events recorded by the short-period elements of the NORESS and ARCESS arrays in Norway, and the GERESS array in Germany (the Oracle database at CSS also includes data from the FINESA array in Finland and a 3-component station in Poland called KSP). The epicentral distances are primarily 50–2000 km, and the magnitudes are primarily 1.0–5.0. Most of the events are mining explosions in the western part of the CIS, Sweden, Finland, Poland and Germany. Also included are 22 presumed underwater explosions, and 51 earthquakes in Fennoscandia that were identified in a regional bulletin produced by the University of Helsinki. Other presumed earthquakes (for which independent bulletin information was not available) include events in the Alps and Mediterranean region that were recorded by GERESS. The Oracle database is in CSS 3.0 format, and the exabyte tapes include waveforms in SAC binary format and parametric data in ASCII tables. Detailed documentation has been developed for each event, and is included in a 13-volume report at the CSS.

## ACKNOWLEDGMENTS

We thank Lori Grant and Jerry Carter at the Center for Seismic Studies for their help in obtaining mine locations in the vicinity of GERESS. This research was funded by the Defense Advanced Research Projects Agency under Contract F19628-90-C-0156 and monitored by Phillips Laboratory.

**(THIS PAGE INTENTIONALLY LEFT BLANK)**



## REFERENCES

- Ahjos, T., M. Uski, and E. Pelkonen, Earthquakes in northern Europe in 1989" *Institute of Seismology, University of Helsinki, Report S-24*, Helsinki, Finland, 1990.
- Anderson, J., W. Farrell, K. Garcia, J. Given, and H. Swanger, Center for Seismic Studies Version 3 Database: Schema Reference Manual, *Tech. Rep. C90-01*, Center for Seismic Studies, Arlington, VA., 1990.
- Bache, T., S. Bratt, J. Given, T. Schroeder, H. Swanger, and J. Wang, The Intelligent Monitoring System Version 2, *Quarterly Tech. Rep. #6 SAIC-91/1137*, Sci. Appl. Int. Corp., San Diego, Calif., 1991.
- Baumgardt, D., and K. Ziegler, Spectral evidence for source multiplicity in explosions *Semiannu. Tech. Rep. SAS-TR-87-01*, Ensco, Inc., Springfield, VA, AFGL-TR-87-0045, ADA187363, 1987.
- Gestermann, N., Interpretation of regional phases recorded at GERESS, paper presented at the *Symposium on Regional Seismic Arrays*, Bavaria, Germany, 22-24 June, 1992.
- Gibowicz, S., NORESS capability for detection and location of mining tremors in the Lubin area of Poland, *Sci. Rep. 2-86/87*, NTNF/NORSAR, Kjeller, Norway, 1987.
- Harjes, H.-P., Siting survey and configuration optimization of a new regional array in the Federal Republic of Germany, *Final Report*, GL-TR-90-0116, ADA223486, 1990.
- Harjes, H.-P., N. Gestermann, M. Jost, J. Schweitzer, J. Wuster, Advanced waveform research methods for GERESS recordings, *Sci. Rep. No. 1*, PL-TR-91-2134, ADA239199, 1991.
- Jurkevics, A., Polarization analysis of three-component array data, *Bull. Seismol. Soc. Am.*, 78, 1725-1743, 1988.
- Lacoss, R., R. Cunningham, S. Curtis, and M. Seibert, Artificial neural networks for seismic data interpretation, *Semiannu. Tech. Rep. ESD-TR-91-058*, Lincoln Laboratory, Massachusetts Institute of Technology, Lexington, MA, ADA239673, 1990.

- Lacoss, R., R. Cunningham, S. Curtis, and M. Seibert, Artificial neural networks for seismic data interpretation, *Semiannu. Tech. Rep. ESD-TR-91-170*, Lincoln Laboratory, Massachusetts Institute of Technology, Lexington, MA, ADA245006, 1991.
- Mortell, M., T. Sereno, G. Patnaik, Data to test and evaluate the performance of neural network architectures for seismic signal discrimination - DARPA Data Set #2, *Tech. Rep. SAIC-91/1243*, Sci. Appl. Int. Corp., San Diego, Calif., 1991.
- Mortell, M., T. Sereno, P. Kelly, and G. Patnaik, Data to test and evaluate the performance of neural network architectures for seismic signal discrimination - DARPA Data Set #3, *Tech. Rep. SAIC-92/1027 (Vol. 1-5)*, Sci. Appl. Int. Corp., San Diego, Calif., 1992.
- Mykkeltveit, S., K. Astebol, D. Doornbos, and E. Husebye, Seismic array configuration optimization, *Bull. Seismol. Soc. Am.*, 73, 173-186, 1983.
- Mykkeltveit, S., and F. Ringdal, New results from processing of data recorded at the new ARCESS regional array, *Sci. Rep. 2-87/88*, NTNF/NORSAR, Kjeller, Norway, 1988.
- Patnaik, G., and T. Sereno, Data to test and evaluate the performance of neural network architectures for seismic signal discrimination - DARPA Data Set #1, *Tech. Rep. SAIC-91/1274 (Vol. 1-7)*, Sci. Appl. Int. Corp., San Diego, Calif., 1991a.
- Patnaik, G., and T. Sereno, Neural computing for seismic phase identification, *Scientific Report No. 1 (Volume II)*, PL-TR-92-2110(II), ADA252442, 1991b.
- Patnaik, G., T. Sereno, and R. Jenkins, Test and evaluation of neural network applications for seismic signal discrimination *Final Report (Volume II)*, PL-TR-92-2218(II), 1992.
- Sereno, T., Data to test and evaluate the performance of neural network architectures for seismic signal discrimination: Event identification - DARPA Data Set #1, *Tech. Rep. SAIC-91/1275*, Sci. Appl. Int. Corp., San Diego, Calif., 1991.
- Sereno, T., and G. Patnaik, Data to test and evaluate the performance of neural network architectures for seismic signal discrimination, *Scientific Report No. 1 (Volume I)*, PL-TR-92-2110(I), 1991. ADA254413
- Sereno, T., H. Swanger, R. Jenkins, W. Nagy, and D. Wahl, Attenuation and travel-time characteristics of regional phases recorded at GERESS, paper presented at the *Symposium on Regional Seismic Arrays*, Bavaria, Germany, 22-24 June, 1992.

Swanger, H., J. Given, and J. Anderson, IMS extensions to the Center Version 3 Database, *Quarterly Tech. Rep. #5 SAIC-91/1138*, Sci. Appl. Int. Corp., San Diego, Calif., 1991.

Uski, M., and E. Pelkonen, Earthquakes in northern Europe in 1990" *Institute of Seismology, University of Helsinki, Report S-29*, Helsinki, Finland, 1991.

Wuster, J., Discrimination of tectonic earthquakes and quarry blasts at regional distances from GERESS, in *Advanced waveform research methods for GERESS recordings* by Harjes, et al., PL-TR-92-2142, 92-136, 1992. ADA253686

Prof. Thomas Ahrens  
Seismological Lab, 252-21  
Division of Geological & Planetary Sciences  
California Institute of Technology  
Pasadena, CA 91125

Prof. Keiiti Aki  
Center for Earth Sciences  
University of Southern California  
University Park  
Los Angeles, CA 90089-0741

Prof. Shelton Alexander  
Geosciences Department  
403 Deike Building  
The Pennsylvania State University  
University Park, PA 16802

Dr. Ralph Alewine, III  
DARPA/NMRO  
3701 North Fairfax Drive  
Arlington, VA 22203-1714

Prof. Charles B. Archambeau  
CIRES  
University of Colorado  
Boulder, CO 80309

Dr. Thomas C. Bache, Jr.  
Science Applications Int'l Corp.  
10260 Campus Point Drive  
San Diego, CA 92121 (2 copies)

Prof. Muawia Barazangi  
Institute for the Study of the Continent  
Cornell University  
Ithaca, NY 14853

Dr. Jeff Barker  
Department of Geological Sciences  
State University of New York  
at Binghamton  
Vestal, NY 13901

Dr. Douglas R. Baumgardt  
ENSCO, Inc  
5400 Port Royal Road  
Springfield, VA 22151-2388

Dr. Susan Beck  
Department of Geosciences  
Building #77  
University of Arizona  
Tucson, AZ 85721

Dr. T.J. Bennett  
S-CUBED  
A Division of Maxwell Laboratories  
11800 Sunrise Valley Drive, Suite 1212  
Reston, VA 22091

Dr. Robert Blandford  
AFTAC/TT, Center for Seismic Studies  
1300 North 17th Street  
Suite 1450  
Arlington, VA 22209-2308

Dr. G.A. Bollinger  
Department of Geological Sciences  
Virginia Polytechnical Institute  
21044 Derring Hall  
Blacksburg, VA 24061

Dr. Stephen Bratt  
Center for Seismic Studies  
1300 North 17th Street  
Suite 1450  
Arlington, VA 22209-2308

Dr. Lawrence Burdick  
Woodward-Clyde Consultants  
566 El Dorado Street  
Pasadena, CA 91109-3245

Dr. Robert Burrige  
Schlumberger-Doll Research Center  
Old Quarry Road  
Ridgefield, CT 06877

Dr. Jerry Carter  
Center for Seismic Studies  
1300 North 17th Street  
Suite 1450  
Arlington, VA 22209-2308

Dr. Eric Chael  
Division 9241  
Sandia Laboratory  
Albuquerque, NM 87185

Prof. Vernon F. Cormier  
Department of Geology & Geophysics  
U-45, Room 207  
University of Connecticut  
Storrs, CT 06268

Prof. Steven Day  
Department of Geological Sciences  
San Diego State University  
San Diego, CA 92182

Prof. Thomas V. McEvilly  
Seismographic Station  
University of California  
Berkeley, CA 94720

Dr. Art McGarr  
U.S. Geological Survey  
Mail Stop 977  
U.S. Geological Survey  
Menlo Park, CA 94025

Dr. Keith L. McLaughlin  
S-CUBED  
A Division of Maxwell Laboratory  
P.O. Box 1620  
La Jolla, CA 92038-1620

Stephen Miller & Dr. Alexander Florence  
SRI International  
333 Ravenswood Avenue  
Box AF 116  
Menlo Park, CA 94025-3493

Prof. Bernard Minster  
IGPP, A-025  
Scripps Institute of Oceanography  
University of California, San Diego  
La Jolla, CA 92093

Prof. Brian J. Mitchell  
Department of Earth & Atmospheric Sciences  
St. Louis University  
St. Louis, MO 63156

Mr. Jack Murphy  
S-CUBED  
A Division of Maxwell Laboratory  
11800 Sunrise Valley Drive, Suite 1212  
Reston, VA 22091 (2 Copies)

Dr. Keith K. Nakanishi  
Lawrence Livermore National Laboratory  
L-025  
P.O. Box 808  
Livermore, CA 94550

Dr. Carl Newton  
Los Alamos National Laboratory  
P.O. Box 1663  
Mail Stop C335, Group ESS-3  
Los Alamos, NM 87545

Dr. Bao Nguyen  
HQ AFTAC/TTR  
Patrick AFB, FL 32925-6001

Prof. John A. Orcutt  
IGPP, A-025  
Scripps Institute of Oceanography  
University of California, San Diego  
La Jolla, CA 92093

Prof. Jeffrey Park  
Kline Geology Laboratory  
P.O. Box 6666  
New Haven, CT 06511-8130

Dr. Howard Patton  
Lawrence Livermore National Laboratory  
L-025  
P.O. Box 808  
Livermore, CA 94550

Dr. Frank Pilotte  
HQ AFTAC/TT  
Patrick AFB, FL 32925-6001

Dr. Jay J. Pulli  
Radix Systems, Inc.  
2 Taft Court, Suite 203  
Rockville, MD 20850

Dr. Robert Reinke  
ATTN: FCTVTD  
Field Command  
Defense Nuclear Agency  
Kirtland AFB, NM 87115

Prof. Paul G. Richards  
Lamont-Doherty Geological Observatory  
of Columbia University  
Palisades, NY 10964

Mr. Wilmer Rivers  
Teledyne Geotech  
314 Montgomery Street  
Alexandria, VA 22314

Dr. George Rothe  
HQ AFTAC/TTR  
Patrick AFB, FL 32925-6001

Dr. Alan S. Ryall, Jr.  
DARPA/NMRO  
3701 North Fairfax Drive  
Arlington, VA 22209-1714

Dr. Richard Sailor  
TASC, Inc.  
55 Walkers Brook Drive  
Reading, MA 01867

Prof. Charles G. Sammis  
Center for Earth Sciences  
University of Southern California  
University Park  
Los Angeles, CA 90089-0741

Prof. Christopher H. Scholz  
Lamont-Doherty Geological Observatory  
of Columbia University  
Palisades, NY 10964

Dr. Susan Schwartz  
Institute of Tectonics  
1156 High Street  
Santa Cruz, CA 95064

Secretary of the Air Force  
(SAFRD)  
Washington, DC 20330

Office of the Secretary of Defense  
DDR&E  
Washington, DC 20330

Thomas J. Sereno, Jr.  
Science Application Int'l Corp.  
10260 Campus Point Drive  
San Diego, CA 92121

Dr. Michael Shore  
Defense Nuclear Agency/SPSS  
6801 Telegraph Road  
Alexandria, VA 22310

Dr. Matthew Sibol  
Virginia Tech  
Seismological Observatory  
4044 Derring Hall  
Blacksburg, VA 24061-0420

Prof. David G. Simpson  
IRIS, Inc.  
1616 North Fort Myer Drive  
Suite 1440  
Arlington, VA 22209

Donald L. Springer  
Lawrence Livermore National Laboratory  
L-025  
P.O. Box 808  
Livermore, CA 94550

Dr. Jeffrey Stevens  
S-CUBED  
A Division of Maxwell Laboratory  
P.O. Box 1620  
La Jolla, CA 92038-1620

Lt. Col. Jim Stobie  
ATTN: AFOSR/NL  
Bolling AFB  
Washington, DC 20332-6448

Prof. Brian Stump  
Institute for the Study of Earth & Man  
Geophysical Laboratory  
Southern Methodist University  
Dallas, TX 75275

Prof. Jeremiah Sullivan  
University of Illinois at Urbana-Champaign  
Department of Physics  
1110 West Green Street  
Urbana, IL 61801

Prof. L. Sykes  
Lamont-Doherty Geological Observatory  
of Columbia University  
Palisades, NY 10964

Dr. David Taylor  
ENSCO, Inc.  
445 Pineda Court  
Melbourne, FL 32940

Dr. Steven R. Taylor  
Los Alamos National Laboratory  
P.O. Box 1663  
Mail Stop C335  
Los Alamos, NM 87545

Prof. Clifford Thurber  
University of Wisconsin-Madison  
Department of Geology & Geophysics  
1215 West Dayton Street  
Madison, WI 53706

Prof. M. Nafi Toksoz  
Earth Resources Lab  
Massachusetts Institute of Technology  
42 Carleton Street  
Cambridge, MA 02142

Dr. Larry Turnbull  
CIA-OSWR/NED  
Washington, DC 20505

DARPA/RMO/SECURITY OFFICE  
3701 North Fairfax Drive  
Arlington, VA 22203-1714

Dr. Gregory van der Vink  
IRIS, Inc.  
1616 North Fort Myer Drive  
Suite 1440  
Arlington, VA 22209

HQ DNA  
ATTN: Technical Library  
Washington, DC 20305

Dr. Karl Veith  
EG&G  
5211 Auth Road  
Suite 240  
Suitland, MD 20746

Defense Intelligence Agency  
Directorate for Scientific & Technical Intelligence  
ATTN: DTIB  
Washington, DC 20340-6158

Prof. Terry C. Wallace  
Department of Geosciences  
Building #77  
University of Arizona  
Tucson, AZ 85721

Defense Technical Information Center  
Cameron Station  
Alexandria, VA 22314 (2 Copies)

Dr. Thomas Weaver  
Los Alamos National Laboratory  
P.O. Box 1663  
Mail Stop C335  
Los Alamos, NM 87545

TACTEC  
Battelle Memorial Institute  
505 King Avenue  
Columbus, OH 43201 (Final Report)

Dr. William Wortman  
Mission Research Corporation  
8560 Cinderbed Road  
Suite 700  
Newington, VA 22122

Phillips Laboratory  
ATTN: XPG  
Hanscom AFB, MA 01731-5000

Prof. Francis T. Wu  
Department of Geological Sciences  
State University of New York  
at Binghamton  
Vestal, NY 13901

Phillips Laboratory  
ATTN: GPE  
Hanscom AFB, MA 01731-5000

AFTAC/CA  
(STINFO)  
Patrick AFB, FL 32925-6001

Phillips Laboratory  
ATTN: TSML  
Hanscom AFB, MA 01731-5000

DARPA/PM  
3701 North Fairfax Drive  
Arlington, VA 22203-1714

Phillips Laboratory  
ATTN: SUL  
Kirtland, NM 87117 (2 copies)

DARPA/RMO/RETRIEVAL  
3701 North Fairfax Drive  
Arlington, VA 22203-1714

Dr. Michel Bouchon  
I.R.I.G.M.-B.P. 68  
38402 St. Martin D'Heres  
Cedex, FRANCE

Dr. Michel Campillo  
Observatoire de Grenoble  
I.R.I.G.M.-B.P. 53  
38041 Grenoble, FRANCE

Dr. Jorg Schlittenhardt  
Federal Institute for Geosciences & Nat'l Res.  
Postfach 510153  
D-3000 Hannover 51, GERMANY

Dr. Kin Yip Chun  
Geophysics Division  
Physics Department  
University of Toronto  
Ontario, CANADA

Dr. Johannes Schweitzer  
Institute of Geophysics  
Ruhr University/Bochum  
P.O. Box 1102148  
4360 Bochum 1, GERMANY

Prof. ~~Hans~~-Peter Harjes  
Institute for Geophysics  
Ruhr University/Bochum  
P.O. Box 102148  
4630 Bochum 1, GERMANY

Prof. Eystein Husebye  
NTNF/NORSAR  
P.O. Box 51  
N-2007 Kjeller, NORWAY

David Jepsen  
Acting Head, Nuclear Monitoring Section  
Bureau of Mineral Resources  
Geology and Geophysics  
G.P.O. Box 378, Canberra, AUSTRALIA

Ms. Eva Johannisson  
Senior Research Officer  
National Defense Research Inst.  
P.O. Box 27322  
S-102 54 Stockholm, SWEDEN

Dr. Peter Marshall  
Procurement Executive  
Ministry of Defense  
Blacknest, Brimpton  
Reading FG7-FRS, UNITED KINGDOM

Dr. Bernard Massinon, Dr. Pierre Mechler  
Societe Radiomana  
27 rue Claude Bernard  
75005 Paris, FRANCE (2 Copies)

Dr. Svein Mykkeltveit  
NTNF/NORSAR  
P.O. Box 51  
N-2007 Kjeller, NORWAY (3 Copies)

Prof. Keith Priestley  
University of Cambridge  
Bullard Labs, Dept. of Earth Sciences  
Madingley Rise, Madingley Road  
Cambridge CB3 0EZ, ENGLAND